POLITECNICO DI MILANO
FACOLTÀ DI INGEGNERIA
CORSO DI LAUREA IN INGEGNERIA MECCANICA

ANALYSIS AND CONTROL OF EFFICIENT BIPEDAL WALKING GAIT

Relatori

Prof. Dott. Ing. Francesco Braghin

Prof. Dott. Ing. Fumihiko Asano

Tesi di laurea di

Alberto Giacomo Piovan

Matr: 725157

Anno Accademico 2010/2011

RINGRAZIAMENTI:
I miei più sentiti ringraziamenti vanno ai Professori
Francesco Braghin *del* Politecnico di Milano
Fumihiko Asano *del* JAIST (Japan Advanced Institute of Science and Technology)
alla mia Famiglia, tutta,
ed in generale a tutte le persone che mi sono state vicine in questa lunga avventura
e che con molta soddisfazione mia, e di molti, è giunta al termine.
Un ringraziamento particolare alla persone che hanno creduto in me
e a quelle che lo faranno.

INDEX

INTRODUCTION **XI**

0.1 INTRODUZIONE - Italiano XI

0.2 INTRUDUCTION - English 1

1 State of Art **3**

1.1 Robots 3

1.1.1 Definition 3

1.1.2 Overview and evolution in the last 50 years 3

1.1.3 Review of the humanoid robots 5

1.1.4 Other Models 14

1.1.5 Main technological improvement of individual components 15

1.2 State of the Art - Modeling 16

1.2.1 Introduction 16

1.2.2 Biped Gait 16

1.2.3 Equilibrium Criteria 17

1.2.4 Zero Moment Point and Foot Rotation Index 18

1.2.5 Center of Pressure 20

1.2.6 Ground Reaction Forces 20

1.2.7 Statically and Dynamically Balanced Gait 21

1.3 Overview of Control Strategies 21

1.3.1 Walking Control 21

1.3.2 Inverted Pendulum Method 23

1.3.3 Passive-Dynamic Walkers 24

1.3.4 Other Control Strategies 24

2 Modeling **27**

2.1 The Mechanical models 27

2.1.1 Model Analysis 28

2.1.2 Dynamic Equations 28

2.1.3 Coordinate re-Labeling Operator 29

2.1.4 Projection Operator 31

2.2 *Knee* Model 34

2.3 *Dribbel* Model 37

2.4 *Compass* Model 39

2.5 Step Model 41

3 Optimization 45

3.1 Optimization Algorithm 45

3.2 Optimization algorithm - General discussion 50

  3.2.1 The Curves routine 51

  3.2.2 The Costfun routine 52

  3.2.3 The Projection routine 52

  3.2.4 The Model routine 53

  3.2.5 The Constraints routine 54

  3.2.6 Optimization - Issues 54

4 *Compass* Model: Optimization and Simulation 57

4.1 Overview 57

4.2 SVD - Singular Value Decomposition 57

4.3 Research of Passive Dynamic Walking (PDW) 61

4.4 PDW - Optimization Part 1 61

  4.4.1 Results Part 1 63

  4.4.2 Simulation and comparing - Part 1 64

4.5 PDW - Optimization Part 2 64

  4.5.1 Results Part 2 65

  4.5.2 Simulation and comparing Part 2 66

5 Kneed Models: Optimization 69

5.1 Optimal Grade of Polynomials 69

5.2 Optimization Results - General 72

  5.2.1 K parameter 72

  5.2.2 Degenerate strikes 72

  5.2.3 Optimizations Parameters 73

  5.2.4 Algorithm to determine the number of possible SMs. 74

5.3 Group 1 - *Dribbel* Optimizations 75

  5.3.1 *Dribbel* - 2 strikes $SM1*$ 75

  5.3.2 *Dribbel* - 3 strikes $SM2*$ 76

5.4 *Knee* Optimization - Overview 77

  5.4.1 Group 2 - 2 strikes SMs 77

  5.4.2 Group 3 - 3 strikes SMs 81

  5.4.3 Group 4 - 4 strikes SMs 87

  5.4.4 Group 5 - 5 strikes SMs 90

5.5 Summarizing the obtained results 93

5.6 Comparison between best models 95

6 Trajectory Tracking Control 97

6.1 *Dribbel* and knee-locking mechanism 97

6.2 Uncontrolled Simulation 99

6.3 Controlled motion 100

  6.3.1 Dynamic Reference 101

  6.3.2 Optimal control parameters 102

6.4 Simulation with optimal control parameters 106

6.5 Compare with other movement trajectories 107

7 Global stability of Dribbel 111
7.1 Introduction 111
7.2 Limit Cycle verification 111
7.3 Global Stability 112

CONCLUSIONS 115

BIBLIOGRAFY 117

LIST OF FIGURES

1.1 Wabot 1 6
1.2 ASIMO 7
1.3 ISAMU 8
1.4 QRIO 9
1.5 Spring Flamingo 11
1.6 HRP-4 13
1.7 WABIAN 14
1.8 Phases of dynamic bipedal gait. 17
1.9 Supporting area during single and double support phase. 18
1.10 Ground projection of Center of Mass (GCoM). 18
1.11 Forces and moments during single support phase. 19
1.12 The possible relative position of ZMP and CoP: dynamically balanced gait (left), unbalanced gait (the system as a whole rotates about the foot edge and overturns) (middle), and intentional foot-edge equilibrium (right). 19
1.13 Inverted Pendolum method 22
1.14 Passive Dynamic Walker 23

2.1 Knee mechanical model. 27
2.2 Dribbel walking motion of the gait. The most important event that characterize its dynamic are highlighted. 28
2.3 Changing of roles between the legs in correspondence of the ground strike (left) and not changing in correspondence of the knee strike (right). . . . 29
2.4 Snapshot of the motion of Knee model with circular feet. 34
2.5 Knee mechanical model. 36
2.6 Knee walking motion of the gait. There are highlighted the most important event that characterize its dynamic. 36
2.7 Dribbel mechanism 37
2.8 Dribbel mechanism 38
2.9 *Dribbel* walking gait 39
2.10 Compass like bepedal walker. 40
2.11 Compass mechanical model. 40
2.12 Compass walking gait. 41
2.13 Knee walking motion of the gait. There are highlighted the most important event that characterize its dynamic. 42

3.1 Walking Cycle. 45

3.2 Pointcaré Map. 47

4.1 Comparison of the hip velocity before ($\dot{q}_-$) and after ($\dot{q}_+$) impact for two impact angles q_4. 59
4.2 Maximum Singolar Value. 60
4.3 Minimum Singolar Value. 60
4.4 Trend of the singular values with mH/m=1. 60
4.5 Optimal position of the coordinates of the Compass model. Opt. 1. . . . 63
4.6 Optimal velocities of the coordinates of the Compass model. Opt. 1. . . 63
4.7 Stick diagram of the optimal gait. Opt. 1. 63
4.8 Comparison between the simulation results and optimization results of the compass like bipedal model (q_o, are the optimized coordinates and q_s are the simulated ones). 64
4.9 Optimal position of the coordinates of the Compass model. Opt. 2. . . . 65
4.10 Optimal velocities of the coordinates of the Compass model. Opt. 2. . . 65
4.11 Stick diagram of the optimal gait. Opt. 2. 66
4.12 Comparison between the simulation results and optimization results of the *Compass* (q_o, are the optimized coordinates and q_s are the simulated ones). 67

5.1 Diagram that shows the minimum number of parameter n that is useful for a proper optimization. 71
5.2 Comparison between the two optimizations with model 2 described before. 71
5.3 Histogram of the error between the two optimization with model 2 described before. 71
5.4 Graph with the areas of the first part and second part of the gait highlighted. 72
5.5 Stick Diagram representing the shape of the gait. 72
5.6 Example of result of an optimization routine. The SM is providing 5 strikes. 73
5.7 Trend of the curves representing the position of the links of the mechanical system (Dribbel) with $SM1*$. In the figure are represented the instants in correspondence of which the strikes happen. 76
5.8 Stick Diagram representing the shape of the gait. 2 strikes $SM1*$ 76
5.9 Histogram representing the cost of actuation with the parameter K for each of the joint actuators. It's referring to the optimization with $SM1*$ 77
5.10 Trend of the curves representing the position of the links of Dribbel with $SM1*$. In the figure are represented the instants in correspondence of which the strikes happen. 78
5.11 Stick Diagram representing the shape of the gait. 3 strikes $SM2*$ 78
5.12 Histogram representing the cost of actuation with the parameter K for each of the joint actuators. It's referring to the optimization with $SM2*$ 79
5.13 Trend of the positions of the links with 2 strikes $SM1$. In the figure are represented the instants (circles) in correspondence of which the strikes happen. 79
5.14 Stick Diagram representing the shape of the gait. 2 strikes $SM1$ 79
5.15 Histogram representing the parameter K. The numbers from 3 to 6 are the torques relative to the i-th joint. 2 strikes $SM1$ 80

5.16 Trend of the positions of the links with the $SM2$. In the figure are represented the instants (circles) in correspondence of which the strikes happen. 80
5.17 Stick Diagram representing the shape of the gait. 2 strikes $SM2$ 80
5.18 Histogram representing the parameter K. The numbers from 1 to 4 are the torques relative to the i-th joint. 2 strikes $SM2$ 81
5.19 Trend of the positions of the links with the $SM1$. In the figure are represented the instants (circles) in correspondence of which the strikes happen. 83
5.20 Stick Diagram representing the shape of the gait. 3 strikes $SM1$ 83
5.21 Trend of the positions of the links with 3 strikes $SM2$. In the figure are represented the instants (circles) in correspondence of which the strikes happen. 83
5.22 Stick Diagram representing the shape of the gait. 3 strikes $SM2$ 83
5.23 Trend of the positions of the links with 3 strikes $SM3$. In the figure are represented the instants (circles) in correspondence of which the strikes happen. 84
5.24 Stick Diagram representing the shape of the gait. 3 strikes $SM3$ 84
5.25 Trend of the positions of the links with 3 strikes $SM4$. In the figure are represented the instants (circles) in correspondence of which the strikes happen. 84
5.26 Stick Diagram representing the shape of the gait. 3 strikes $SM4$ 84
5.27 : Histogram representing the cost of actuation of the torques singularly, in which is highlighted the share between the two parts of the gait. It's referring to the optimization with $SM2$. 85
5.28 Histogram representing the cost of actuation of the torques singularly, in which is highlighted the share between the two parts of the gait. It's referring to the optimization with $SM4$. 85
5.29 Histogram representing the cost of actuation of the torques singularly, in which is highlighted the share between the two parts of the gait. It's referring to the optimization with $SM1$ 87
5.30 Trend of the curves representing the position of the links of the mechanical system with the $SM1$. In the figure are represented the instants in correspondence of which the strikes happen. 89
5.31 Stick Diagram representing the shape of the gait. 4 strikes $SM1$ 89
5.32 Trend of the curves representing the position of the links of the mechanical system with the $SM2$. In the figure are represented the instants in correspondence of which the strikes happen. 89
5.33 Stick Diagram representing the shape of the gait. 4 strikes $SM2$ 89
5.34 Trend of the curves representing the position of the links of the mechanical system with the $SM3$. In the figure are represented the instants in correspondence of which the strikes happen. 90
5.35 Stick Diagram representing the shape of the gait. 4 strikes $SM3$ 90
5.36 Histogram representing the comparison between the K parameters of the optimizations with $SM2$ and $SM3$. 91
5.37 Trend of the curves representing the position of the links of the mechanical system with the $SM3$. In the figure are represented the instants in correspondence of which the strikes happen. 92

5.38 Stick Diagram representing the shape of the gait. 5 strikes $SM3$ 92
5.39 Trend of the curves representing the position of the links of the mechanical system with the $SM4$. In the figure are represented the instants in correspondence of which the strikes happen. 93
5.40 Stick Diagram representing the shape of the gait. 5 strikes $SM4$ 93
5.41 Values of the OFs of the best optimization of each group. 95
5.42 Comparison between the best SMs of Dribbel and Knee optimizations. 95
5.43 Histogram reporting the K parameters of the $SM1*$ with Dribbel mechanism. 96
5.44 Histogram reporting the K parameters of the $SM1$ with Knee mechanism with 3 strikes. 96
5.45 Trend of the curves representing the position of the links of the mechanical system (Dribbel) with the $SM1*$. In the figure are represented the instants in correspondence of which the strikes happen. 96

6.1 The four phases of the down-hill walking with Dribbel 98
6.2 Comparison between the simulation of the uncontrolled *Dribbel*, and the optimized curves. Dash line are the optimized curves, and solid line is the simulation. 99
6.3 Problem of trajectory tracking for hibrid mechanical systems. 100
6.4 Dynamic reference mechanis. 101
6.5 Particular of the knee strike of a simulation result. 102
6.6 Surface representing the work of the actuators varying the control input parameters. 103
6.7 Surface representing the work of the actuators varying the control input parameters. It's a detail of the figure 6.6. 104
6.8 Surface representing the RMS of the error between simulated and reference curves varying the control input parameters. 105
6.9 Trend of the simulated and reference coordinates with optimal control law. 106
6.10 Error between the real positions and the reference of the three coordinates.107
6.11 Work per step; the three columns azure, purple and pink are represented the work of the toque 3, 5 and 6 respectively. 107
6.12 Trend of the curves representing the optimizaed coordinates. 108
6.13 Trend of the simulated and reference coordinates with optimal control law befined in the previous pharagraph. 108
6.14 Work per step; the three columns azure, purple and pink are represented the work of the toque 3, 5 and 6 respectively. 108
6.15 Trend of the curves representing the optimizaed coordinates. 109
6.16 Trend of the simulated and reference coordinates with optimal control law befined in the previous pharagraph. 109

7.1 Limit Cycle Diagram. The dark marks indicate the state value of the steps initial conditions. 112
7.2 Basin of attraction $\Delta\dot{q}_6$ - $\Delta\dot{q}_5$ 113
7.3 Basin of attraction $\Delta\dot{q}_6$ - $\Delta\dot{q}_3$ 113
7.4 Basin of attraction $\Delta\dot{q}_5$ - $\Delta\dot{q}_3$ 114

LIST OF TABLES

2.1 Scheme for the evaluation of number of possible SMs for the imposed number of strikes . . . 30
2.2 Physical parameters of Knee model. . . . 35
2.3 Physical parameters of Dribbel model. . . . 38
2.4 Physical parameters of *Compass*. . . . 41
2.5 Nomenclature and symbolism used to completely determine a Step Model. 43

3.1 Main Constaints of the minimization problem . . . 48
3.2 Main Constaints of the minimization discetized problem . . . 49
3.3 Parameters of the optimization routine . . . 50
3.4 Sub-routines of the minimization algorithm . . . 51

4.1 Parameters of the optimization routine 1 - Compass Model . . . 62
4.2 Physical Parameters of Compass Model . . . 62
4.3 Optimization results 1 . . . 62
4.4 Optimization results 2 . . . 65

5.1 Step Models for the definition of the optimal degree of polynomials . . . 70
5.2 Scheme for the evaluation of number of possible SMs for the imposed number of strikes . . . 78
5.3 Scheme for the evaluation of number of possible SMs for the imposed number of strikes . . . 82
5.4 Tables representing the values of velocities just before the knee1 impact, and just after that. The values refers to the optimization results with the SM2. . . . 86
5.5 Tables are reporting the velocity values just before and just after the knee2 impact. The values are referred to the optimization with SM2. . . 86
5.6 Scheme for the evaluation of number of possible SMs for the imposed number of strikes . . . 87
5.7 Scheme for the evaluation of number of possible SMs for the imposed number of strikes . . . 91

INTRODUCTION

0.1 INTRODUZIONE - Italiano

In questa tesi si affronta il tema della camminata bipede in generale e nel suo specifico, in riferimento ad alcuni dei più comuni (e semplici) sistemi camminatori di cui è semplice descirverne la dinamica nel piano. I sistemi camminatori considerati nel seguito della trattazione, sono: Il sistema a 2 g.d.l. chiamato *Compass*, quello a 3 d.o.f. chiamato *Dribbel*, ed infine, un sistema a 4 d.o.f. chiamato *Knee*.

Il modello *Compass* è il modello camminatore bipede planare più semplice che si possa pensare. *È* composto da due lik (che fungono da gambe) rigidi, uniti in corrispondenza del punto di hip dal quale si diparte il busto. La massa dei due link viene concentrate nei punti di "hip" e a mezza lunghezza delle due gambe.

Il sistema può prevedere una camminata passiva in presenza di un suolo in discesa, e con una particolare distribuzione dei parametri fisici.

Il modello meccanico *Dribbel* prevede 4 link, e quindi le ginocchia, e si impone che la gamba di sostegno resti diritta, e che la gamba sollevata possa flettersi fino al momento in cui avviene la prima completa estensione ("strike" al ginocchio). Da questo momento in poi, fino alla fine del passo, il modello della camminata prevede che, attraverso il meccanismo di blocco del ginocchio, la gamba rimanga diritta e faccia *sí* che il sistema evolva fino alla fine come il sistema *Compass* descritto il precedenza.

Il modello *Knee*, prevede anch'esso 4 link ma non prevede il blocco della gamba di sostegno per tutta la durata del passo, n*é* il blocco del ginocchio al primo strike. Tutti e tre i modelli presentano la medesima descrizione dell'impatto al suolo, oltre alla definizione delle coordinate ottime visto come problema di minimizzazione di una data funzione obiettivo, e al controllo del sistema di tipo inseguimento di traiettoria.

Il modello di contatto è stato implementato considerando le superfici a contatto idealmente rigide. Si è inoltre suppesto che la condizione di entrambe le gambe a terra sia istantanea. Questa permette di definire due fasi della camminata ben distinte. La prima, descritta dalla dinamica continua, durante la fase di oscillazione della gamba che inizia con lo stacco da terra di quest'ultima a seguito dello strike al suolo del passo precedente; la seconda, descritta dalla dinamica impulsiva, quando il sistema bipede impatta con il suolo.

Con lo stesso criterio sono stati modellati gli strike che avvengono in corrispondenza delle ginocchia.

Altro minimo comune denominatore è la definizione delle coordinate ottime per un sistema bipede che percorre un tratto in discesa di pendenza 3°. In questa tesi, infatti, si è cercato il movimento del sistema più efficente in termini di energia spesa per attuare i giunti del meccanismo attraverso degli attuatori considerati comunque ideali e non

dissipativi. I sistemi sono considerati totalmente attuati con attuazione co-locata.
Il caso limite del movimento efficiente di un sistema camminatore bipede è il caso in cui il sistema evolva nel tempo senza bisogno di attuazione. Questo è il caso dei sistemi con dinamica passiva per i quali la perdita di energia meccanica associata alla dinamica impulsiva del sistema (strike al ginocchio o al suolo) è completamente sopperita dal contributo di energia potenziale dovuto al dislivello tra inizio e fine passo.
È stato dimostrato che la dinamica passiva esiste per alcuni sistemi bipedi ed in partiolare per il modello *Compass* analizzato in questa tesi. Ovviamente il comportamento passivo del sistema dipende anche dalla sua distribuzione di massa e dalla pendenza del suolo. Oltre a questi parametri fisici, il comportamento passivo si manifesta solamente con determinate condizioni iniziali (stato iniziale del sistema).
Il movimento passivo del sistema *Compass* è stato indagato tramite l'algoritmo di ottimizzazione spiegato in seguito. Il compotamento passivo è stato verificato con una simulazione del modello meccanico partendo da condizioni iniziali ottime. In aggiunta si è indagata la postura ottima che permetterebbe al modello *Compass* di minimizzare la perdita di energia cinetica all'impatto con il suolo. Per far questo si è analizzata la perdita di energia cinetica all'impatto con un'analisi ai valori singolari definendo delle direzioni di massima e minima perdita di energia al variare dello stato assunto all'istante precedente l'impatto.
In seguito si sono analizzati i modelli provvisti di ginocchia e si è cercato il loro movimento ottimo in riferimento ai parametri della camminata in analisi. La ricerca del movimento ottimo dei sistemi viene affrontata come un problema di minimizzazione di una certa funzione obiettivo che tiene conto della richiesta di coppia da parte degli attuatori co-locati rispetto alle coordinate libere.
L'algoritmo di minimizzazione ottimizza la funzione obiettivo (OF) ottenuta mediante la risoluzione della dinamica diretta del sistema attraverso la definizione delle coordinate libere (e velocità e accelerazioni) come funzioni polinomiali del tempo. In questo modo, i parametri da ottimizzare sono i coefficienti dei polinomi che definiscono le coordinate libere, oltre ai valori degli istanti temporali in cui avvengono gli strike che sono previsti nel modello del passo.
Il passo infatti è caratterizzato dal numero (e tipo) di strike, nonché dal loro ordine temporale di accadimento. Il movimento ottimo per il tipo di camminata analizzata (camminata in discesa con pendenza 3°), è risultato essere quello del modello *Dribbel* in presenza di due strike, il primo in corrispondenza del ginocchio della gamba che oscilla, e il seecondo al suolo a fine del passo.
Il risultato dell'ottimizzazione è il movimento ottimo in termini di energia richiesta agli attuatori. In seguito si è proceduto all'analisi della stabilità in grande della camminata mediante simulazione numerica attribuendo come riferimento del controllo degli attuatori, le curve ottime definite in fase di ottimizzazione. L'inseguimento delle curve ottime è stato realizzato mediante un semplice controllore PD (proporzionale e derivativo).
I coefficienti proporzionale e derivativo del controllo sono stati scelti in modo da minimizzare in lavoro compiuto dagli attuatori. La determinazione e taratura dei parametri è stata effettuata considerando il sistema che evolve partendo dallo stato iniziale ottimo definito dalla routine di ottimizzazione implementata precedentemente. I parametri trovati sono dunque i parametri ottimi che permettono al sistema di inseguire il suo riferimento minimizzando il lavoro richiesto dagli attuatori. Con la legge di controllo appena definita, si analizza la stabilità del sistema in grande andando a simulare la

camminata perturbandone lo stato iniziale nell'intorno dello stato iniziale ottimo. Le basi di attrazione definite per l'analisi di stabilità mostrano come il sistema controllato sia molto robusto riuscendo a gestire perturbazioni anche di entità rilevante. Va detto che in questa fase, non sono state implementate le saturazioni che caratterizzano gli attuatori reali.

0.2 INTRUDUCTION - English

This Thesis was developed in Japan during my stage at JAIST (*Japan Advanced Institute of Science and Technology*). The purpose of the thesis was to analyse and develop an efficient walking movement for the walking humanoids robots proceeding down-hill. The main feature of such robots is the so-called hibrid dynamics i.e. the congiunction between continuous dynamics equations of the links of the robots during the single-support phase and impulsive dynamic equations in correspondence of the strikes that happen during the gait.
The specific goals of this thesis are as follows.

- Develop a systematic way to construct an optimization algorithm in order to find the most natural trend of coordinates for the walking robots treated in this thesis.
- Investigate the presence of the passive dynamic walking and verify the optimization results trough simulation.
- Investigate the optimal movement of bipedal mechanisms with knees in order to testify their natural walking and applying a control law in order to simulate the walking down-hill, designing an energy efficient controller.

The search for the most efficient walking behavior has been faced combining the hybrid dynamics with an optimization algorithm that allows to determine the time histories of the free coordinates that minimize a specific cost function related to the torques of the actuators.
The optimization algorithm is adaptable to the three different humonoids robots considered in this thesis: the *Compass* model, the *Dribbel* model and the *Knee* model, and has shown that the best humanoid robot for walking down-hill is the *Compass* one, that is able to walk down-hill without the necessity of actuations i.e. the so-called passive dynamic walking.
Only considering the kneed models, *Dribbel* is the best for an efficient down-hill walking and for this model it was introduced and an easy control law to let the system walk. In fact, for the chosen characteristics of the model, no passive dynamic walking was found, and so, it requires a control law in order to not falling down. The control law was a trajectories tracking control law that uses like reference, the optimal trajectories coordinates defined with the optimization algorithm. In the end, was tested the stability of the walking perturbing the velocities of the free coordinates and observing its basin of attraction. The results showed that the designed control law is really robust because the basin of attraction are really large specially along some specific coordinates.

CAPITOLO 1

State of Art

1.1 Robots

1.1.1 Definition

Robotics is a branch of science and engineering dealing with the study of robots. A robot is a virtual or mechanical artificial agent. In practice, it is usually an electro-mechanical machine which is guided by computer or electronic programming, and is thus able to do tasks on its own. The mechanics of the robot, in the strict sense, is the geometric, kinematic, dynamic and functional study of the robot. Typical arguments are the determination of the geometrical structure of the robots and their components, the determination of the trajectories, velocities and accelerations, the determination of the forces and torques necessary to achieve the desired movements. In recent years, robotics feeds relating to the advancement of innovative systems and mechatronics, and due to developments in miniaturization, has left the bounds in the industry to integrate, more and more, into social and relational life of individuals. According to the report World Robotics 2010 Service Robots published in mid-September by the Statistics Department of IFR (International Federation of Robotics), at the end of 2009 there were 76,600 commercial robots non-manufacturing active worldwide, with a total value of 13.2 billion dollars. Of these 30% (23,200 units) was used for defense, 25% of applications for agricultural or livestock (mainly milking) and 8% were cleaning robots and robot for medical use. To follow with 7% were robots for underwater activities, with 6% , both those used in the construction and demolition and those mobile robot platforms for general use, with 5%, the robots used in logistics and finally, with 4% those for rescue and safety. To the service commercial robots are then added those for household use that, at the same date of 2009, amounted to about 5.6 million units: in almost all of these cases, they are entertainment robots, robot vacuum cleaner and a small part, is the robot mower. Still limited is the market for robots to assist the handicapped, however, that, according to the report of the IFR, is expected to grow substantially over the next 10 years. Will increase, in the near future, the market for robots for personal transportation and for security and home surveillance.

1.1.2 Overview and evolution in the last 50 years

Around the world, a world leader in robotics is of course Japan, South Korea may follow, but also America and Europe are challenging for the top three places with ups and downs. There are many projects that are especially made for industrial robotics and biomedical robotics.

- U.S.A. military and space robotics - biomedical robotics
- EUROPE: Industrial robotics, biomedical robotics
- JAPAN: Industrial robotics - Personal robotics - Humanoids
- SOUTH KOREA- Humanoids -Services robotics - Personal robotics

Japan

The Japanese government has provided substantial aids to support the development of robotic technologies, and in general, of the industrial activities. Research in robotics has been driven primarily by MEXT (Ministry of Education, Culture, Sports and Technology) by METI (Ministry of Economy and Industry) and even the Ministry of Interior, Posts and Telecommunications. For this reason, research robotics in Japan is very active in all fields, especially in the field of humanoid robots and the human-robot interaction. The industry, however, is very active in developing industrial robots, advanced and increasingly independent, by using A.I. and advanced sensors. The government for its part, has been active in promoting and supporting various programs with the aim of developing more and more not only to robotics but also the industrial activity associated and induced. However, it seems important to emphasize that Japan can put forward about the double of European researchers, but that the quality of the researchers on the study level and qualification is lower than America or Europe. The largest of these project in the recent years, plans to send humanoid robots to the moon by il2020. At the Waseda University in Tokyo this project is led by Katsuhiko Shirai and the cost is 2.2 billion dollars. By 2015 should be placed in orbit around the moon, robots that would be able to monitoring and studying the moon. Then by 2020 there would be the descent on the moon of the droids that would be laid near the lunar south pole. Weighing approximately 330 kg and equipped with powerful tracks, the robot is energized by solar panels due to some envelopes.

South Korea

In South Korea, the robotics research are stimulated by massive government investments in three ministries MIC, MOCIE and MOST, respectively, the Ministry of Information and Communication Ministry of Commerce, Industry and Energy, Ministry of Science and Technology that are developed in a variety of special plans of industries. She has also been created Academic Society for Engineering Robotics, which has acquired a central role in the Korean community. It has the task of encouraging the dissemination of knowledge in robotics into other institutions to organize robotic competitions that have the purpose to create and stimulate a playful market.

United States of America

The research is on many fronts simultaneously. It has developed both in academic and government centers, both in the private industrial sector and foundations. National priorities have turned to nanotechnology, environment and information technology. The military research of the DARPA (Defense Advanced Research Program Agency) had a big increase in their scope and it may extend to security. Even in space applications, as is traditional in the USA, is deeply felt, and, in these recent years, there is the project developed jointly by NASA and General Motors, which has generated ROBONAUT the first robot in space.

Europe

Europe currently represents an interesting situation in full and complete development both as a market and as a researcher. In fact, the new European Union has opened up new potential for market expansion and then the overall well-being of robotics. One of the aims is to increase the integration between the countries of the union, another is to encourage industry to innovate in order to increase overall competitiveness. For this, were born EURON (European Robotics Network) and EUROP (European Robotics Platform) that seeks to link the industrial and university programs in order to allow the European potential to express themselves fully in the global competition of robotics. The most important industries of Europe are ABB (Automation Brown Boveri) and KUKA ROBOTIC. European companies are used to supplies outsources of specific parts such as motors and sensors, in contradiction, for example, to the Japanese companies that emphasize the vertical integration within them.

1.1.3 Review of the humanoid robots

The modern era of humanoid robotics began in 1973 with HIROKAZU KATO, a professor of Waseda University (Tokyo). He oversaw the construction of a Wabot, the first humanoid robot. Since 1990 many projects have been launched especially humanoid robots in Japan, Europe and the United States. In Japan, as well as university and research centers, including the Honda Corp has dealt with success of this argument by presenting Asimo. Honda has built the first artificial legs in 1986. Even Sony has been dedicated to projects of biped robots. In the U.S.A., larger projects have been developed at the University of Utah, Vanderbilt University, NASA and MIT. In South Korea is studied, at this time, the bipedal walking robot that is able to interact with humans. In Europe, the most radical technological innovations come from nature. The biorobotics and in particular the biometric robotics are areas where were studied biological systems and developed technologies that replicate the solutions devised taking inspiration from nature of animals and even plants. It 's the case for example of the OCTOPUS project coordinated by the Scuola Superiore Sant'Anna in Pisa, where the study of the common octopus is leading to the creation of new robotic technologies with variable stiffness, and is leading to the construction of a robotic arm solely with innovative materials, but able to perform actions of achievement and taking. The Politecnico di Torino, after producing Isaac, has been working from years to organize the Robocup with the aim to spread the interest in this type of study and be able to design a humanoid team that can beat our National football team! Germany for its part, has designed RunBot who beat the world record in speed which was held from Spring Flamingo created by MIT. The problem of building a humanoid robot is very complex. In fact, analyzing the human body from the point of view of the complexity of motion, you get about 92 degrees of freedom. This is why people often prefer to divide the problem into sub-problems and focus on the implementation of sub-parts of humanoid robots. Future promises the presence of many robots in everyday life. Therefore it is very important to study the perhaps most human characteristic of all: the uniquely human features of flexibility and adaptability.
A number of the most successful biped robots is presented in the following:

WABOT-1

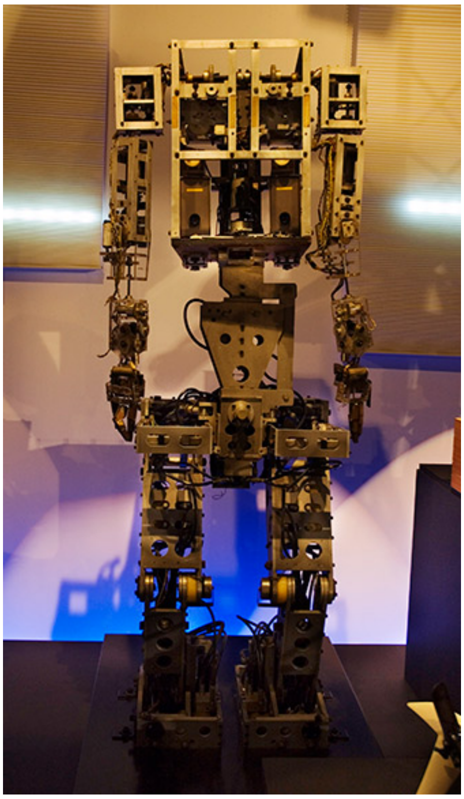

Figura 1.1: Wabot 1

WABOT-1 was the first modern prototype humanoid robot. Its name derives from a contraction of Waseda and robots.It 'was built under the supervision of Hirokatsu Kato in the Department of Science and Engineering of the Waseda University in Tokyo in 1973. This robot is able to move with small steps with two legs, grasp simple objects with two hands and is able to execute some basic speech interaction with people. It has, in fact, a control system of the walk, a vision system and a voice system. It moves in the environment thanks to the ability to assess directions and distances from the objects using external sensors, including artificial eyes. Grab and transport objects using hands with tactile sensors. Communicate with people in Japan using artificial mouth and ears.

ASIMO

Asimo is a humanoid robot who has overcome the challenges and obstacles of walking technology to tour the world and demonstrate his amazing feats of human activity. ASIMO, a humanoid robot, was created by the Honda Motor Company, a producer of cars, motorcycles and power products, as a new challenge in mobility — the development of a two-legged humanoid robot that can walk. Standing at 4 feet 3 inches and

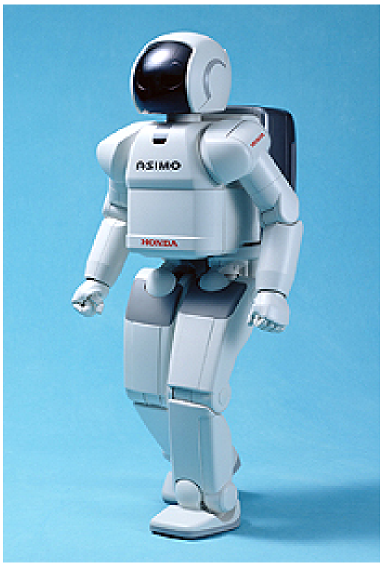

Figura 1.2: ASIMO

weighing 119 pounds, the robot resembles a small astronaut wearing a backpack and can walk or run on two feet at speeds up to 3.7 mph.

The Concepts Behind Asimo Back in 1986, the main concept behind Honda's robot was to create a robot with more viable mobility that would allows robots to help and live in harmony with people. Research began by envisioning the ideal robot form for use in human society. The idea was that the robot would need to be able to maneuver between objects in a room and be able to go up and down stairs. For this reason it had to have two legs, just like a person. In addition, if two-legged walking technology could be established, the robot would need to be able to walk on uneven ground and be able to function in a wide range of environments. Although considered extremely difficult at the time, Honda set itself this ambitious goal and developed revolutionary new technology to create a two-legged walking robot.

The Challenge of Two-Legged Walking Technology To achieve stable walking, the following issues needed to be addressed:

- Not falling down even when the floor is uneven.
- Not falling down even when pushed.
- Being able to walk stable on stairs or slopes.

This is achieved by three posture controls that achieve stable walking. The first is Floor Reaction Control which absorbs irregularities in the floor and controls the placement of the soles of the feet when falling is imminent. For example, if the tip of the robot's toe steps on a rock, the actual center of ground reaction shifts to the tip of the toe. The floor reaction control then causes the toe to rise slightly, returning the center of ground reaction to the target ZMP, or Zero Moment Point when the total inertia force is zero. The target ZMP control, the next posture control, operates to prevent the robot from falling if the robot leans too far over. The target ZMP control maintains the robot's stability. For example, if the robot starts to fall forward, its walking speed is accelerated forward from the ideal walking pattern. As a result, the target ZMP is shifted rearward from the actual floor reaction action point and a rearward falling force is created which corrects the robot's position. The final posture control, the Foot Planting Location Control, uses side steps to adjust for irregularities in the upper torso caused by target ZMP control. This stepping placement control idealizes the stride to ensure the ideal relationship between torso speed and length of stride is maintained.

ISAMU

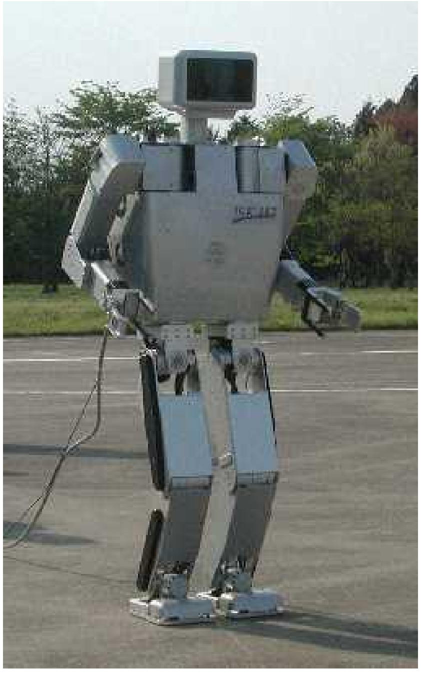

Figura 1.3: ISAMU

Isamu is a joint project of the University of Tokyo's Jouhou System Kougaku Laboratory (JSK Lab) and the Aircraft and Mechanical Systems Division of Kawada Industries, Inc. (Tokyo, Japan). To date, the two organizations have teamed up to build two Isamu robots - dubbed H6 and H7. The purpose of the project is to develop test-beds for research into a wide range of applications for human interactive motion control technology. For example, Kawada Industries intends to use Isamu as a platform to explore potential commercial applications in markets like construction systems, disaster relief, aids for the handicapped, rehabilitation and training devices, and amusement. In an effort to mimic a degree of human-like movement, Isamu is endowed with thirty-two degrees of freedom – six for each leg, one for each foot (toe joint), seven for each arm, one for each gripper, two for the neck, and three for the eyes. The onboard computer, equipped with dual 750MHz Pentium III processors running RTLinux, provides real-time servo and balance compensation, and coordinates the robot's 3D vision and motion-planning software modules.Thanks to an ample battery pack, a wireless Ethernet interface, and the powerful onboard computer, Isamu can operate without the need for external cables or constant human intervention. A joystick can be used to control the robot's movements when direct human control is desired. It is able to walk back and forth shifting of 25 cm at every step. Isamu is 1.5 meters high, weighs 55 kg and walks at speed of 2km / h. Isamu's bipedal walk control system software was developed by the Inoue-Inaba Laboratory, while the hardware and robotics structures, including the servo-based level control system, were developed by Kawada Industries. Kawada applied aircraft technologies to the body frame, resulting in a strong and light structure.

QRIO

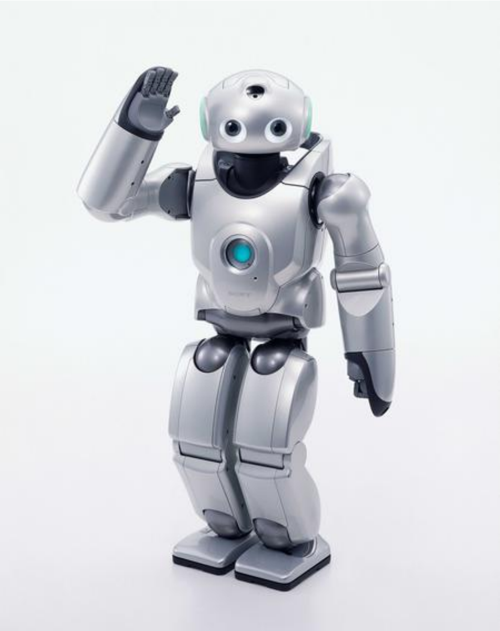

Figura 1.4: QRIO

QRIO is a humanoid robot, equipped with the latest in advanced recognition, motional control communications, information technology, and artificial intelligence. Its programming allows it to protect itself should it lose balance, and should it fall, it checks front and back, left and right, before getting up without any assistance. It can distinguish individual faces and voices, and can learn and memorize new words. Sony explains that QRIO can also communicate with people based on internal judgments, and express feelings through movements, conversations, and the use of a lighting system.Looking like child astronauts, they can balance and dance with motor control so smooth and fluid as to make grown men weep. In other respects, QRIO is a little disappointing. His walking marks an improvement in robot technology, but it is still much more of a shuffle than a stride. There are people doing more impressive robot control. Intelligent servo actuators enable Qrio to walk on two feet, dance, climb and descend stairs, not fall over when shoved, and even pick itself up when it takes a tumble. Using twin CCD (charge coupled device) cameras, it can also recognize and identify faces. Equipped with seven microphones and a speaker, Qrio is able to identify voices, talk, sing, and understand about 20,000 words. It can also exhibit some limited emotional responses, according to Sony. QRIO can walk on two feet and dance dynamically. To make its arms and legs strong, and yet able to move fluidly, it was necessary to develop an entirely new joint actuator. The realization of this Intelligent Servo Actuator (ISA) made it possible to build a robot with compact body design that could move its body smoothly and dynamically. QRIO moves with dynamic walking. Static walking means the robot keeps its center of gravity within the zone of stability – when the robot is standing on one foot, its center of gravity falls within the sole of that foot, and when it is standing on two feet it falls within a multi-sided shape created by those two feet – causing it to walk relatively slowly. In dynamic walking, on the other hand, the center of gravity is not limited to the zone of stability – in fact it often moves outside of it as the robot walks. People move using dynamic walking. It is equipped with technology that uses a wide range of sensors to detect changes in the walking surface and respond accordingly. QRIO determines the condition of the walking surface using four pressure sensors in the sole of each foot to gather data on the amount of force being received from the walking surface. If pushed by someone, QRIO will take a step in the direction it was pushed to keep from falling over. The control system senses that it has been pushed through the pressure sensors in the soles of its feet and its position sensors, and acts to maintain stability. It can detect an outside force acting on it from front, back, right or left. When QRIO determines that its actions will not prevent a fall, it instinctively sticks out its arms, swivels its hips, and assumes an impact position. At the same time, the control system instantaneously commands the servos in the joint actuators to relax slightly. In this way it lessens the shock of the fall, enabling it to survive unscathed.

Spring Flamingo

Is a planar bipedal walking robot. This robot was developed as an experimental platform for implementing:

- Various walking algorithms
- Motion description and control techniques, particularly Virtual Model Control
- Force control actuation techniques, particularly Series Elastic Actuation

The goals of Spring Flamingo were the following (all have been met):

- Walk fast (0.75 meters/second). [Fastest speed achieved was 1.2 meters/second!]

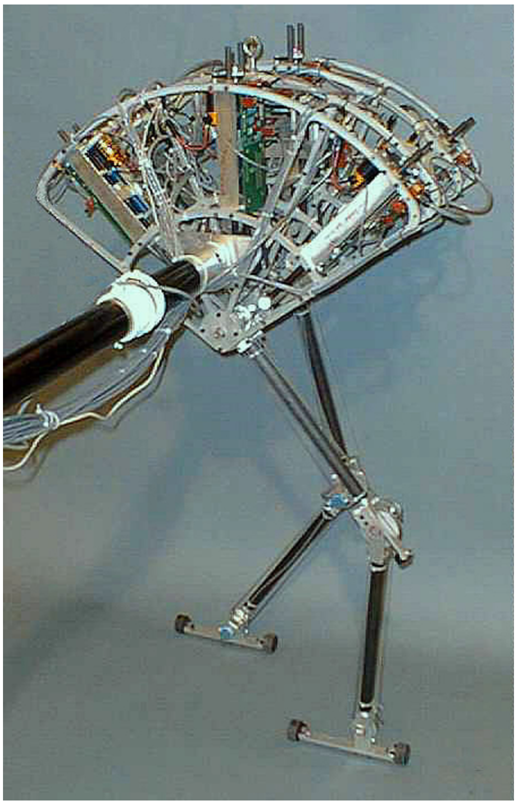

Figura 1.5: Spring Flamingo

- Walk efficiently. [Joint power – sum of torques times velocities – during walking was as low as 15 Watts!]
- Be reliable (work 9 out of 10 attempts). [Over 200 successful demos covering over 15 miles of walking!]
- Have a large margin of stability and be robust to small disturbances (reasonable pushes) [Recovered after being wacked by a pugil stick!]
- Be confident looking. [Fairly graceful looking when walking well.]
- Become a robotic workhorse - a robot which can be reliably used to perform experiments without breaking. [Operational for over 3 years before breaking a leg! Will be operational longer once leg is fixed.]
- Teach us how feet and actuated ankles can help in bipedal walking. [Taught quite a bit! See papers below.]

Spring Flamingo was designed, built, and controlled by Jerry Pratt in 1996-2000. The actuators were based on a design and prototype by Mike Wittig done for his Undergraduate Thesis in 1995-1996. Robert Ringrose helped with the development software which was a modification of his creature library and other lab simulation software.

Dave Robinson helped with design advice, foot design, and machining. Dan Paluska helped with assembly. Ann Torres helped with machining and named the robot based on its appearance. However, Spring Flamingo doesn't walk like a flamingo, nor is it intended to. The robot has an actuated hip, knee, and ankle on each leg. An un-actuated boom constrains Spring Flamingo's roll, yaw, and lateral motion thereby reducing it to a planar robot. All of Spring Flamingo's motors are located in its upper body, with power being transmitted to the joints via cable drives. Series Elastic Actuation is employed at each degree of freedom, allowing for accurate application of torques and a high degree of shock tolerance. The maximum torque that can be applied to the hips and ankles is approximately 16 Nm while approximately 24 Nm can be applied to the knees. The force control bandwidth we achieve is approximately 20 Hz. Spring Flamingo weighs in at approximately 30 lbs (13.5 kg) and stands 3 ft (90 cm) tall. Rotary potentiometers at the hips, knees, ankles, and boom measure joint angles and body pitch. Linear compression springs are located in the actuators to implement Series Elastic Actuation. Linear potentiometers measure the spring compression. In all there are six actuators and thirteen sensors on Spring Flamingo. We have implemented simple walking algorithms for walking on flat terrain. With these algorithms, we have successfully compelled the robot to reliably take consecutive un-aided laps as shown in the MPEG video below. As of April 8, 1998, we have developed algorithms for sloped terrain up to 15 degrees, as shown in the MPEG video below. As of Summer 1999 we have developed walking algorithms for fast walking up to 1.2 meters per second. Some of these algorithms exploit the natural dynamics of the robot to allow for simpler control with a more graceful result.

HRP-4

Japan has added another soldier to its humanoid robot army following last year's fembot supermodel.. The HRP-4 is the latest edition in the state-backed humanoid project. It's leaner, lighter, and can balance itself with yogic ease.Developed by bridge builder Kawa Industries and the National Institute of Advanced Industrial Science and Technology (AIST), the HRP-4 can stand on one leg, track faces and objects, and respond to voice commands. HRP-4 sports a RoboCop look, but it's more C-3PO. Designed under the theme of a slim athlete, it weighs a mere 86 pounds including battery. That's about 9 pounds less than its sister bot HRP-4C, which made waves last year modeling a dress at a bridal fashion show in Osaka, as well as Japan Fashion Week in Tokyo. HRP-4 stands nearly 5 feet tall and has 34 moving joints, with seven in each arm, as well as fingers than can move more precisely than earlier HRP models. Each arm has a load capacity of about 1 pound. All joint motors are less than 80 watts for design safety. A compact notebook computer can be installed in HRP-4's back to increase onboard data processing. Kawada and AIST have previously shown off how HRP bots can be useful around the house, wielding power tools and pouring drinks. The HRP-2 Promet has been shown walking on uneven terrain and even helping install wall paneling. The video below shows HRP-4 introducing itself, showing off some moves and tracking a man's face (it stands on one leg at around 4:25). HRP-4 is the result of over a decade of research by the public and private sector in Japan, and inherits technology originally developed by Honda. The droid will go on sale for around 26 million yen (some $ 300,000; software not included) starting in January. Kawada and AIST are targeting foreign and domestic research centers and universities as potential

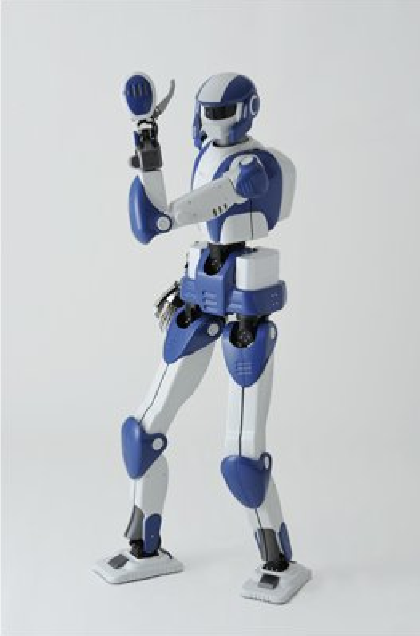

Figura 1.6: HRP-4

buyers. While I doubt they'll find many, I'm glad to see the HRP project is moving to commercialization after vast sums in investment. My fave HRP moment to date was when it performed a charming folk dance several years ago. I hope it becomes not only entertaining, but useful.

Wabian II

The acronym Wabian stands for Waseda BIpedal HumANoid. Wabian is a humanoid robot equipped with a system control, capable of replicating the human walking. It uses a sophisticated system of balance that, by coordinating the movement of the legs and torso, is able to keep it in balance. The walk is balanced by using the movement of the trunk. The movements are calculated offline by a method of learning. WABIAN has a compliance control of the joints. The joints have a high damping coefficient for shock absorption. The purpose with Wabian is to develop the mechanism for monitoring the movement of human beings in terms of robotics and establish a technology base for building the personal robots of the future. Specifications of Wabot are:

- Degrees of freedom 35
- Weight 107 kg
- Height 1.66 m
- Actuators AC servomotors, DC servomotors

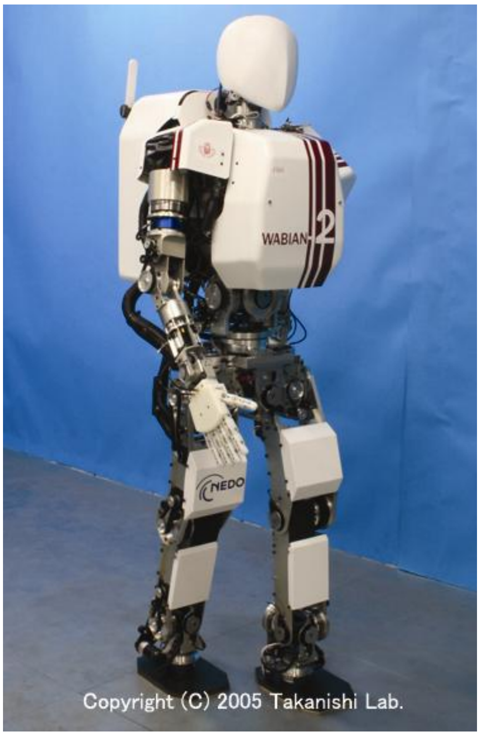

Figura 1.7: WABIAN

- control unit operations and Walking, PC / AT Pentium CPU board
- power cable
- speed 0.2 m / s for the transport of 2 kg

Wabian boasts a new swiveling pelvis and the ability to walk taking heel-to-toe strides extending its leg much like humans do. This new design allows for a much more natural looking walking motion. One of Wabian's weak points is its immense power consumption that only allows it to remain operational for 15 minutes when it is not attached to an external power source. In addition, it appears that achieving the more natural walking gate comes at a high price since Wabian is not able to negotiate even the smallest of obstacles in its path. There are different versions of Wabian. The version described here is carried out in 1995. Otherversions differ in terms of size and implementation in general. For example Wabian-R2 is able to dance through the development of coordination of the movements.

1.1.4 Other Models

In the following are reported other robots with a small description just to complete the list of the most significant models that have been made.
RunBot is a bio-mechanical system of legs. Developed in Germany in 2006 by dr. Tao Geng, it broke the record in speed, running at 3.5 leg lengths per second. It is direct

controlled by the neurons - motors of its neuronal controller that is similar to what occurs in human feet. Simulates a mechanism of synaptic plasticity that allows it to adapt its locomotion to different soils. The robotic system has three levels (biomechanical, spinal reflex and postural reflex).

ISAAC is a biped humanoid robot designed by the Politecnico di Torino in 2007. Initially, the project's purpose was purely scientific but the fields of application are various and embrace ideas from different disciplines starting with therapeutic ideas for people with disabilities. The lower limbs are in fact able to reproduce the natural movements of human legs using 6 degrees of freedom. Isaac is annually involved in RoboCup.

ATHLETE was created in 2009 by Ryuma Niiyama. This robot has real legs with a design that mimics the musculoskeletal human body shape. Athlete's legs contain seven sets of artificial muscles, with six individually designed pneumatic actuators each, like muscles of the human leg. To solve the problem of balance was mounted on the trunk an inertial measurement unit that helps the body to orient properly, while the touch sensors on each foot perceive the movements and sensations. Unlike traditional humanoid running by changing the position of their joints, Athlete moves more like a human being using their muscles and tendons to bounce on the ground and go.

MAHRU was presented in 2010. It 's a project of South Korean scientists who created the Institute for Science and Technology in Seoul. It is capable of performing various household tasks but also to interact with humans. Can dance and imitate human expressions, can do even the faces. These capabilities make it to be the first emotional robot. A humanoid capable of reacting to stimuli and stresses coming from outside.

SUREÑA 2: In date July 5, 2010 Iran, the University of Tehran, has unveiled its first humanoid robot that looks a lot like ASIMO. It weighs 45 kg, is 1.45 m tall and moves rather slowly. Iran has not dwelt in great detail during the presentation and the only thing we know is that his name derives from an ancient Persian warrior.

1.1.5 Main technological improvement of individual components

Into the field of sensors, as well as vision sensors, the challenge is based on three interrelated areas: the time response more and more high with more suitable sensors for real-time, the use of network sensors (with its fusion-data) that can provide the robot more flexibility for all types of activities, both traditional and advanced, and the use of VR (Virtual Reality) to study architecture and FSR (Sensor Fusion Structures) for the new robots. In the field of actuators, the advanced state of such equipment, is essentially based on the miniaturization of classical systems and using new materials that increase the efficiency. The class of actuators, however, is that which has undergone minor changes since its birth. The evolution that most concerns this topic is that relating to nano-materials that have allowed the design of artificial muscles used in the latest prototypes.

The key point about the structure of an autonomous robot is navigation and control. In this areas, the technologies are in possession of the U.S.A. , while for navigation in structured environments, the scepter is held by the European Union has developed many service robots. The most radical innovations draw from nature. The bio-robotics and in particular the biometric robotics are areas where are studied biological systems and are developed technologies that replicate the solutions devised by nature for animals and even plants. It 's the case for example of the OCTOPUS project coordinated by the Scuola Superiore Sant'Anna in the study of the common octopus is leading to the creation of new robotic technologies with variable stiffness, and is leading to the construction of a robotic arm solely with innovative materials, but able to perform actions of achievement and taking.

1.2 State of the Art - Modeling

1.2.1 Introduction

The basis for current humanoid walking research has been laid by Vukobratovic in 1969 [1] who was one of the first to analyze biped walking [2] and establish criteria for balanced gait [3]. Since then, most research on biped walking is rooted in these fundamental investigations. Trying to implement human-like locomotion capabilities for robots, researchers have always been torn between a technological approach and a biological approach. The former relies on concepts and techniques known from robotics, where abilities are realized departing deliberately from the solution chosen by the natural archetype. This approach can either be motivated by the attempt to find a better solution or a lack of comprehension of nature. The biological approach on the other hand starts by thoroughly analyzing the functioning of animals or humans. These mechanisms are then adapted and translated into algorithms understandable to machines. Information processing in animal and human brains is rather complex and an analysis is often not possible with current technology; therefore assumptions on the functioning of natural signal processing can be validated by implementing the concept in a robot and observing its effect. Hence, there is a mutual benefit of a collaboration for engineering, biology and neuroscience. This chapter gives a condensed summary of the state of the art in humanoid biped walking after more than three decades of research. Starting with an analysis of human gait, Sec 1.2 introduces some notions commonly used in humanoid walking and criteria for balanced gait. An overview of the most important control strategies is than given in Sec. 1.3.

1.2.2 Biped Gait

From the technical point of view, humanoid gait is often divided into different phases. This discrimination is made, as bipeds show very different dynamical properties depending on the number of ground contact points and the contact type. As shown in Fig. 1.8, humanoid walking can generally be split into the double support phase, where both feet have ground contact, and the single support phase with one foot being at on the ground, while the other swings through the air. Especially for fast walking, the swing phase is further classified into a pre-swing and a post-swing phase. During the pre-swing phase the swing foot rolls about the toes, and the post-swing phase is characterized by the swing foot landing on its heel and rolling about it.

Depending on the type of gait, not all phases can be observed. When robots are walking very slowly, the pre- and post-swing phase are generally omitted, thus always keeping the sole of the feet parallel to the ground. In very fast and dynamic motion on

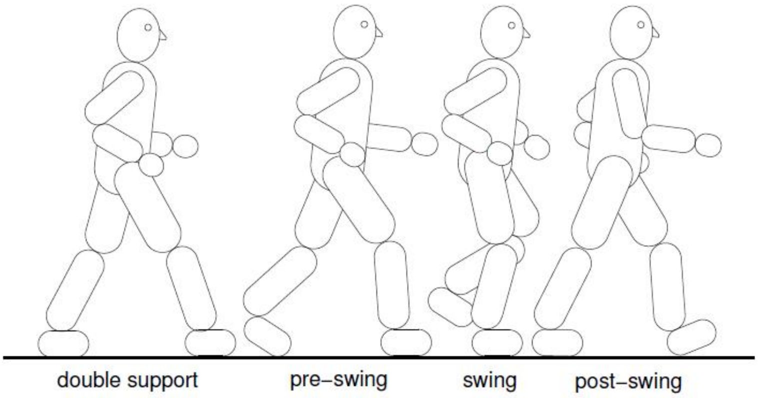

Figura 1.8: Phases of dynamic bipedal gait.

the other hand, the double support phase, with both feet on the ground, often is not distinguishable; running is even characterized by a complete lack of a double support phase, the single support phases are separated by a flight phase. The ground contact being the supporting basis has a substantial influence on the ability to balance the robot in an upright position. The great variety of ground contact situations however constitutes the necessity for a more generic description of the foot contact situation. Therefore the term supporting area has been introduced:

Definition 2.1: Supporting Area The supporting area is formed by the convex hull about the ground support points.

Fig.1.9 illustrates this definition in the case of single and double support. During the single support phase with only one foot having ground contact, the supporting area is the convex hull about the foot contact area. The supporting area in double support phase, however, comprises the contact area of both feet as well as the domain between them.

The feet of walking robots are not attached to the ground and can slip or lift off. Hence, forces can only be transmitted in one direction and friction forces and the gravitational force alone ensure, that the support foot remains at a fixed position on the ground. Therefore, the weight of the robot limits the applicable force and the lever arm becomes decisive for the achievable torque. The lever arm being essentially determined by the contact area, the supporting area becomes especially important for balanced walking. Therefore the supporting area is a central part of all commonly used equilibrium criteria.

1.2.3 Equilibrium Criteria

To implement biped walking controllers it is essential to determine whether the robot is in danger of tilting. Therefore, mathematical criteria for this property are discussed in the following.

Ground Projection of Center of Mass

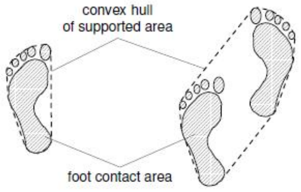

Figura 1.9: Supporting area during single and double support phase.

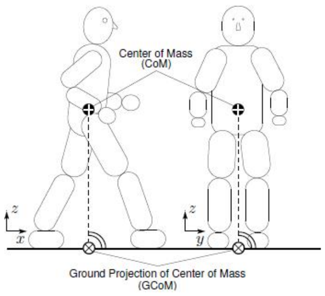

Figura 1.10: Ground projection of Center of Mass (GCoM).

A motionless robot only experiences gravitational forces, which are exerted on all parts of the robot. These forces can be replaced by a virtual force acting at the center of mass (CoM)

$$\boldsymbol{p}_{CoM} = \frac{\sum_i m_i \boldsymbol{p}_i}{\sum_i m_i} \tag{1.1}$$

of the robot, where denotes the mass of the -th link of the robot and the position of its center of mass. The location of the center of mass is decisive for the equilibrium of the robot. Its orthogonal projection to the ground is commonly referred to as the Ground Projection of Center of Mass (GCoM) or the Normal Projection of the Center of Mass (NPCM), see Fig.**??**. The location The location $\boldsymbol{p}_{GCoM}$ of the GCoM is the point that fulfills the relation:

$$\sum_i ((\boldsymbol{p}_{GCoM} - \boldsymbol{p}_i) \times m_i \boldsymbol{g}) = \boldsymbol{0} \tag{1.2}$$

i. e. the GCoM is the point on the ground, where the sum of all moments exerted on the motionless robot is zero. If the GCoM resides within the supporting area, the gravitation force does not generate a tilting moment and the robot remains standing. However, during fast locomotion, dynamic forces dominate static forces. As the GCoM does not take these dynamic forces into account, it becomes meaningless and bipeds may fall over although the GCoM resides within the supporting area. Hence other criteria must be applied.

1.2.4 Zero Moment Point and Foot Rotation Index

Rotation of an object about a given axis requires the presence of a torsional moment. Therefore, if the robot does not encounter a moment about the horizontal axes x and y, i. e.

$$M_x = 0 \quad M_y = 0 \tag{1.3}$$

the robot is balanced.
From (1.3) follows the Definition of the Zero Moment Point:

Definition 2.2: Zero Moment Point (ZMP). The Zero Moment Point x_{ZMP} is the point, where the ground reaction force F_R has to act to compensate all horizontal moments M_x and M_y. See Fig.**??** [4].

Hence, the robot is equilibrated, if the ZMP is within the supporting area. During locomotion the robot experiences - besides the gravitation force $F_{G,i}$ acting at the center of mass $\boldsymbol{p}_i$ of the i-th link - dynamic forces: Accelerating masses entails an inertial force $F_{I,i}$ and the corresponding moment $M_{I,i}$, which also acts at $\boldsymbol{p}_i$. Furthermore there is a resultant ground reaction force $\boldsymbol{F}_R$, which can be decomposed into a vertical component $\boldsymbol{F}_{R,v}$ and a horizontal component $\boldsymbol{F}_{R,h}$, i. e. $\boldsymbol{F}_R = \boldsymbol{F}_{R,v} + \boldsymbol{F}_{R,h}$. Accordingly the moment can be broken up into $\boldsymbol{M} = \boldsymbol{M}_v + \boldsymbol{M}_h$. Thus, the dynamic equilibrium during motion is expressed by the equilibrium of forces and moments:

$$\boldsymbol{F}_{R,v} + \boldsymbol{F}_{R,h} + \sum_i (\boldsymbol{F}_{I,i} + \boldsymbol{F}_{G,i}) = \boldsymbol{0} \tag{1.4}$$

$$\boldsymbol{p}_{ZMP} \times \boldsymbol{F}_R + \sum_i \boldsymbol{p}_i \times (\boldsymbol{F}_{I,i} + \boldsymbol{F}_{G,i}) + \sum_i \boldsymbol{M}_{I,i} + \boldsymbol{M}_{ZMP,h} + \boldsymbol{M}_{ZMP,v} = \boldsymbol{0} \tag{1.5}$$

According to (1.3), the horizontal component of the moment is zero, $\boldsymbol{M}_{ZMP,h} = 0$. Substituting in (1.5), solving (1.4) for $\boldsymbol{F}_R$ and inserting into (1.5), solving (1.5) yields

$$(\boldsymbol{p}_i - \boldsymbol{p}_{ZMP}) \times (\boldsymbol{F}_{I,i} + \boldsymbol{F}_{G,i}) + \sum_i \boldsymbol{M}_{I,i} = \boldsymbol{0} \tag{1.6}$$

Equation (1.6) allows another interpretation of the ZMP: The Zero Moment Point (ZMP) is the point on the walking ground surface at which the horizontal components of the resultant moment generated by active forces and moments acting on human/humanoid links are equal to zero [4].

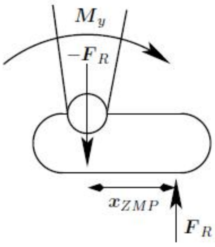

Figura 1.11: Forces and moments during single support phase.

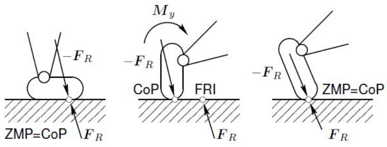

Figura 1.12: The possible relative position of ZMP and CoP: dynamically balanced gait (left), unbalanced gait (the system as a whole rotates about the foot edge and overturns) (middle), and intentional foot-edge equilibrium (right).

In 1999, Goswami [5] introduced the notion of foot rotation indicator (FRI), also known as imaginary ZMP (iZMP) [4]. The FRI is physically identical to the ZMP and both points coincide as long as ZMP/FRI remain inside the supporting area. But unlike the ZMP, the FRI is allowed to leave the supporting area, see Fig. 16. Although the gait is not balanced anymore (unbalanced gait), the FRI still has a useful interpretation: the distance of the FRI to the supporting area is a measure for the degree of instability of the gait and hence can give some invaluable information when controlling a stumbling biped. Technical feasibility of such motion is not clear and has not been proven yet. The concept of the ZMP being a physical approach, is very useful in numerical simulations, as it can easily be calculated from the system state. In hardware experiments however, this information is not necessarily known and measurement often is subject to considerable noise. Hence, another criterion, that can be evaluated more easily, is desirable.

1.2.5 Center of Pressure

Most humanoid robots are equipped with force-torque-sensors at the feet of the robot. Therefore the Center of Pressure criterion results directly from evaluating those sensors.

Definition 2.3: Center of Pressure. The Center of Pressure (CoP) is defined as the point on the ground where the resultant of the ground reaction forces acts [6].

There are two types of interaction of the foot with the ground: the normal forces $\boldsymbol{F}_{N,i}$ and the frictional tangential forces $\boldsymbol{F}_{T,i}$. The CoP is the point:

$$\boldsymbol{p}_{CoP} = \frac{\sum_i \boldsymbol{p}_i F_{N,i}}{\sum_i F_{N,i}} \tag{1.7}$$

where the resultant $\boldsymbol{F}_R = \sum_i \boldsymbol{F}_{N,i}$ acts; $\boldsymbol{p}_i$ is the vector from the origin to the point of action of force $\boldsymbol{F}_{N,i}$ and $F_{N,i} = |\boldsymbol{F}_{N,i}|$. As the interaction between foot and ground is always unilateral, $F_{N,i} \geq 0$ holds. Hence, $\boldsymbol{p}_{CoP}$ always lies within the supporting area. In [6], Goswami proved that ZMP and CoP are identical during single support phase for balanced walking. This identity implies that definitions referring to the ZMP can be applied accordingly using the CoP. The ZMP is easy to compute and therefore well suited for gait generation, while the CoP can easily be measured and hence is more suitable for control of a walking robot. Due to their identity, these criteria can be used interchangeably thus facilitating computation. Besides criteria for a balanced robot, there are restrictions on the ground reaction forces to avoid slipping or lifting off.

1.2.6 Ground Reaction Forces

As already mentioned, the ground reaction forces determine fixed contact of the support foot with the ground. Therefore, to maintain ground contact, the vertical component

$$F_{R,v} > 0 \tag{1.8}$$

of the ground reaction force $\boldsymbol{F}_R$ as defined in Fig.**??**, must always be positive. Otherwise the foot lifts off the ground and the robot cannot be controlled anymore. Slipping of the support foot is avoided by restricting the horizontal component $\boldsymbol{F}_{R.h}$ to remain within the so-called friction cone

$$\sqrt{F_{R,x}^2 + F_{R,y}^2} = F_{R,h} \leq \mu_R F_{R,z} \tag{1.9}$$

where μ_R is the friction coefficient. The equilibrium criteria introduced in this chapter are evaluated in most walking control algorithms. Furthermore, they help to determine the difference between slow, static motion and fast, dynamic walking.

1.2.7 Statically and Dynamically Balanced Gait

As already mentioned, dynamic forces like Coriolis, centrifugal and inertial forces, dominate the static gravity forces with increasing walking velocity. The dynamic forces can usually be neglected in slow motion, hence a common classification of walking gait distinguishes between statically and dynamically balanced gait.

Definition 2.4: Statically balanced motion. The movement of a robot is called statically balanced, if the GCoM and the ZMP always remain within the supporting area during the entire motion [7].

Accordingly, fast motion taking into account dynamic forces is referred to as dynamically balanced motion.

Definition 2.5: Dynamically balanced motion. If the ZMP resides within the supporting area during the motion of a human / humanoid while the GCoM leaves the supporting area, then this motion is called dynamically stable.

Note that Def.1.2.7 is a special case of Def. 2.5, as GCoM and ZMP are identical for a motionless robot. Obviously, the maximum achievable step length for statically balanced gait is limited compared to dynamically balanced gait [8]. The terms and criteria explained in Sec. **??** are the fundament for humanoid walking control. The following section gives an overview of the most commonly used control strategies.

1.3 Overview of Control Strategies

For humanoid biped robots, the problem of equilibrated robust walking is most fundamental and current solutions yet remain unsatisfactory for real world application. There are three fundamentally different approaches to humanoid walking control: One strategy assumes very accurate models of the real robot and its environment. Using this model for physically consistent motion generation, the approach relies on close accordance of the calculated dynamics with the real hardware behavior. Another starting point is to use a rather simple and abstract model of the dynamic behavior and achieve accordance with reality by feedback control. The third research direction can be subsumed as nature inspired control techniques. These include methods based on neural networks, fuzzy logic or genetic algorithms and are generally inspired by the idea to enable robots to act in unknown environments and to react on unforeseen events. One of the most popular approaches based on a simplified model is the inverted pendulum method belonging to the category of strategies relying on feedback control.

1.3.1 Walking Control

A core task for humanoid walking robots is the actual walking controller, generally consisting of a gait pattern generator and the balance control. For this problem, there exist two fundamental approaches: one possibility to set about this matter is to rely on a very accurate model of the walker and to compute gait trajectories trusting in sufficient accordance of the model with reality. The other direction relies an on approximating the robot dynamics by a simple model with reduced system states, e. g. an inverted pendulum. Accordance of the simplified model with the real dynamics is ensured by

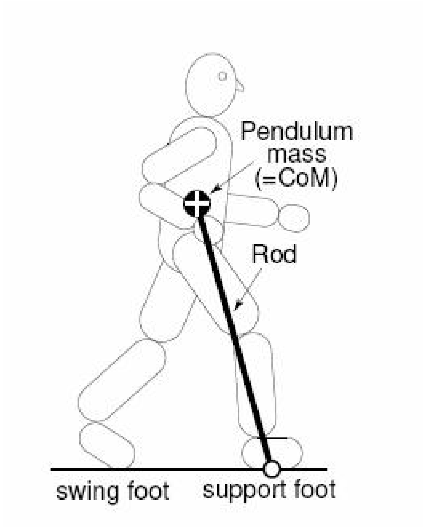

Figura 1.13: Inverted Pendolum method

feedback control. In the first approach, the trajectories are generally computed offline incorporating many constraints like balanced or energy efficient walking. As the trajectories are inherently balanced, only little control is required to compensate disturbances. Besides the accurate model of the robot dynamics, this method also assumes that commanded gait trajectories are closely matched by the real motion. Another difficulty arising from the approach with pre-calculated walking patterns is the size of the necessary database with gait trajectories, as variations in step length, walking direction, speed or ground inclination generally require recalculated dedicated walking patterns. Therefore it is useful to have a means of correcting the posture of the robot by superposing the pre-calculated pattern with a correction term thus correcting posture errors or adapting trajectories to new situations, e.g. adjusting at ground trajectories to walking on slopes. A method allowing such modifications is named Jacobi Compensation. The method uses Jacobian matrices to translate desired cartesian motions of selected parts of the body into corresponding joint space motions. The inverted pendulum method is a walking control strategy that classes as a simplified model approach. The robot dynamics are described by an inverted pendulum where the pendulum base coincides with the robot support foot and the pendulum mass represents robot center of mass. Most of the control methods of bipedal walking requires reference trajectories, including continuous-time methods based on PID controllers, computed torque and sliding mode control, etc. Traditionally, the main control problem is how to specify the trajectories that have to be followed (In this thesis was developed an optimization method for the specification of the coordinates trajectories). Only few methods adopt control strategies without need for a reference trajectory.

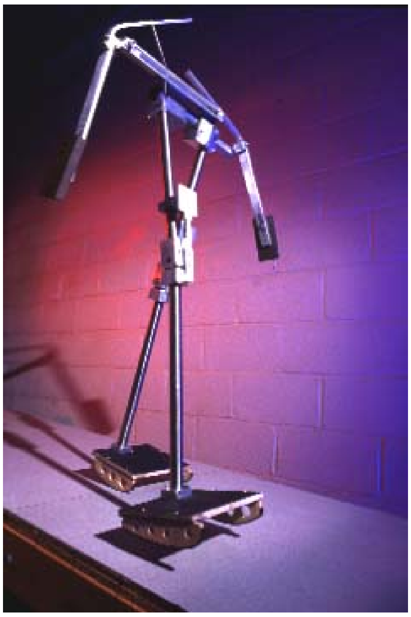

Figura 1.14: Passive Dynamic Walker

1.3.2 Inverted Pendulum Method

Miura and Shimoyama [9] studied the inverse pendulum approximation for the control of the Biper-3 robot. Later on, Kajita et al. [10] extended the inverse pendulum approach and tested its validity on various robots. In this approach, the dynamics of the robot are approximated by those of an inverted pendulum linearized about the upper equilibrium point. The mass is concentrated at the center of mass (CoM) of the robot, and the base of the pendulum coincides with the support foot of the robot, as illustrated in Fig.19. Based on this dynamic model, an appropriate location for the foot placement can be computed in order to counterbalance the tilting motion. Errors between the computed motion of the inverted pendulum and the real motion of the robot must be compensated by feedback control. One solution is to use the actuated ankle joint and apply a small correction torque. However, the single mass inverted pendulum is a non-minimum phase system, which imposes problems for controlling the ZMP. Therefore Napoleon et al. [11] proposed an extension towards a two mass inverted pendulum to overcome this deficiency. Sugihara [21] proposed a method to manipulate the location of the center of mass using the whole body motion, and to control the evolution of the inverted pendulum through ZMP manipulation. As the Inverted Pendulum Method is very flexible and gait patterns can be computed online, it is used in many humanoids.

1.3.3 Passive-Dynamic Walkers

Contrary to the previous active control methods, where joint angles and ground reaction forces are measured and precisely controlled, passive dynamic walkers achieve biped walking without electronic support. Passive dynamic walkers [13] are mechanical devices designed specifically for walking down shallow slopes. They have no motors or controllers, yet they can exhibit humanlike motions. This is achieved by exploiting their natural dynamics, i. e. passive walkers have been mechanically designed such that a machine of this class will settle into a steady, periodic gait without active control or energy input. Energy loss due to friction or impact is compensated by utilizing the potential energy of the slope converting it into kinetic energy. This idea was first introduced and examined by McGeer ([14] and [14]) in 1989. One very interesting observation with passive walking are very smooth trajectories giving the impression of human-like gait. This reinforces the observation of high energy efficiency of human gait. In 2001, Ruina et al. [16] succeeded in building the first three-dimensional, kneed, two-legged, passive-dynamic walking machine, the Cornell Passive Walker, see Fig. 20. Thus they proved the theoretic considerations to be valid. In this experiment, the two dimensional model by McGeer is extended by adding specially curved feet, a compliant heel and mechanically constrained arms thus achieving a harmonious and stable gait. However, passive walkers are very sensitive to initial conditions and can only walk at a dedicated speed imposed by the mechanical construction. Thus transferring the idea of passivity to actuated humanoids is an interesting challenge addressed by many researchers. An intermediate mixture between passive walkers and actuated humanoids has been introduced by Spong [17], who showed that by adding a single actuator to a passive walker, energy loss can be compensated. It is even possible to add energy to the system such that the robot can climb up slopes. Various energy efficient biped walkers have been built [18], e. g. the Cornell Biped shown in Fig. 1.14, the Delft biped, or the MIT learning biped. An established measure to compare efficiency between humans and bipeds of different size is the cost of transportation:

$$c_t = (\text{energyused}) \,/\, (\text{weight} \times \text{distancetraveled}) \tag{1.10}$$

It is useful to distinguish between the specific energetic cost c_{et} of transportation and the specific mechanical cost c_{mt} of transport, where c_{et} reflects the total energy consumed by the system and c_{mt} only considers the mechanical work of the actuators. The 13-kg Cornell Biped, for example, walking at 0.4 m/s has and . Humans are similarly energy effective, walking with $c_{et} \approx 0.2$, as estimated by the volume of oxygen they consume, and $c_{mt} \approx 0.05$. By contrast, the Honda humanoid Asimo is estimated to have $c_{et} \approx 3.2$ and $c_{mt} \approx 1.6$. Thus Asimo uses at least 10 times the energy (scaled) of a typical human. These data confirm that adopting concepts from passive walkers to humanoid robots constitutes an important aspect towards autonomous and energy efficient walking.

1.3.4 Other Control Strategies

There are various other methods to achieve balanced humanoid walking. Yamaguchi et al. [19] solved the problem to obtain trajectories inversely from a desired ZMP movement; the upper body motion is used to compensate the moment about the desired ZMP. This strategy has been implemented in the Waseda Leg and Wabian series. Miura and Shimoyama [20], who developed the Biper robots, controlled his robots by foot placement feedforward control. This method yields an asymptotically stable periodic gait. A method to manipulate the ZMP has been presented by Sugihara ([21] , [22]). Based on an inverted pendulum model, the CoM is controlled through a Jacobian such that the ZMP shows the desired behavior. Apart from these classical control approaches, there are approaches to mimic the human neuro-system by employing neural networks [23] or to emulate the central pattern generator [24] as it can be found in human beings. Another direction employs genetic algorithms or neural networks to acquire and improve gait trajectories on an evolutionary basis [25].

CAPITOLO 2

Modeling

2.1 The Mechanical models

The mechanical models treated in this thesis are of three kinds. One of them is the most simple walking mechanism that should show a passive behavior walking downhill; it is the Compass like bipedal robot It will called Compass. The second one, is the bipedal walking robot with knees, with 3 d.o.f. that is a mechanism that is a little bit more complicated rather than the compass one, and has a behavior that's much closer to the human walking. This mechanism is called in literature Dribbel, and so, it will call. The third, again, is a bipedal walking robot with knees wih 4 d.o.f. and the assumption will be really different from the ones done for the 3 d.o.f. It will called Knee model. All the models can be practically obtained from the model Knee simply eliminating one or two of the four degrees of freedom that Knee has.

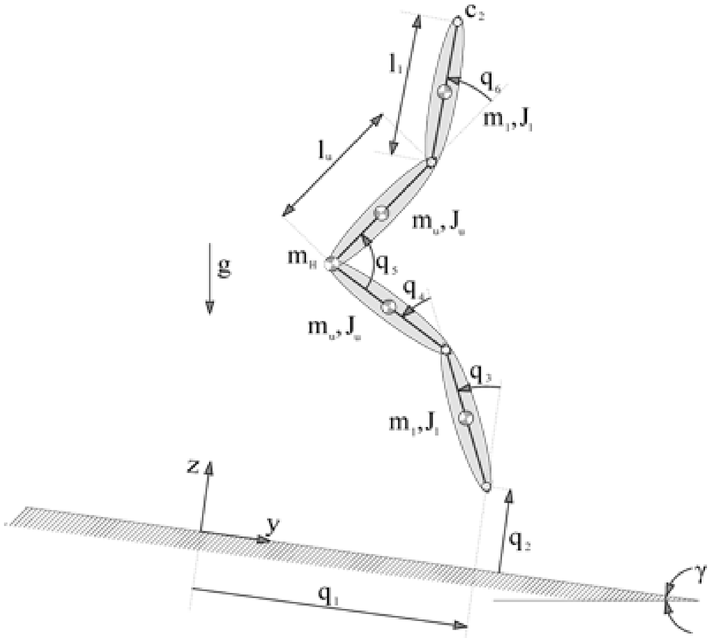

Figura 2.1: Knee mechanical model.

Taking a look to the Fig.2.1, if the stance leg is blocked (means that the coordinate $q_4 = 0$) it is obtained the Dribbel model. Otherwise, if are blocked both the legs (

$q_4 = 0$ and $q_6 = 0$), it's obtained the model Compass. That's, for allow us to say that everything (every equation or matrix or relation) proposed in the following, can be derived from the relative one referred to the model Knee. How can be noticed in the figure 2.1, the walking model present not only the minimum set of coordinates for describing its dynamic, but present also two coordinates (q_1 and q_2) that define the position along the slope, of the stance leg's foot. These two cooridinates are important for describing the velocities constraints at the moment of the ground impact.

2.1.1 Model Analysis

To obtain a model of one of the mechanisms that is suitable for the analysis, we make the assumptions that only one foot is on the ground at the same time, the double-supporting phase is instantaneous, the gait is symmetric, and the motion of the mechanism is such that the stance leg's foot remains on the ground throughout the whole step.

A step starts at $t = 0$ with the swinging leg that begin to swing along the walking direction. Then, the walking motion continues smoothly until the instant $t = Tkneej > 0$ that could happen on the swing or on the stance leg's knee. This strike couldn't happen if, for example, we are considering the Compass model. After that, the swing phase continue, and depending on how many knee strikes will occur, it is possible to individuate as many time instants $Tknee_j$, where $j = 1 \cdots N_s - 1$, that refers to the instants of the knees strikes. After all the knees strikes, if they occur, the continuous dynamic develop until a time instant $t = T$ in which happen the strike on the ground of the swing foot. Under those assumptions, the analysis model of a step of one of the three models proposed in this thesis, can be split into N_s continuous phases, each delimitated between the time instants outlined before. The figure 2.2 below, is showing a typical walking motion of the model with 3 d.o.f. (*Dribbel*) with just two strikes per single gait; the first happen on the knee and the last one on the ground. The red leg indicates the swinging leg and with the azure, is indicated the stance leg.

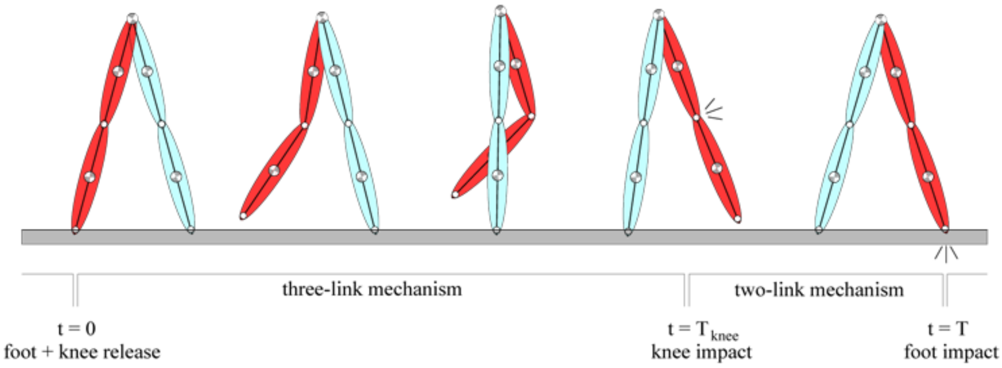

Figura 2.2: Dribbel walking motion of the gait. The most important event that characterize its dynamic are highlighted.

2.1.2 Dynamic Equations

The three models proposed, present, obviously, different motion equations but they can be simbolically expressed by the same matricial equation:

$$\boldsymbol{M}\left(\boldsymbol{q}\right)\ddot{\boldsymbol{q}} + \boldsymbol{C}\left(\boldsymbol{q},\dot{\boldsymbol{q}}\right)\dot{\boldsymbol{q}} + \boldsymbol{V}\left(\boldsymbol{q}\right) = \boldsymbol{\tau} \tag{2.1}$$

Where $\boldsymbol{M}\left(\boldsymbol{q}\right) \in \mathbb{R}^{m\times m}$ is the mass matrix of the system and collects the inertial terms, $\boldsymbol{C}\left(\boldsymbol{q},\dot{\boldsymbol{q}}\right) \in \mathbb{R}^{m\times m}$ collects together elements of centrifugal force and Coriolis forces, the term $\boldsymbol{V}\left(\boldsymbol{q}\right) \in \mathbb{R}^{m\times 1}$ collects the elements of gravity, while $\boldsymbol{\tau} \in \mathbb{R}^{m\times 1}$, Is the vector of torque applied to the system. m is the number of degrees of freedom of the considered mechanism (the length of the vector $\boldsymbol{q}$).

2.1.3 Coordinate re-Labeling Operator

The coordinate relabeling operator is a matrix that has the task to re-label the coordinate after a single strike if it needs to be re-labeled. In fact, in correspondence of the ground strike, the coordinates have to be re-labeled because there is the change of roles between the two legs: the leg was swinging become the stance, and the opposite. Despite of this, in correspondence of the knee strike, no re-labeling operator is needed because there is no change of roles between the legs.

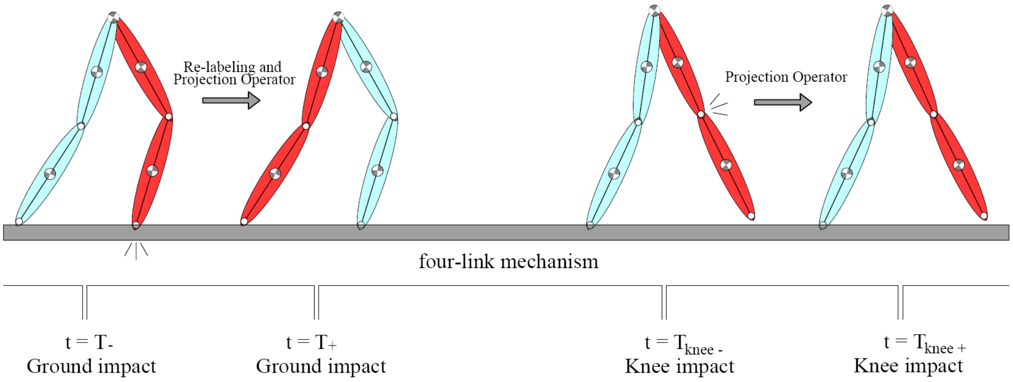

Figura 2.3: Changing of roles between the legs in correspondence of the ground strike (left) and not changing in correspondence of the knee strike (right).

Depending on the considered mechanical system, the re-labeling operator changes, but there is a common base over the three different proposals. First of all, it needs to be defined the variables vectors of the different mechanisms that are reported in the table 2.1

Where $\boldsymbol{q}_i$ is the vector of coordinates that really explain the dynamic of the system, while $\bar{\boldsymbol{q}}_i \in \mathbb{R}^{m+2\times 1}$ is the vector of generalized and extended coordinates including the two coordinates q_1 and q_2 that define the position of the stance leg's foot. With $i = K, D, C$. The i, with one of its three meanings, stands for the model that begins with that letter.

$$K = Knee \quad D = Dribbel \quad C = Compass \tag{2.2}$$

In the following, the various models can be considered how derived from the much complex one that is Knee. In fact, Dribbel is the model obtained from Knee just

Knee	$\boldsymbol{q}_K = \begin{bmatrix} q_3 \\ q_4 \\ q_5 \\ q_6 \end{bmatrix}$	$\bar{\boldsymbol{q}}_K = \begin{bmatrix} q_1 \\ q_2 \\ q_3 \\ q_4 \\ q_5 \\ q_6 \end{bmatrix}$
Dribbel	$\boldsymbol{q}_D = \begin{bmatrix} q_3 \\ q_5 \\ q_6 \end{bmatrix}$	$\bar{\boldsymbol{q}}_D = \begin{bmatrix} q_1 \\ q_2 \\ q_3 \\ q_5 \\ q_6 \end{bmatrix}$
Compass	$\boldsymbol{q}_C = \begin{bmatrix} q_3 \\ q_5 \end{bmatrix}$	$\bar{\boldsymbol{q}}_C = \begin{bmatrix} q_1 \\ q_2 \\ q_3 \\ q_5 \end{bmatrix}$

Tabella 2.1: Scheme for the evaluation of number of possible SMs for the imposed number of strikes

imposing the coordinate $q_4 = 0$ for all the gait long. As so, Compass is obtained imposing $q_4 = 0$ and $q_6 = 0$. Dough, it is possible to define the re-labeling operator for the model Knee, and then, evaluate the operator $\boldsymbol{G}_i$ of the other models like a consequence. The re-labeling operator for Knee, is defined like:

$$\begin{bmatrix} q_1 \\ q_2 \\ q_3 \\ q_4 \\ q_5 \\ q_6 \end{bmatrix} = \bar{\boldsymbol{q}}_K \rightarrow \boldsymbol{q}_K = \begin{bmatrix} q_3 \\ q_4 \\ q_5 \\ q_6 \end{bmatrix} \rightarrow \boldsymbol{G}_K = \begin{bmatrix} 1 & 1 & 1 & 1 \\ 0 & -1 & 0 & 0 \\ 0 & 0 & -1 & 0 \\ 0 & 0 & 0 & -1 \end{bmatrix} \tag{2.3}$$

The other re-labeling operators $\boldsymbol{G}_D$ and $\boldsymbol{G}_C$ are evaluated considering the matrix full of zeros and on the first row the value 1, and on the main diagonal, the value -1 but on the position $\boldsymbol{G}_i\,(1,1) = 1$. The size of the matrix is $m \times m$, remembering that m is the number of degree of freedom of the considered mechanism, and so, is equal to the size of the vector $\boldsymbol{q}_i$. So, we obtain the following other operators:

$$\boldsymbol{G}_D = \begin{bmatrix} 1 & 1 & 1 \\ 0 & -1 & 0 \\ 0 & 0 & -1 \end{bmatrix} \quad \boldsymbol{G}_C = \begin{bmatrix} 1 & 1 \\ 0 & -1 \end{bmatrix}$$

The matrix $\boldsymbol{G}_i$ relates the coordinates before and after the impact to the ground of the relative mechanism.

$$\begin{cases} \boldsymbol{q}_i\,(t_+)_r = \boldsymbol{G}_i \boldsymbol{q}_i\,(t_-) \\ \dot{\boldsymbol{q}}_i\,(t_+)_r = \boldsymbol{G}_i \dot{\boldsymbol{q}}_i\,(t_+) \end{cases} \tag{2.4}$$

Where $\boldsymbol{q}_i\left(t_+\right)_r$ and $\dot{\boldsymbol{q}}_i\left(t_+\right)_r$ are the relabeled coordinate and velocity vectors of the i-model at the initial instant of the next step, and $\boldsymbol{q}_i\left(t_-\right)$ and $\dot{\boldsymbol{q}}_i\left(t_-\right)$ are the coordinate and velocity vectors of the i-model at the final instant of the current step.

2.1.4 Projection Operator

Rigid Contact

The Euler-Lagrange differential equation works well to describe the dynamics of a biped robot while one foot is on the ground and the other leg is swinging above the ground. However, kinetic energy is lost when the swinging foot strikes the ground, resulting in a dramatic change in the Lagrangian of the robot. We might modify the Euler-Lagrange equations at the time of the ground impact to model the continuous loss of energy. Some researchers have attempted this task by modeling the surface of the ground as a series of springs and dampers ([27] and [28]). While such a model results in continuous equations that hold throughout the impact, it does so at the cost of increased complexity. For example, the compliant contact model described by [26] allows for a wide range of surface properties and other situations. However, for the purpose of modeling walking robots, it has two main problems. The first problem is that as the surfaces in contact become stiffer, the dynamics in the collision phase become faster. This leads to a dynamic model described by stiff differential equations; a model with relatively fast dynamics (the collision dynamics) as well as relatively slow dynamics (the other motions of the system). Simulation of such system requires special integration methods in order to ensure the accuracy of the results as well as acceptable simulation speeds, and simulation of the collision phase will be relatively slow. The second problem relates to the analysis of the models. A walking cycle of a robot consists of a single-support phase, in which one foot is more or less fixed to the ground and one foot is above the ground, and a double-support phase, in which both feet are on the ground and support is transferred from one foot to the other. Of these two phases, the single support phase is generally the longest, and for some walking configurations, the double-support phase completely disappears as the surface stiffness increases. However, the compliance in the contact model prevents the stance foot from being exactly fixed to the ground, and the double-support phase from being exactly instantaneous, thus making the analysis of the overall cycle overly cumbersome. For these two reasons, in this section, it is presented a simpler contact model. This model is suitable for contact situations in which the stiffness and damping are large enough to permit approximating them by an instantaneous dissipation of energy on impact. The advantage of this model is that the analysis becomes simpler, especially for certain types of walking robots where the double support phase becomes a simple momentum reset between consecutive steps. In general, it is not so easy to replace compliant contact by instantaneous impulsive contact. Aspects that are unimportant in compliant modeling (such as the exact order in which points of the bodies come in contact with each other) suddenly change the outcome of the simulation significantly in the case of impulsive contact modeling (Acary & Brogliato 2003 [29]). Furthermore, the presence of finite friction and slip requires various extra modeling assumptions to ensure a single deterministic solution of the dynamic equations (Glocker 2001 [30], Glocker 2004 [31]). To avoid such problems, it was chosen to restrict the work to the following class of contact situations:

- Instantaneous and fully plastic contact (zero restitution).
- No simultaneous collisions.
- No sideways slipping.
- Support is instantaneously transferred from the stance leg to the swing leg.

These assumptions are a reasonable approximation for most walking robots.
As the starting point for the rigid contact model, it is taken a mechanical system of the form:

$$\begin{cases} \bar{\boldsymbol{M}}_i\left(\bar{\boldsymbol{q}}_i\right)\ddot{\bar{\boldsymbol{q}}}_i + \bar{\boldsymbol{C}}_i\left(\bar{\boldsymbol{q}}_i, \dot{\bar{\boldsymbol{q}}}_i\right)\dot{\bar{\boldsymbol{q}}}_i + \bar{\boldsymbol{V}}_i\left(\bar{\boldsymbol{q}}_i\right) = \boldsymbol{\tau}_i - \boldsymbol{J}_I\left(\bar{\boldsymbol{q}}_i\right)^T \boldsymbol{\lambda}_I \\ \boldsymbol{0} = \boldsymbol{J}_I\left(\bar{\boldsymbol{q}}_i\right)\dot{\bar{\boldsymbol{q}}}_i \end{cases} \tag{2.5}$$

Where $\bar{\boldsymbol{M}}_i\left(\bar{\boldsymbol{q}}_i\right) \in \mathbb{R}^{m+2\times m+2}$ is the enlarged mass matrix of i-model by considering variables the vector $\bar{\boldsymbol{q}}_i \in \mathbb{R}^{m+2\times 1}$ and no more $\bar{\boldsymbol{q}}_i \in \mathbb{R}^{m+2\times 1}$, $\boldsymbol{J}_I\left(\bar{\boldsymbol{q}}_i\right) \in \mathbb{R}^{m+2\times 2}$, is the jacobian matrix obtained from the geometrical conditions at impact if the strike is the one on the ground, and $\boldsymbol{J}_I\left(\bar{\boldsymbol{q}}_i\right) \in \mathbb{R}^{m+2\times 2}$, if the strike is the one on the knees. The rows of $\boldsymbol{J}_I\left(\bar{\boldsymbol{q}}_i\right)$ descibe the direction of the contact wrenches and contain information from the contact kinematics, in order to know when and at what position the contact forces act. $\boldsymbol{\lambda}_I \in \mathbb{R}^2$ is the vector of undetermined Lagrange multipliers in the context of the impulsive forces, while the relation $\boldsymbol{0} = \boldsymbol{J}_I\left(\bar{\boldsymbol{q}}_i\right)\dot{\bar{\boldsymbol{q}}}_i$ represents the conditions of the constraints of the velocities. The rigid contact model describe what happen on impact, i.e. when impulsive constraint forces $\boldsymbol{\lambda}_I$ set the velocities of the contact point to zero. There are defined t_i as the time of impact, and t_- and t_+ as the time instants just before and just after impact, i.e. mathematically as $t_- = t_i - \varepsilon$ and $t_+ = t_i + \varepsilon$ with $\varepsilon \to 0$. Using this notation, can be indicated the velocity constraint of equation 2.5 as

$$\boldsymbol{J}_I\left(\bar{\boldsymbol{q}}_i\right)\dot{\bar{\boldsymbol{q}}}_i\Big|_{t=t_+} = \boldsymbol{0} \tag{2.6}$$

Where were used t_+ (the time just after impact) since the momentum $(\bar{\boldsymbol{M}}_i\dot{\bar{\boldsymbol{q}}}_i)$ is discontinuous at impact $t = t_i$ and hence, not well defined. Can be integrated the dynamic equation (2.5) over the impact phase, i.e. from t_- to t_+, which results in the following.

$$\int_{t_-}^{t_+} \bar{\boldsymbol{M}}_i\ddot{\bar{\boldsymbol{q}}}_i dt = \int_{t_-}^{t_+} \left(-\bar{\boldsymbol{C}}_i\dot{\bar{\boldsymbol{q}}}_i - \bar{\boldsymbol{V}}_i + \boldsymbol{\tau}_i - \boldsymbol{J}_I^T\boldsymbol{\lambda}_I\right) dt \tag{2.7}$$

$$\bar{\boldsymbol{M}}_i\dot{\bar{\boldsymbol{q}}}_i\left(t_+\right) - \bar{\boldsymbol{M}}_i\dot{\bar{\boldsymbol{q}}}_i\left(t_-\right) = -\boldsymbol{J}_I^T \int_{t_-}^{t_+} \boldsymbol{\lambda}_I dt \tag{2.8}$$

Where it is assumed that the terms $-\bar{\boldsymbol{C}}_i\dot{\bar{\boldsymbol{q}}}_i - \bar{\boldsymbol{V}}_i$ and $\boldsymbol{\tau}_i$ have finitely large magnitude and hence, zero integral between t_- and t_+. If sobstitute the expression (2.8) for $\bar{\boldsymbol{M}}_i\dot{\bar{\boldsymbol{q}}}_i\left(t_+\right)$ into (2.7), we obtain an expression for $\boldsymbol{\lambda}_I$ as

$$\boldsymbol{0} = -\boldsymbol{J}_I^T\left(\bar{\boldsymbol{q}}_i\right)\bar{\boldsymbol{M}}_i\left(\bar{\boldsymbol{q}}_i\right)^{-1}\left(\bar{\boldsymbol{M}}_i\dot{\bar{\boldsymbol{q}}}_i\left(t_-\right) + \boldsymbol{J}_I^T\left(\bar{\boldsymbol{q}}_i\right)\int_{t_-}^{t_+} \boldsymbol{\lambda}_I dt\right) \tag{2.9}$$

$$\int_{t_-}^{t_+} \boldsymbol{\lambda}_I dt = \left(\boldsymbol{J}_I\left(\bar{\boldsymbol{q}}_i\right)\bar{\boldsymbol{M}}_i\left(\bar{\boldsymbol{q}}_i\right)^{-1}\boldsymbol{J}_I^T\left(\bar{\boldsymbol{q}}_i\right)\right)^{-1}\boldsymbol{J}_I\left(\bar{\boldsymbol{q}}_i\right)\dot{\bar{\boldsymbol{q}}}_i\left(t_-\right) \tag{2.10}$$

The inverse of the matrix $\boldsymbol{J}_I\bar{\boldsymbol{M}}_i^{-1}\boldsymbol{J}_I^T$ exists if and only if the rows of $\boldsymbol{J}_I^T$ are linearly indipendent, i.e. if the constraint force magnitudes $\boldsymbol{\lambda}_I$ are uniquely determined. Instead of explicity computing and using $\boldsymbol{\lambda}_I$, can be also substitute eqaution (2.10) into equation (2.8) to obtain an expression for the velocity after impact $\dot{\bar{\boldsymbol{q}}}_i\left(t_+\right)$ as

$$\dot{\bar{\boldsymbol{q}}}_i\left(t_+\right)=\left(\boldsymbol{I}-\bar{\boldsymbol{M}}_i^{-1}\boldsymbol{J}_I^T\left(\boldsymbol{J}_I\bar{\boldsymbol{M}}_i^{-1}\boldsymbol{J}_I^T\right)^{-1}\boldsymbol{J}_I\right)\dot{\bar{\boldsymbol{q}}}_i\left(t_-\right)=\boldsymbol{P}_{proj}\dot{\bar{\boldsymbol{q}}}_i\left(t_-\right) \tag{2.11}$$

The Projection Operator $\boldsymbol{P}_{proj}$ assume different shape in according with the considered mechanism, and according with the considered strike (if it happen on the stance leg's knee or on the swing leg's knee or on the ground). $\dot{\bar{\boldsymbol{q}}}_i\left(t_+\right)$ and $\dot{\bar{\boldsymbol{q}}}_i\left(t_-\right)$ are respectively the vectors of velocities before and after impact of the i-model. $\boldsymbol{J}_I\left(\bar{\boldsymbol{q}}_i\right)$ is the generic Jacobian setting the geometrical conditions at a generic impact, and so, it may vary depending on the considered strike of one of the three models.
It is possible to consider the Jacobian for the model *Knee* and then, evaluate the others of *Dribbel* and *Compass* with simple considerations like done before for the re-labeling operator. The Jacobian for the strike to the ground, for model *Knee* is defined by $\boldsymbol{J}_{Kf}\left(\bar{\boldsymbol{q}}_K\right)$:

$$\boldsymbol{J}_{Kf}\left(\bar{\boldsymbol{q}}_K\right)=\begin{bmatrix} 1 & 0 & J_{13} & J_{14} & J_{15} & J_{16} \\ 0 & 1 & J_{23} & J_{24} & J_{25} & J_{26} \end{bmatrix} \tag{2.12}$$

Where:

$$J_{13}=-l_l\cos\left(q_3\right)-l_u\cos\left(q_3+q_3\right)+l_u\cos\left(q_3+q_4+q_5\right)+l_l\cos\left(q_3+q_4+q_5+q_6\right)$$

$$J_{14}=-l_u\cos\left(q_3+q_3\right)+l_u\cos\left(q_3+q_4+q_5\right)+l_l\cos\left(q_3+q_4+q_5+q_6\right)$$
$$J_{15}=l_u\cos\left(q_3+q_4+q_5\right)+l_l\cos\left(q_3+q_4+q_5+q_6\right)$$
$$J_{16}=l_l\cos\left(q_3+q_4+q_5+q_6\right)$$
$$J_{23}=-l_l\sin\left(q_3\right)-l_u\sin\left(q_3+q_3\right)+l_u\sin\left(q_3+q_4+q_5\right)+l_l\sin\left(q_3+q_4+q_5+q_6\right)$$
$$J_{24}=-l_u\sin\left(q_3+q_3\right)+l_u\sin\left(q_3+q_4+q_5\right)+l_l\sin\left(q_3+q_4+q_5+q_6\right)$$
$$J_{25}=l_u\sin\left(q_3+q_4+q_5\right)+l_l\sin\left(q_3+q_4+q_5+q_6\right)$$
$$J_{26}=l_l\sin\left(q_3+q_4+q_5+q_6\right)$$

That Jacobian matrix defined above, is the one referred to the strike on the ground. The other Jacobian matrix are evaluated simply remembering the relation in terms of coordinate variables between the mechanisms. In fact, The Jacobian matrix for *Dribbel* striking on the ground is obtained deleting the fourth column of the matrix $\boldsymbol{J}_{Kf}\left(\bar{\boldsymbol{q}}_K\right)$ and imposing the coordinate $q_4=0$ into the other members. In particular will see in the latter, that *Dribbel* has the characteristic to behave like a 2 d.o.f. model (like *Compass*) the end of the gait, and so, the Jacobian $\boldsymbol{J}_{Df}\left(\bar{\boldsymbol{q}}_D\right)$ is evaluated deleting also the sixth column of $\boldsymbol{J}_{Kf}\left(\bar{\boldsymbol{q}}_K\right)$ and imposing the coordinate $q_6=0$ in the other members. With the same considerations The Jacobian matrix of Compass $\boldsymbol{J}_{Cf}\left(\bar{\boldsymbol{q}}_C\right)$ is evaluated in the same way and it is equal to the $\boldsymbol{J}_{Df}\left(\bar{\boldsymbol{q}}_D\right)$.

$$J_{Cf}\left(\bar{\boldsymbol{q}}_C\right)=\boldsymbol{J}_{Df}\left(\bar{\boldsymbol{q}}_C\right)=\left[\begin{array}{cccc} 1 & 0 & 0 & \left(l_l+l_u\right)\cos\left(q_3\right) \\ 0 & 1 & -2\left(l_l+l_u\right)\sin\left(q_3\right) & -\left(l_l+l_u\right)\sin\left(q_3\right) \end{array}\right] \quad (2.13)$$

Note that we can use the same coordinate vector $\bar{\boldsymbol{q}}_C$ because of the compass posture that the two model assume at the end of the gait. In this formulation was imposed the symmetry of the gait at the end with the relation $q_5 = -2q_3$. For the strikes on the knees, the jacobian matrix is simpler and starting from the one related to the mechanism *Knee*, we can find the two $\boldsymbol{J}_{Kk1}$ and $\boldsymbol{J}_{Kk2}$ related to the two possible strikes on the *knee1* (of the stance leg) and *knee2* (of the swing leg):

$$\boldsymbol{J}_{Kk1}=\left[\begin{array}{cccccc} 0 & 0 & 0 & 1 & 0 & 0 \end{array}\right] \quad \boldsymbol{J}_{Kk2}=\left[\begin{array}{cccccc} 0 & 0 & 0 & 0 & 0 & 1 \end{array}\right] \quad (2.14)$$

Dealing about the other mechanisms, the only other that can exibit one strike on the knee, is *Dribbel*, and in particular can exibit the only strike on the knee2 (swing leg). The related jacobian is obtained like before, eliminating the fourth column from the $\boldsymbol{J}_{Kk2}$. It is obtained the vector $\boldsymbol{J}_{Dk2}$:

$$\boldsymbol{J}_{Dk2}=\left[\begin{array}{ccccc} 0 & 0 & 0 & 0 & 1 \end{array}\right]$$

Where $\boldsymbol{J}_{Dk2} \in \mathbb{R}^{m+2\times 1}$

2.2 *Knee* Model

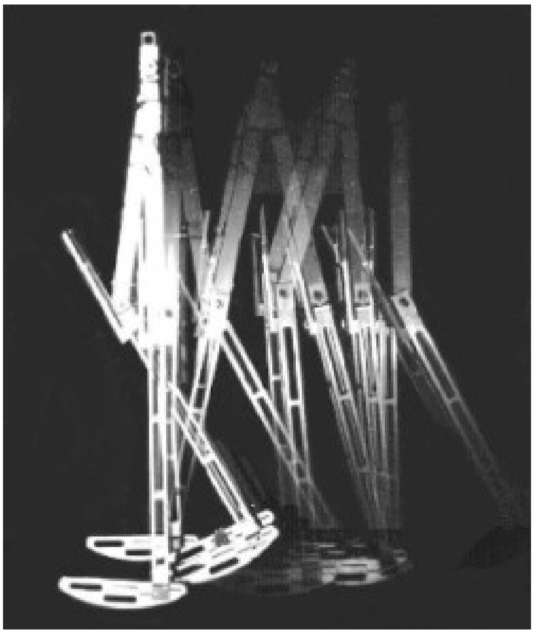

Figura 2.4: Snapshot of the motion of Knee model with circular feet.

. The figure (2.4) shows *Knee* model movement with a series of napshot. The model in the figure has circular feet but the mechanism's model we will study in the following doesn't provide circular feet. The mechanism consists of four legs that are connected in pairs so that both, internal and external legs are moving synchronously. This type of connection was used for the first time by British researcher McGeer (1991) [**?**]. He discovered this interesting way to build a three-dimensional walker mechanism (robot), behaves essentially as a two-dimensional mechanism. The pairs of legs, in fact, preserve the robot from falling sideways. The leg pairs are joined in two concentric aluminum tubes, which contain most of the electronics as well as a motor and a torque sensor. The knees of the robots are equipped with mechanical stops (knee-cups) whose function is to avoid over-extension of the legs. The robot's feet are small plates of metal U-shaped and are aligned with the leg kept simple elastic bands. The robot is implemented as fully actuated with the presence of actuators in rotational joints (knees and chest) and ankles.

Dynamic model of Knee

Simulation Model

In order to develop a simulation of the model *Knee*, we make the assumption that the links of the robot are considered rigid and the joints, ideals. Assuming values taken from literature for the main physical characteristics of the system, looking at the figure 2.5, we recognize 3 characteristic points of our model: The Hip point, and those which characterize the knee joints. The model thus provides a concentrated mass at Hip point , another one in the middle of the upper part of each leg and another one in the bottom part of the legs. Each concentrated mass has inertia associated with its corresponding. Other physical parameters of the robot in question are the lengths of the upper and lower part of the leg respectively defined by the parameters l_l and l_u. The feet are modeled in order to make the contact happen on a single point and they have no spatial extension and coincide with the end point of the lower part of the legs. Have been used the values of the mass, center of mass, and inertia of these four rigid bodies as adopted in Duindam and Stramigioli dissertation [26]. There were assumed the mass of the links to be distributed uniformly, and the mass of the joints to be concentrated in a point. The values of physical parameters are shown in table 2.2 below.

m_H	3,0 [kg]
m_l	1,6 [kg]
m_u	1,52 [kg]
J_l	0,0592 [mm^4]
J_u	0,0663 [mm^4]
l_l	0,43 [m]
l_u	0,47 [m]

Tabella 2.2: Physical parameters of Knee model.

From the Fig.2.5 we can see the degrees of freedom (d.o.f.) of the model. The degrees of freedom are four (or six if we consider the coordinates that links the robot's position at the origin of the reference system) and are defined with that nomenclature: q_1, q_2, q_3, q_4, q_5 and q_6. The coordinates q_1 and q_2, are those that define the position of the foot of the stance leg with respect to fixed reference system. The remaining coordinates q_3, q_4, q_5 and q_6, are the rotational coordinates of the rotations of linear elements that constitute the legs of the robot. The first coordinate q_3, is absolute because it

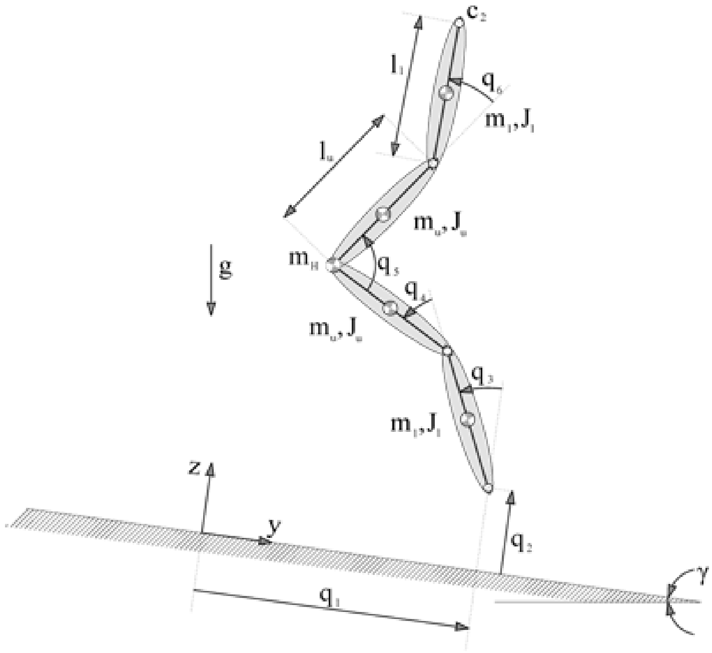
c_2
l_l
q_6
m_l,J_l
l_u
m_u,J_u
g
m_H
q_5
q_4
m_u,J_u
q_3
m_l,J_l
z
y
q_2
q_1
γ

Figura 2.5: Knee mechanical model.

is the rotation of the stance leg respect to the perpendicular to the ground, while the remaining q_4, q_5 and q_6 are related to rotations are immediately preceding, and so are relative coordinates. The system is moving along a downhill with a slope γ and in the following is shown an example of the walking gait.
It is show the movement behavior of the *Knee* mechanism highlighting the main important events that happen during the walking. The step model used, provides the presence of three strkes during the gait.

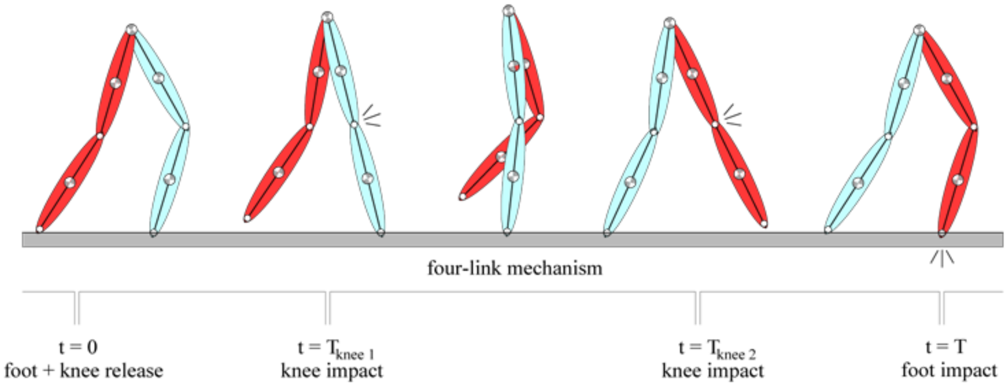
four-link mechanism
t = 0
foot + knee release
t = T_knee 1
knee impact
t = T_knee 2
knee impact
t = T
foot impact

Figura 2.6: Knee walking motion of the gait. There are highlighted the most important event that characterize its dynamic.

The step model presented in Fig.2.6 is providing a series of three strikes that happen with this order: the first strike happen on the knee of the stance leg (*knee1*), the second one on *knee2* and the last one on the ground. The model develop like a four-link mechanism for all the duration of the gait.

2.3 *Dribbel* Model

Fig.2.7 shows *Dribbel*, the kneed walking robot developed by Dertien (2005) [33], Beekman (2004) [32] and van Oort (2005) [34] at the University of Twente. It is a mechanism consisting of four legs (the same treated for the model *Knee*), which are connected in pairs, such that both the two outer legs and the two inner legs move together. The knees of the robot have mechanical kneecaps that prevent them from hyper-extending. They also contain electromagnets that can be actuated in order to hold the leg straight. The feet of the robot are same described with the *Knee* model. Finally, all joints are equipped with rotational encoders that measure the joint angles. Inspired by human locomotion, we choose to activate the magnets on the knees during the whole stance phase, such that knee buckling is prevented. When the stance foot releases the ground (as detected by the contact switch), the magnet is deactivated and the knee is free to flex during the swing phase. Then, before the lower leg hits the kneecap on its forward swing, the magnet is reactivated in order to catch and hold the lower leg straight for the subsequent stance phase. Dribbel is similar to the planar kneed robot developed before. The only differ on the fact that *Knee* model doesn't provides the mechanical locking at the kneecup that the *Dribbel* do.

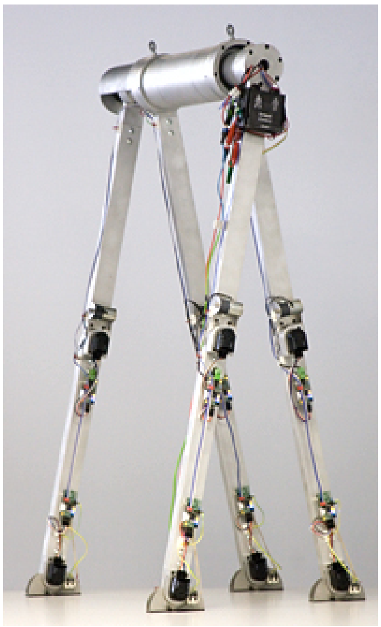

Figura 2.7: Dribbel mechanism

Dynamic model of Dribbel

Simulation model

To develop a simulation or an optimization model of Dribbel, we make the assumption that the links of the robot are rigid and the joints ideal as previously. We also assume that the legs move in pairs, meaning that the inner legs move together and the outer legs move together, in particular the lower legs. Have been used, in addition, the same values of mass, center of mass, and inertia of the ones used with *Knee*. Take a look to the table 2.3 and the figure 2.8 that highlights the *Dribbel's* physical parameters (the same of *Knee* model) and also the position of the joints, and the setup of the coordinates q_1 through q_6 as indicated.

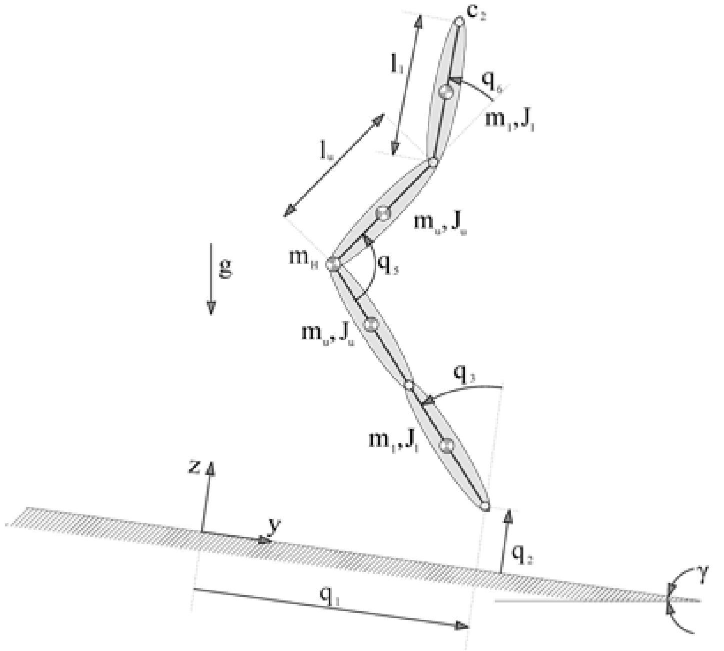

Figura 2.8: Dribbel mechanism

m_H	3,0 [kg]
m_l	1,6 [kg]
m_u	1,52 [kg]
J_l	0,0592 [mm^4]
J_u	0,0663 [mm^4]
l_l	0,43 [m]
l_u	0,47 [m]

Tabella 2.3: Physical parameters of Dribbel model.

Since the robot was constructed to behave like a planar walker, we construct a mechanical model that only represents the lateral behavior of the robot. In addition, was modelled the feet as point feet, and possible contact with the ground as rigid contact. The resulting model can be used for simulation of the planar behavior of Dribbel. The particular thing that differs from the *Knee* model, is the fact that the coordinate $q_4 = 0$ for all the duration of the gait.

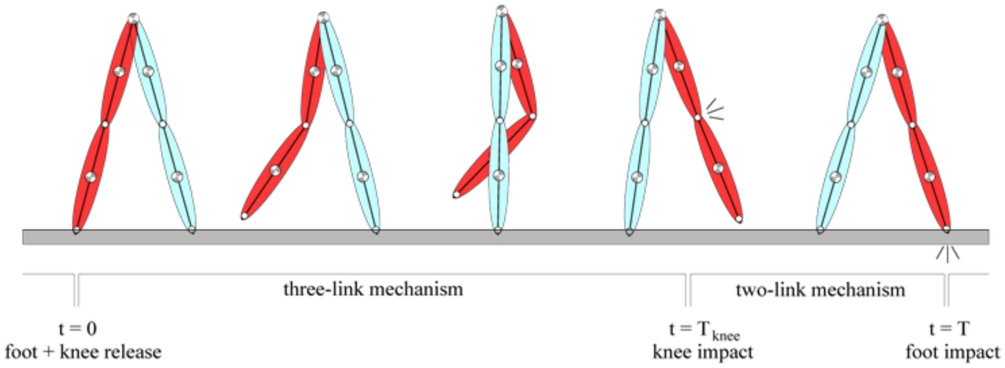

Figura 2.9: *Dribbel* walking gait

Figure 2.9 shows a single step of *Dribbel* that is split into two phases: the first phase from foot lift-off until knee strike (modeled as a three-link mechanism), and the second phase from knee strike until foot strike (modeled as a two-link mechanism). It is possible to swich between these two configurations due to the knee locking mechanism implemented for *Dribbel*. This mechanism, consists in mechanically lock the swing leg in correspondence of the knee strike before the one on the ground. The locking happen introducing a desired torque acting to the relative coordinate q_6 that has the purpose to keep the leg straight till the end of the gait.

2.4 *Compass* Model

The compass model is the one like in the figure 2.10. Compass was developed by many authors since a long time but the main important results in studing this kind of mechanism were proposed by Goswami 1998 [5] and [5], with his studies involving stable passive limit cycles and bifurcations. It is a mechanism consisting of four strigth legs which are connected in pairs, such that both the two outer legs and the two inner legs move together. The feet are little wheels and that means that the surface of the feet in contact with the ground is circular, thing that, how proved by F. Asano [38], is very effective on the walking efficiency.

Compass has characterized by the fact that is one of few models that can exibit a passive dynamic walking proceding downhill along a certain slope with some particular physical characteristics. The model is simply made by two straight legs jointed at the hip point through a rotational joint. How can be easily noticed from the figure 2.10, the walker needs to be tested with help of some platforms that ensure that the model doesn't fall down cause of premature strikes on the ground of the swing leg's foot (this could happen cause of the same length of the two legs). These strikes can happen due to some perturbations of the walking behavior or because not optimal initial conditions.

Dynamic model of *Compass*

Simulation Model

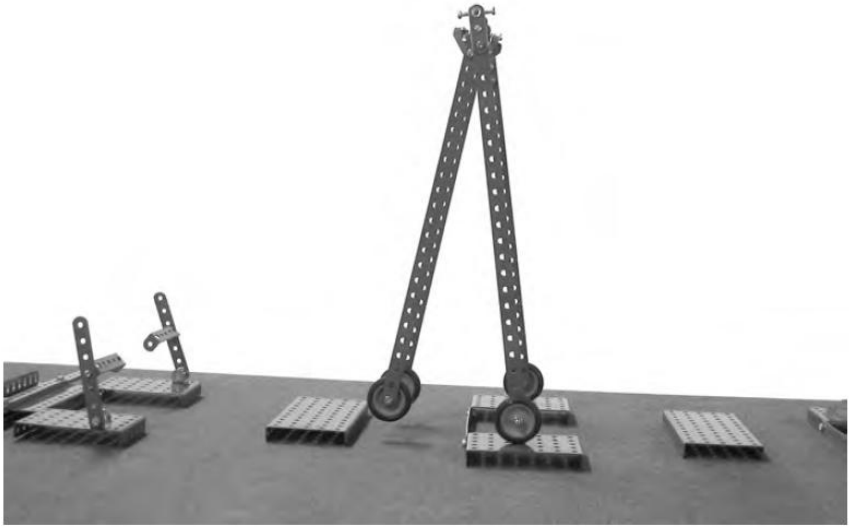

Figura 2.10: Compass like bepedal walker.

To develop a simulation model of Compass, is assumed that the links of the robot are rigid and the joints ideal. It is also assumed that the legs move in pairs, meaning that the ineer legs move together with the outer legs. The value of mass that have been used are summarized in the table below:

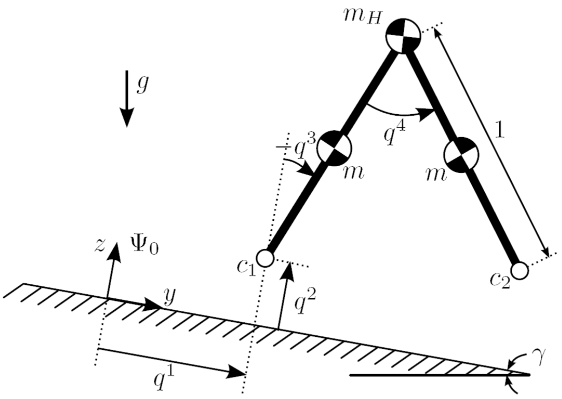

Figura 2.11: Compass mechanical model.

The physical values are taken from Goswami 1998 [6]. The physical parameters are shown also in the figure 2.11 where are shown also the coordinates from q_1 to q_4. Since the robot was constructed to behave like a planar walker, we construct a mechanical model that only represents the lateral behavior of the robot. In addition, was modeled the feet as point feet, and possible contact with the ground as rigid contact. The re-

m_H	5,0 [kg]
m	1,0 [kg]
l	1,0 [m]

Tabella 2.4: Physical parameters of *Compass*.

sulting model can be used for simulation of the planar behavior of Compass.

The model consists of two legs with a concentrated mass m in the middle of each leg, linked with a joint in top position of mass m_H. The feet come in contact with the ground which is tilted of an angle γ as shown in the figure 2.11.

The figure 2.12 below, is representing the walking gait in which are highlighted the main important instants.

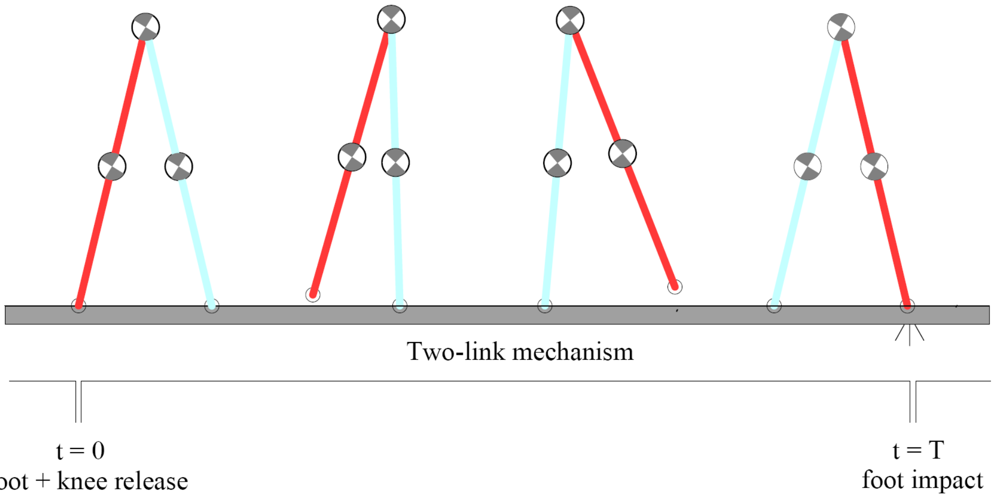

Figura 2.12: Compass walking gait.

2.5 Step Model

The hypothesis of this thesis are that the entire walking cycle is symmetric. That means the gait is the same considering the phase in which the left leg of the system is pivoted on the ground for walking, and the phase in which the right leg do it. That is possible only after the re-labeling operator that re-allocate the right coordinates to the right joints.

The Step Model (SM) is the precise description of the most significant events that characterize the step during its developing. In order to clarify the concept, we must assume that the dynamics of a walker mechanism, such as those analyzed in this thesis, is an impulsive dynamic, as a sequence of impulsive events (strikes) interacting with the continuous dynamic of its own mechanism. The model is, thus, a characterization of the walk carefully defined the number of strikes and their temporal order of occurrence. The number of strikes and the order have to be, obviously congruent with the physical constraints and with the symmetry of the walking cycle. Take a look to the figure below:

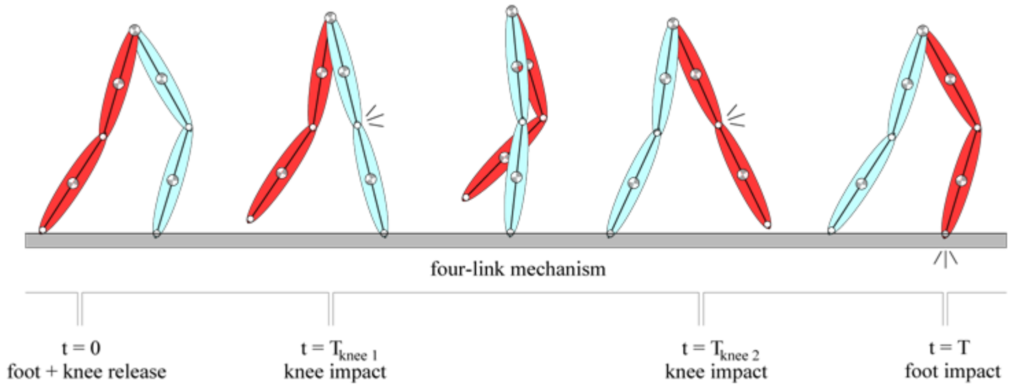

Figura 2.13: Knee walking motion of the gait. There are highlighted the most important event that characterize its dynamic.

Making an example, can be noticed how the step model (SM) shown in the figure 2.13 above is defined. The mechanical model used for this example is *Knee*. The Step Model provides three different strikes in the following order:

- Strike of the knee of the stance leg (*knee1*)
- strike of the knee of the swing leg (*knee2*)
- strike of the foot of the swing leg on the ground (final instant of the gait)

That step's model highlights the main important instants of the walking in correspondence of which, the impulsive dynamic interact with the continuous one. With those assumptions, the analysis model of a step brings that the gait can be split into three continuous phases: between $t = 0$ and $t = Tknee1$, then between $t = Tknee1$ and $t = Tknee2$ and then, between $t = Tknee2$ and $t = T$. Where $Tknee1$ is the instant of the strike that happen on the knee of the stance leg (relative to the coordinate q_4), $Tknee2$ is the same of before for the swing leg's knee (relative to the coordinate q_6) and T is the final time of the gait in which happen the strike to the ground. The SM considered with this example, is one of the possible SMs can be created just, for example, adding other strikes referring to the stance or to the swing leg. This concept has been introduced in order to investigate the influence of the impulsive dynamic on the continuous dynamic of the walking system. In fact, the optimization routine implemented in the next chapter, was designed considering the SM of the walking gait like an input of the routine and so, modifying this inputs, we will investigate the effects of the impulsive dynamic (referring to the number of strikes and their order) over the continuous (referred to the natural walking behavior of the mechanisms). The optimization algorithm, as constructed, requires that have been set, in advance, the SM we want to investigate, and this brings as a consequence, that a huge number of optimization routines have to be performed in order to give a sort of generality to the research. This is a limitation for the algorithm. This problem was studied, but the problem is the very functioning of the optimization routines that did not allow great results in this direction. I found it difficult for the optimization to combine the management of continuous parameters such as coefficients of polynomials (these will be the parameters of the optimization routines better described in the following paragraph), with the management of discrete parameters as required, moreover, from the introduction of parameters like the number of strikes and the order of occurrence of the latter. Furthermore, the automatically recognition of the strike (if there is) by the MatLab routine is an operation that is hard to reconcile with the optimization of the parameter's vector $\boldsymbol{x_p}$, since the very advent of the strike made sure that the parameters that in this moment are satisfying the constraints of the optimization, immediately after the strike, they don't do it anymore, (due to the projection and re-labeling operator) and this ensure that the optimizer diverges from that position that, just an instant before it, he evaluated be good and in the direction of the optimal solution. These and other problems are the basis of the decision to drop the general optimization algorithm (i.e. that would be responsible not only to optimize the parameters vector $\boldsymbol{x_p}$ but also the number and order of timing of any strikes of the model, if they occur), and to concentrate on an algorithm that would be of general validity, however, but that is capable to optimize the coordinates of the system with the number and temporal order of the strikes assigned. This type of algorithm is valid, in general, if it's possible to establish that any other SM produce an optimization worse (from the point of view of the objective function) than the considered one. This was faced performing a huge amount of optimizations, varying a great amount of possible SMs and evaluating from time to time the Objective Function (OF) value J. The table3.2 below is showing the nomenclature and symbolism used to completely determine a SM.

Symbol	**Description**
str	Locate the strike of any kind (to the ground or knee).
N_s	Number of strikes.
γ	Slope of the terrain. $[rad]$
$*\_*\_*$	Temporal order of occurrence of strikes (E.g. 1_2_gr. - 1 and 2 refer to the strike taking place at the knee, respectively, for the stance leg and for the swing leg).
n	Degree of the polynomials which represents the independent coordinates.
$\gamma n N_s str * \_ * \_ *$	Acronym that identify the step's model with all its parameters.
gr	Reference to the strike that happens to the ground at the end of the gait.

Tabella 2.5: Nomenclature and symbolism used to completely determine a Step Model.

For example, one SM defined: $345str1\_1\_2\_1\_gr$, is a model that provides the descent of the mechanism on a plane with a slope of three degrees, with a grade of polynomials equal to four, which presents five strikes. The first two occur at the knee of the stance leg (which can be identified with the number 1 that refers, precisely, to the stance leg), then one at the knee of the swing leg (number 2 is referring to the swing leg), then again another one at the knee of the stance leg and at the end, of course, the one that happens on the ground (gr). As one can easily imagine, for the three mechanical models I had considered in this chapter (i.e. *Knee*, *Dribbel* and *Compass*), but in general, for any bipedal walker, cannot be present a number of strikes less than one per gait that correspond to the only presence of the strike to the ground at the end of the gait. That is, in addiction, a binding condition for the optimization.

CAPITOLO 3

Optimization

3.1 Optimization Algorithm

In order to study walking behavior, we have to find walking gaits of a mechanism: periodic motions of the links of the mechanism that, together with interactions with the ground, produce a net overall displacement along the ground. Next section describes a technique to find efficient walking gaits using numerical optimization. The following section then, describe the modeling and analysis of the three proposed walking mechanisms: *Compass*, *Dribbel* and *Knee*. The simplified models, which were developed in the previous sections, as in general any mechanism that can be thought, has a dynamic that is described by a set of differential equations that describe the movement, and so the continuous dynamic, since the beginning of the step up to the end. Then, there are the equations of projection and re-labeling that link the positions and angular velocities in correspondence of the strikes, to the positions and velocities just after the strike. The structure of the walking is, more or less, the same for all the models proposed in this thesis, and figure 3.1 is giving an example: The figure 3.1 illustrates the model of a planar bipedal walking robot with knees (*Dribbel* model) and highlights a certain period of time for the walk cycle that consists of two steps, one with his left foot centered on the floor and one on his right foot.

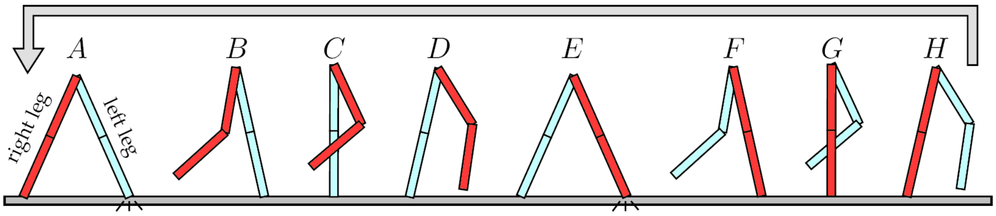

Figura 3.1: Walking Cycle.

The cycle of the walk is considered as the union of the step during which acts as a pivot the left leg, plus the phase in which acts as a pivot the right leg. This cycle is repeated over time (starting from point A after posture H), and is also symmetric with respect to both left and right legs. If we use the coordinates $\boldsymbol{q}(t)$ to describe the movement of the robot with the left foot centered on the ground, we can then use a mapping $\boldsymbol{G}$ to describe the symmetrical movement focusing on the right foot. The cycle of the total movement $A - E - A$ can also be represented as a conjunction of two single gaits (the one starting from A to E and the other starting from E to A again) of which the first

is described by the coordinates $\boldsymbol{q}\,(t)$ and the second, by the coordinates $\boldsymbol{Gq}\,(t)$.
An important aspect of the research of efficient walking is what is called the Passive Dynamic Walking, which is the search for natural, not actuated, periodic movement of the mechanism (also called passive limit cycle), that appears sometimes in circumstances that have a path with a sharp downhill slope along the way.
The existence of this limit cycle depends on the configuration of the robot, its mass distribution and of the presence, of course, of a downhill sole. If a passive limit cycle exists, this may be attractive (stable) or not (unstable). For defining a limit cycle we have firstly introduce the state variables vector defined like:

$$\boldsymbol{x} = [\boldsymbol{q}, \dot{\boldsymbol{q}}]^T$$

The flow of $\boldsymbol{x}$ is the trajectory which begins at the initial condition $\boldsymbol{x}\,(0) = \boldsymbol{x}_0$ and ends at $\boldsymbol{x}\,(t)$. The flow is denoted $\phi\,(\boldsymbol{x}_0, t)$ to explicitly show dependence on initial condition and time. If, for some initial condition $\boldsymbol{x}^*$ and some time T.

$$\phi\,(\boldsymbol{x}^*, t) = \boldsymbol{x}^* \tag{3.1}$$

we say the flow $\phi\,(\boldsymbol{x}^*, t)$ is a *periodic solution*. Although difficult to visualize in higher dimensions, a periodic solution in two or three dimensions would look like a closed loop (take a look to the figure 3.2). If the periodic solution is isolated - that is, there is a neighborhood around it containing no other periodic solutions - then we call it a limit cycle. If all trajectories beginning in some neighborhood around a limit cycle converge to the limit cycle, we say it is stable. We give the name basin of attraction to the neighborhood surrounding a stable limit cycle which contains all the initial conditions that will converge to the limit cycle. For our robot models, a limit cycle in the state space indicates that a physical robot will walk continuously under the same initial conditions. We can start the robot with an initial set of joint angles and angular velocities and allow it to evolve over time until the nonsupport foot strikes the ground. If, after the ground impact, the robot begins its step with positions and velocities identical to the previous step, we see a periodic solution of the flow. If it turns out that the robot returns to the periodic solution despite small perturbations, we conclude that this periodic behavior is a stable limit cycle. A passive limit cycle draws energy solely from the acceleration of gravity, replacing the kinetic energy lost during impacts with energy gained from the change in potential energy during each step. The biped walking system *Compass* described in this thesis demonstrated passive limit cycle ([5], [38], [39]); it was shown how the system walk continuously down shallow slopes. Mechanisms to be able to perform a passive dynamic walking, have an autonomous dynamic and therefore the initial conditions completely determine the motion. The deterministic function $\boldsymbol{F}(*)$ that maps the initial conditions at the beginning of a step up to the initial ones of the next step, then the combination of continuous dynamics, projection operator and the re-labeling operator of coordinates, is called return map (*stride function*) and it serves as a *Pointcaré map* for the system that maps the the state values of the system from one step to another into the Pointcaré surface. A Poincare surface samples the flow (defined before $\phi\,(\boldsymbol{x}^*, t)$) once every period. The effect is much like a strobe light that illuminates a walking human at the same time during each step. If, over time, the strobed images become identical, the human has settled into a stable walking pattern. In a similar manner, if the points on a Poincare surface converge to a single point, we have found a stable limit cycle. As the name suggests, a Poincare map is a mapping from one point to another on the Poincare surface. For an example take a look to the figure 3.2.

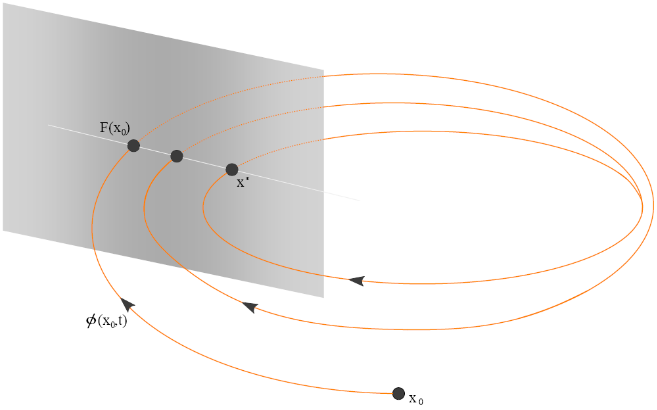

Figura 3.2: Pointcaré Map.

The map shows the initial conditions of the mechanism that map themselves through the integration of continuous dynamic and through the projection operators and, the relabeling operator. Since the Poincaré map involves integration of nonlinear differential equations, it is usually not available symbolically, and searching for fixed points is hence a numerical problem. As an example, see Goswami et al. (1998), [36] for a detailed study of the Poincaré map of the compass-gait walker. The approach of searching for fixed points of the Poincaré map is very useful in passive dynamic walking, as it has few degrees of freedom (just the initial conditions of the system, which are often partially fixed due to the choice of the starting point of a cycle). However, it relies on the restriction to autonomous systems, i.e. systems with zero control input, or at least an input that is chosen a priori. When walking down a slope, zero-input limit cycles have been shown to exist for various walking mechanisms. However, for walking on level ground, purely passive walking cycles generally do not exist, since the kinetic energy lost during impact cannot be recovered fromgravity. Some ideal walking mechanisms can be found that touch the ground with zero velocity (Gomes & Ruina 2005 [40]) and hence do not loose energy on impact, but these are exceptions. Thinking about walking on general surfaces (whether uphill or downhill), we don't have to carry out a search for the pure passive movement, but at this point it is possible looking for a natural and efficient one. In this way, however, we must consider the mechanism directly and fully actuated (are actuated all the coordinates of the system) by ideal back-driveable motors, and therefore, the natural and efficient movement of the mechanism is the one for which the actuators are required to spend the small amount of torque that's possible. Passive dynamic walking, in fact, is solely the extreme case that does not require any torque to the actuators, but if this movement does not exist, the best we can do is to find the movement that requires the least amount of torque that's possible. Here, then, we can refer the problem to an optimization problem which aim is to find the optimal movement in terms of energy consumption of the actuators in order to make the system be able to make a step consistent with the physical and kinematic constraints of the walking. In order to properly determine a measure for the amount of torque, we define a function in the space of torques representing the cost of actuation.

For convenience we consider a function defined in the form $\boldsymbol{\tau}^T \boldsymbol{Q}(t)\,\boldsymbol{\tau}$, a quadratic form in the space of torques $\boldsymbol{\tau}(t) = \boldsymbol{\tau}(\boldsymbol{q}(t), \dot{\boldsymbol{q}}(t), \ddot{\boldsymbol{q}}(t))$, dependent of the time and of the configuration of the robot and of its velocities and accelerations. So we can define the problem of finding an efficient step as the following minimization problem: The problem of search for an efficient step is the problem of finding the coordinates of the joints $\boldsymbol{q}(t)$ that solve,

$$\min_{\boldsymbol{q}(t)} \int_0^T \boldsymbol{\tau}^T(t)\,\boldsymbol{Q}(t)\,\boldsymbol{\tau}(t)\,dt \tag{3.2}$$

Where the matrix $Q(t)$ is semi-positive definite. The minimization algorithm is then liable to the following constraints:

$\boldsymbol{\tau}(t) = \boldsymbol{\tau}(\boldsymbol{q}(t), \dot{\boldsymbol{q}}(t), \ddot{\boldsymbol{q}}(t))$	This equality constraint forces the optimization, and then the research of the optimal coordinate, to be bound to the dynamics dictated by its dynamic equation.
$q_{+r} = Gq_-$	Equality constraint which expresses the relationship between coordinates at the beginning of step $\boldsymbol{q}_{+r}$ and coordinates at the end of step $\boldsymbol{q}_-$ through the re-labeling operator.
$\dot{q}_{+r} = G \cdot P_{proj}(q_-) \cdot \dot{q}_-$	Equality constraint that represent the link defined by the operator of projection of the velocity after a strike.

Tabella 3.1: Main Constaints of the minimization problem

Where $\boldsymbol{\tau}(\boldsymbol{q}, \dot{\boldsymbol{q}}, \ddot{\boldsymbol{q}})$ is the dynamics of the system, $\boldsymbol{G}$, describes the re-labeling of the coordinates, $\boldsymbol{P}_{proj}(\boldsymbol{q})$ is the projection of the moment due to the impact (a generic impact - ground or knee), and where $\boldsymbol{q}_- = \boldsymbol{q}(t_-)$ and $\boldsymbol{q}_{+r} = \boldsymbol{q}(t_+)_r$, are respectively the coordinates at the instant before impact, and at the instant immediately after that, with re-labeling.

The problem is therefore to find the coordinates of the joints $\boldsymbol{q}(t)$ for a step (between $t = 0$ and $t = T$) so that the total integration of the torque $\boldsymbol{\tau}(t)$ is minimized in the metric $\boldsymbol{Q}(t)$, and so that the initial conditions $(\boldsymbol{q}_{+r}, \dot{\boldsymbol{q}}_{+r})$, are compatible with the final conditions ($\boldsymbol{q}_-, \dot{\boldsymbol{q}}_-$) projected and re-labeled. The relation, for example, between $\dot{\boldsymbol{q}}_{+r}$ and $\dot{\boldsymbol{q}}_-$ is the successive projection $\boldsymbol{P}_{proj}(\boldsymbol{q})$ of the moment due to of the impact and the re-labeling of the projected velocities with the operator $\boldsymbol{G}$. Additional constraints may be added, for example, to enforce a certain walking speed or to require that the period of the walk $T > 0$, or many others. Find the optimal trajectories $\boldsymbol{q}(t)$ that solve the problem defined above, is a problem of infinite dimensions, and then we introduce an approximation in finding the optimum gait. Then the trajectories of the joints are parameterized as polynomial functions of time:

$$\boldsymbol{q}^i\,(t) = \sum_{j=0}^{n} b_{ij}\boldsymbol{t}^j = b_{i0} + b_{i1}\boldsymbol{t} + b_{i2}\boldsymbol{t}^2 + ... + b_{ik}\boldsymbol{t}^n \tag{3.3}$$

For each coordinate $\boldsymbol{q}^i\,(t)$ and for some integer constant $n > 0$. The i runs the related coordinate from 1 to m where m is the number of degrees of freedom of the mechanism under analysis. The advantage of taking a polynomial base to build the coordinates upon is that's easy to derive and the calculation of velocities and accelerations of the coordinates of joints ($\dot{\boldsymbol{q}}\,(t)$ and $\ddot{\boldsymbol{q}}\,(t)$), are of immediate resolution, and also for the fact that they are suitable for approximating functions that change slowly over time,just as I expect the coordinates to be. This is because rapid changes in the functions imply a large amount of torque of the actuators, but the optimization algorithm obtain the movement with the minimum actuation. The problem then is modified as follows: The problem of finding an efficient and approximate gait, is the problem of finding the parameters b_{ij} that solve:

$$\min_{b_{ij}} \frac{T}{N} \sum_{p=1}^{N} \boldsymbol{\tau}^T\,(t_p)\,\boldsymbol{Q}\,(t_p)\,\boldsymbol{\tau}\,(t_p) \tag{3.4}$$

Where $\boldsymbol{Q}\,(t)$ is a semi - positive definite matrix and N is a positive integer, and T is the period of the gait. The problem is subject to the following constraints:

$\boldsymbol{\tau}\,(t_p) = \boldsymbol{\tau}\,(\boldsymbol{q}\,(t_p)\,, \dot{\boldsymbol{q}}\,(t_p)\,, \ddot{\boldsymbol{q}}\,(t_p))$	This equality constraint forces the optimization, and then the research of the optimal coordinate, to be bound to the dynamics dictated by its dynamic equation.
$\boldsymbol{q}^i\,(t) = \sum_{j=0}^{k} b_{ij}\boldsymbol{t}^j$	Constraint linking the parameters to optimize b_{ij} to the evaluation of the coordinates.
$q_{+r} = Gq_-$	Equality constraint which expresses the relationship between coordinates at the beginning of step $\boldsymbol{q}_{+r}$ and coordinates at the end of step $\boldsymbol{q}_-$ through the re-labeling operator.
$\dot{q}_{+r} = G \cdot P_{proj}\,(q_-) \cdot \dot{q}_-$	Equality constraint that represent the link defined by the operator of projection of the velocity after a strike.

Tabella 3.2: Main Constaints of the minimization discetized problem

Where $\boldsymbol{\tau}\,(\boldsymbol{q}, \dot{\boldsymbol{q}}, \ddot{\boldsymbol{q}})$ is the dynamics of the system, $\boldsymbol{G}$, describes the re-labeling of the coordinates, $\boldsymbol{P}_{proj}\,(\boldsymbol{q})$ is the projection of the moment due to the impact (a generic impact - ground or knee), and where $\boldsymbol{q}_- = \boldsymbol{q}\,(t_-)$ and $\boldsymbol{q}_{+r} = \boldsymbol{q}\,(t_+)_r$, are respectively the coordinates at the instant before impact, and at the instant immediately after that, with re-labeling.

The result of the optimization problem is the vector of coordinates $\boldsymbol{q}(t)$ representing the trajectories more natural and efficient in terms of actuation. This means that the algorithm can be used to find a natural and efficient step also for mechanisms moving up-hill or in other circumstances in which the passive dynamic walking does not exist.

3.2 Optimization algorithm - General discussion

In this section, there will be presented all the routines that constitute the optimization algorithm. There are presented in order to describe the meaning and the function of every subroutine, and how these interact to each other. The algorithm was implemented in MatLab and consist essentially in using the function *fmincon* from the library of MATLAB functions. This function allows us to find the minimum of a function that's subject to nonlinear equality or inequality constraints. The algorithm minimizes a certain objective function J defined in the space of torques $\boldsymbol{\tau}(\boldsymbol{q}, \dot{\boldsymbol{q}}, \ddot{\boldsymbol{q}})$ (See previous section 3.1) to obtain the optimal curves that represent mechanism's coordinates in the space of a step. For the optimization, needs to be defined the mechanical system used, and the Step Model (SM). The considered parameters are, therefore, the coefficients of polynomials b_{ij} and the time instants when the strikes occur. That said, a kind of optimization routines includes a *main script* from which are set all the sensitive parameters, of the optimization of the model we are considering:

Parameters	*Description*
links	Number of links that make up the analyzed mechanism.
n	Degree of polynomials representing the coordinates of the system.
P_T	Number of stikes (depending on the analyzed model).
P_M	Number of the intrinsic parameters of the system (mass, inertia and length of links).
γ	Downhill slope of the terrain.
x_p	Vector containing the parameters to optimize.

Tabella 3.3: Parameters of the optimization routine

The variables of the optimization are all collected into the parameter's vector $\boldsymbol{x}_p$ defined as

$$\boldsymbol{x}_p = \begin{bmatrix} b_{11} & b_{12} & \dots & b_{1j} & b_{21} & b_{22} & \dots & b_{2j} & \dots & param\_body & param\_time \end{bmatrix}^T \tag{3.5}$$

Where *param_body* is the vector that collect all the physical parameters (the ones are keps constrained during the these optimizations), and *param_time* is the vector that collect all the time instant of the various strikes provided by the SM. The parameters b_{ij} are in number equal to $n \cdot P_T \cdot links$ and define all the $P_T \cdot links$ parts of coordinates with a polynomial of grade equal to n.

Here in the table 4.1 are defined also the references to the others MatLab subroutines, each performing some specific functions required by the optimization.

Sub-routine	*Description*
Costfun	The routine in MatLab, which defines the objective function we want to minimize. (the same for all configurations).
Constraints	The routine in MatLab, which defines the constraints of equality and inequality that has the system.
Curves	MatLab routine that builds, getting input vector $\boldsymbol{x}_p$ of the parameters to optimize, the curves representing the coordinates of the system.
Model	The routine that solves the direct dynamic of the system with the coordinates like input.
Projection	The routine implements the operator of projection and re-labeling of the coordinates when a strike occurs.
Plotstep	The routine does the representation of the optimized curves, represent the stick-diagram of the gait, and, in general, all the graphs or diagram useful for represent the results of the optimization.

Tabella 3.4: Sub-routines of the minimization algorithm

The parameters called *param_body* that, as I previously mentioned, are all intrinsic parameters of the system (mass, inertia, and lengths of links). These were considered in the algorithm, not as external and fixed parameters, but as internal parameters, and they also need to be optimize with the criterion of minimization previously shown. For the study and analysis that is presented, we need to consider the system, with the physical parameters fixed. For this reason, the physical parameters of the system were included as constraints in the *Constraints* routine in order to un-constrain these bonds if you want to optimize one or another physical parameter.

3.2.1 The Curves routine

The parameters to optimize are dependent on the mechanical model and the SM. These are the coefficients b_{ij} of polynomials of degree n defined in the section 3.1, which represent the coordinates of the mechanism. In addition to these factors, are optimized also the time-instants when the strikes defined in the SM occur. The time period of the duration of the step (which coincides with the time at which the last strike, the ground strike, happens), is, therefore, considered to be broken into as many parts as dictated by the number of strikes (N_s) used in the optimization model. In this way, the coordinates will be broken too and evaluated in multiple time periods. Each subinterval is then, time basis for the definition of coordinates of the given subinterval. Then we will get a set of parameters to optimize that will be, in number, amounting to

$n \cdot links \cdot P_T$, in addition to the parameters that identify the time values of strikes, plus the ones defining the prysical parameters. n is the grade of the polynomials representing the coordinates, *links* is the number of links which make up the system, and P_T, is the number of strikes occurring during the gait. For each subinterval of time, therefore, will be defined a number equal to *links* curves obtained using the relationship defined in the previous paragraph:

$$\boldsymbol{q}^i\left(t\right) = \sum_{j=0}^{n} b_{ij}\boldsymbol{t}^j = b_{i0} + b_{i1}\boldsymbol{t} + b_{i2}\boldsymbol{t}^2 + ... + b_{ik}\boldsymbol{t}^n \tag{3.6}$$

Where i is the index that runs the values between 1 and the value *links* , while j runs values from 0 up to n . This report is implemented in the routine of MatLab *Curves* , evaluating on time $t \in [0, T_k]$ (Where T_k is the i-th generic instant at which a strike occur), and as coefficient b_{ij} the values that are evaluated from each iteration to another of the optimization.

3.2.2 The Costfun routine

The routine *Costfun*, however, implements the calculation of the objective function that we want to minimize in the optimization process. The routine includes in its implementation another routine (*Model*), which calculates the direct dynamics of the mechanical system and obtains the value of the energy of torques of actuators that are equal, in number, to the degrees of freedom of the system (bacause the system is fully actuated). The calculation of the value of the actuation $\boldsymbol{\tau}_k$ (Value of the actuation for the individual k-th time interval), is used to calculate the objective function that we want to minimize. It is reproduced below:

$$J = \sum_{k=1}^{params} \left(\frac{T_k}{N_k} \sum_{p=1}^{N_k} \boldsymbol{\tau}_k^T\left(t_{p,k}\right) \boldsymbol{Q}\left(t_{p,k}\right) \boldsymbol{\tau}\left(t_{p,k}\right) \right) \tag{3.7}$$

Where $\boldsymbol{Q}\left(t_{p,k}\right)$ is the weights matrix semi-definite positive and N_k is a positive integer that defines the number of points of discretization which is discretized the k-th time interval, and T_k is the k-th period that goes from the initial instant of time ranging to T_1 , if we consider the first interval, and ranges from T_{k-1} to T_k for subsequent periods. The function thus defined, is a quadratic function of the actuation of the system and presents a matrix of weights that for simplicity and generality have been considered always equal to the identity matrix in the various optimizations .

3.2.3 The Projection routine

The entire optimization algorithm also presents an additional routine that serves to implement the projection function of speed and re-labeling of the coordinates after each strike. In particular, the function of re-labeling and the projection of velocities are implemented in a routine called *projection* performing both operations simultaneously: First, the projection of the velocity after a strike is expressed by the following relationship,

$$\dot{\boldsymbol{q}}_i\left(t_+\right) = \left(\boldsymbol{I} - \bar{\boldsymbol{M}}_i^{-1}\boldsymbol{J}_I^T\left(\boldsymbol{J}_I\bar{\boldsymbol{M}}_i^{-1}\boldsymbol{J}_I^T\right)^{-1}\boldsymbol{J}_I\right)\dot{\boldsymbol{q}}_i\left(t_-\right) = \boldsymbol{P}_{proj}\dot{\boldsymbol{q}}_i\left(t_-\right) \tag{3.8}$$

The second (i.e. the operator to re-label), however, is not always present (this is only for the strike to the ground), and when present, is characterized by the matrix $\boldsymbol{G}$. The operation is implemented using the following equation:

$$\left\{ \begin{array}{l} \boldsymbol{q}\left(t_{+}\right)_{r} = \boldsymbol{G}\boldsymbol{q}\left(t_{-}\right) \\ \dot{\boldsymbol{q}}\left(t_{+}\right)_{r} = \boldsymbol{G}\dot{\boldsymbol{q}}\left(t_{+}\right) \end{array} \right. \tag{3.9}$$

Before making the re-labeling operation, there is the need of making an extraction operation from the vector $\dot{\bar{\boldsymbol{q}}}\left(t_{+}\right)$. In fact, after the projection operator, is obtained, like result, the vector $\dot{\bar{\boldsymbol{q}}}\left(t_{+}\right)$ that is different from the one used by the re-labeling operator ($\dot{\boldsymbol{q}}\left(t_{+}\right)$). For obtaining the vector $\dot{\boldsymbol{q}}\left(t_{+}\right)$ needs just a simple extraction operation due to the matrix $\boldsymbol{E}_{ex}$ defined below:

$$\dot{\boldsymbol{q}}\left(t_{+}\right) = \boldsymbol{E}_{ex}\dot{\bar{\boldsymbol{q}}}\left(t_{+}\right) \quad \boldsymbol{E}_{ex} = \begin{bmatrix} 0 & 0 & 1 & 0 & 0 & 0 \\ 0 & 0 & 0 & 1 & 0 & 0 \\ 0 & 0 & 0 & 0 & 1 & 0 \\ 0 & 0 & 0 & 0 & 0 & 1 \end{bmatrix} \tag{3.10}$$

With regard to the relations just given, $\bar{M}\left(\bar{q}\right) \in \mathbb{R}^{m+2\times 2}$ is the mass matrix of the system, the matrix $\boldsymbol{G}$, is the operator of re-labeling, while the function $\boldsymbol{P}_{proj}$ is the projection operator of the velocities operating between the velocities just before impact and getting those one immediately after that. This is subsequently re-labeled for obtaining $\dot{q}\left(t_{+}\right)_{r}$. As is easily understood, if the strike is one of those that occur at the level of the knees of the system, the model does not need to re-label the coordinates after the strike, while if this happens on the ground, the matrix $\boldsymbol{G}$ exists, and has different forms depending on the mechanical model considered. The matrix $\boldsymbol{J}_{I}$, as seen above, that is the Jacobian matrix, obtained by setting the geometric condition at the impact. Obviously $\boldsymbol{J}_{I}$ changes depending on the impact (strike) and the model considered.

3.2.4 The Model routine

The routine Model takes care of solving the continuous dynamic of the mechanical system. The routine implements the resolution of the differential, second order matrix equation that defines the system's dynamics. The equation is presented in most cases with the following form:

$$\boldsymbol{M}\left(\boldsymbol{q}\right)\ddot{\boldsymbol{q}} + \boldsymbol{C}\left(\boldsymbol{q},\dot{\boldsymbol{q}}\right)\dot{\boldsymbol{q}} + \boldsymbol{V}\left(\boldsymbol{q}\right) = \boldsymbol{S}\left(\boldsymbol{q}\right)\boldsymbol{u} \tag{3.11}$$

Where $\boldsymbol{M}\left(\boldsymbol{q}\right) \in \mathbb{R}^{m\times m}$ is the mass matrix of the system and collects the inertial terms, $\boldsymbol{C}\left(\boldsymbol{q},\dot{\boldsymbol{q}}\right) \in \mathbb{R}^{m\times m}$ collects together elements of centrifugal force and Coriolis forces, the term $\boldsymbol{V}\left(\boldsymbol{q}\right) \in \mathbb{R}^{m\times 1}$ contains the terms due to the potential energy of the system, while is the control action and $\boldsymbol{S}\left(q\right)$, because of the co-location of the actuators, in the cases analyzed, will always be considered equal to the identity matrix. m is the number of degrees of freedom of the considered mechanism (the length of the vector $\boldsymbol{q}$). In practice, the routine solves the equation above, obtaining values $\boldsymbol{\tau} \triangleq \boldsymbol{S}\left(\boldsymbol{q}\right)\boldsymbol{u}$ and then evaluating the objective function. To do that takes as inputs the coordinates, velocities and accelerations ($\boldsymbol{q}\left(t\right)$, $\dot{\boldsymbol{q}}\left(t\right)$, $\ddot{\boldsymbol{q}}\left(t\right)$) previously evaluated by the routine *Curves*, and calculate the direct dynamic.

3.2.5 The Constraints routine

The routine called *Constraints* is the one that contains all the inequality and equality constraints that drive in a certain way the optimization. The script manages two large matrix in which are defined the constraints of strict inequality (matrix $\boldsymbol{C}$), and the the equality constraints (matrix $\boldsymbol{C}_{eq}$). Many of the constraints that are set in routine, derive from considerations dictated by common sense and by my own, but also our own, experience (we humans) on bipedal walking and on constraints that the walker requires.

Others are purely dictated by mechanical constraints of the walk and by the model itself, as, for example, prevention of over-extension of the two links (that make up the leg) straddling the knees (not for *Compass*), or as the constraint of no penetration of the foot of the system in the ground during the swing phase (ground clearance), etc. Additional constraints are dictated by the fact that is considered just a single step for the optimization of the system and, therefore, the walk is considered symmetrical respect the two phases of the walking cycle (symmetric respect the phases in which is the left leg to be focused on the ground and the other in which is the right one to be focused). This type of constraints ensures that the angular positions (the degrees of freedom of the model are all revolute-type) of the coordinates are the same at the beginning and at the end of the step, naturally taking into account the re-labeling operator.

One of the constraints derived, for example, by common sense and human experience, is the constraint to limit the flexion of the leg in a narrower range, or to limit the amplitude of the decoupling between the two legs with the related rotational coordinate q_5 . Or again, to set manually the preferential direction towards which the system will evolve with his continuous dynamic.

As is known, for optimization of highly non-linear objective functions, and in general, very complex and having several parameters, it is often necessary to use re-iterations of the optimization routines un-constraining, iteration after iteration, further constraints constructed ad hoc to allow the optimizer to proceed groping toward the optimal solution. Therefore, the additional constraints to guide the research are: constraints on the velocity of the rotational joints, and constraints on time instants, constraint on the final instant (strike to the ground) or to the instants in which the knee strikes happen. These constraints will be unlocked now and again, to get the best seeked results.

3.2.6 Optimization - Issues

The problems of the optimization routines are those outlined in the section 3.1. In addition there is the fact that the optimization algorithm, and in general the optimizations of very non linear functions, are very dependent by the initial condition. In that case, the vector ($\boldsymbol{x}_p$) of the parameters to be optimized has to be initialized at the beginning of the optimization routine. The inizialization was done imposing random values to each of the parameters composing the $\boldsymbol{x}_p$ vector. The results, generally are strongly influenced by the chosen initial condition; for that reason, every singol optimization made for apport the results to this thesis was launched several times with different initial conditions, in order to validate the obtained results. The correct result was the one that showed the best trajectory behavior in terms of actuation cost. This problem, in other words, is related to the presence (because of the non linearity of the motion equations) of relative minimum points of the Objective Function (OF) toward which the optimization algorithm could tend because of the choice of the initial conditions. Changing the initial conditions (for several times - generally three times), assure that there are much more possibilities to tend toward the absolute minimum of the OF despite of the relative one. There are some cases in which the optimization algorithm doesn't converge to a reasonable solution, and there is the need to ever-constrain the optimization in order to drive the routine in the fisrt iterations. For doing that, there is the need to over-constrain the optimization for the first iteration steps, and then, unlock these, continuing the algorithm. For that reason, the result is strongly influenced by the choice of the additional constraints added because of this problem. These constraints, so, have to be congruent with the expected walking and with the physical limits of the system. In the majority of the cases, the most common constraints used for drive the optimization toward a reasonable direction are those one dictated by the common sense of what the walking should be, and by our own personal experience of human walkers. Some of those are the ones trated in the section 3.2.5 and generally they refers to physical constraints dealing with penetration into the soil, walking direction, over-extension of the legs, etc. and to human walking knowledge dealing with ranges into which the coordinates of the system may vary. All those constraints may influence the result of the optimization and so, could be appropriate vary the additional constraints between the various optimizations tests of the singol step model in order to better validate the obtained results.

CAPITOLO 4

Compass Model: Optimization and Simulation

4.1 Overview

In this chapter is analyzed the simpler mechanical bipedal model (*Compass*) walking down-hill. The purpose is to show the Passive Dynamic Walking (PDW) that this mechanism can exhibit with some characteristics of slope and physical parameters. Those characteristics were taken from Goswami 1998, [36] that was one of the first researcher to demonstrate, in simulation, the PDW of *Compass*. In this chapter was firstly analyzed the impact posture and characteristics of the final conditions though the singular value analysis, and then, was developed the optimization routine for the optimal coordinates of Compass, and then it is tested its dow-hill walking behavior in simulation. It is expected that the coordinates trends found with optimization and simulation routines are almost equal.

4.2 SVD - Singular Value Decomposition

The efficiency of a walking cycle is partly determined by the mechanical energy loss during the cycle, and partly by the non-idealness of the actuators of the system. The first aspect is analyzed in this section and the second one, is not treated in this thesis. More precisely, we focus here on the energy loss due to the impact of the feet with the ground at the end of each step. Other mechanical losses, such as friction are ignored. As I showed in the chapter 2, the relation between velocities before and after impact (section 2.1.4) can be useful to express the lost of the kinetic energy on impact written in terms of velocities as:

$$\Delta E_{hs} = \frac{1}{2}\left(\dot{\bar{\boldsymbol{q}}}_{+}\right)^{T} \bar{\boldsymbol{M}}\left(\bar{\boldsymbol{q}}\right)\dot{\bar{\boldsymbol{q}}}_{+} - \frac{1}{2}\left(\dot{\bar{\boldsymbol{q}}}_{-}\right)^{T} \bar{\boldsymbol{M}}\left(\bar{\boldsymbol{q}}\right)\dot{\bar{\boldsymbol{q}}}_{-} \leq 0 \tag{4.1}$$

By substituting (2.11) into (4.1) and eliminating $\dot{\bar{\boldsymbol{q}}}_{+}$, we can arrange ΔE_{hs} as follows:

$$\Delta E_{hs} = \frac{1}{2}\left(\dot{\bar{\boldsymbol{q}}}_{-}\right)^{T} \boldsymbol{J}_I^T \boldsymbol{X}_I^{-1} \boldsymbol{J}_I \dot{\bar{\boldsymbol{q}}}_{-} \tag{4.2}$$

And considering $\dot{\bar{\boldsymbol{q}}}_{-} = \boldsymbol{H} \cdot \dot{\boldsymbol{q}}_{-}$ Where

$$\boldsymbol{H} = \begin{bmatrix} 0 & 0 \\ 0 & 0 \\ 1 & 0 \\ 0 & 1 \end{bmatrix} \tag{4.3}$$

just because the velocities of the coordinates q_1 and q_2 are zero in correspondence of the instant immediately before the strike. this yields:

$$\begin{cases} \Delta E_{hs} = \frac{1}{2}\left(\dot{\boldsymbol{q}}_-\right)^T \boldsymbol{H}^T \boldsymbol{J}_I^T \boldsymbol{X}_I^{-1} \boldsymbol{J}_I \boldsymbol{H} \dot{\boldsymbol{q}}_- \\ \boldsymbol{X}_I = \left(\boldsymbol{J}_I \bar{\boldsymbol{M}}^{-1} \boldsymbol{J}_I^T\right)^{-1} \end{cases} \tag{4.4}$$

Note, here, that $\boldsymbol{H}$, $\boldsymbol{J}_I$ and $\boldsymbol{X}_I$ are only function matrices of q_i . $\boldsymbol{H}$ is a matrix that has the purpose to construct the vector $\dot{\bar{\boldsymbol{q}}}_-$ from $\dot{\boldsymbol{q}}_-$. This is possible just because during the swing phase the two velocities $\dot{q}_1$ and $\dot{q}_2$ are zero.

J_I is the jacoian matrix defined in the section 2.1.4.

Let α (in radians) be the absolute value of the half inter-leg angle at the transition instant. The angular position in Figure 4.1 (posture at the impact) can be expressed as $q_3 = -\alpha$ and $q_4 = 2\alpha$. The following matrix $D \in \mathbb{R}^{2\times 2}$.

$$\boldsymbol{D} := \boldsymbol{H}^T \boldsymbol{J}_I^T \boldsymbol{X}_I^{-1} \boldsymbol{J}_I \boldsymbol{H} \tag{4.5}$$

Only becomes a function matrix of α . The dissipated kinetic energy finally yields

$$\Delta E_{hs} = -\frac{1}{2}\left(\dot{\boldsymbol{q}}_-\right)^T \boldsymbol{D}(\alpha)\, \dot{\boldsymbol{q}}_- \tag{4.6}$$

The matrix D was treated as a matrix function of α and m_H/m , the ratio between the hip point mass and the mass of each leg.

The kinetic energy loss on impact is hence, a quadratic function of the impact velocities at the last instant of the gait $(\boldsymbol{q}(T))$ depending generally on the inertial properties of the system as well as the posture (the coordinates $\boldsymbol{q}(T)$) on impact. If we consider *Compass*, and assume a symmetric walking cycle with instantaneous double-support phase, we can write the energy loss as a quadratic function of only $\dot{q}_3$ and $\dot{q}_4$, with $\boldsymbol{D}(\alpha)$ a positive semi-definite 2×2 matrix. For general m and m_H , the symbolic representation of $\boldsymbol{D}(\alpha)$ is too large to fit here, but for $m \to 0$, it is simply:

$$\boldsymbol{D}(\boldsymbol{q})\,|_{m\to 0} = \begin{bmatrix} m_H \sin^2(q_4) & 0 \\ 0 & 0 \end{bmatrix} \tag{4.7}$$

This make sense intuitively: for $m = 0$, the velocity $\dot{q}_4$ does not influence the energy loss, since the inertia of the swing leg around the hip is zero and hence, no energy is stored in the swing leg. Furthermore, as illustrated in figure 4.1, the velocity of the hip mass changes from being tangent to a circle around one leg, to tangent a circle around the other leg, and the impulsive force on impact removes the part of the pre-impact velocity that is not along the post-impact circle.

Hence, if the circles are close to each other, little is removed and hence little energy is lost, whereas if the circles are orthogonal to each other, the remaining velocity is zero and hence all energy is lost. For general nonzero m , the matrix $\boldsymbol{D}(\boldsymbol{q})$ is too complex to study directly. Instead, we study its generalized principle directions (i.e. the velocity directions that result in minimal and maximal energy loss on impact. The principle directions of a real symmetric matrix $\boldsymbol{X}$, are given by the singular value decomposition (Trefethen & Bau 1997 [41]) i.e. the decomposition of $\boldsymbol{X}$ as:

$$\boldsymbol{X} = \boldsymbol{U}\boldsymbol{\Sigma}\boldsymbol{V}^T = \boldsymbol{U}\boldsymbol{\Sigma}\boldsymbol{U}^T = \boldsymbol{U}\begin{bmatrix} \sigma_1 & & 0 \\ & \ddots & \\ 0 & & \sigma_n \end{bmatrix} U^T \quad \sigma_1 \geq \ldots \geq \sigma_n \geq 0 \tag{4.8}$$

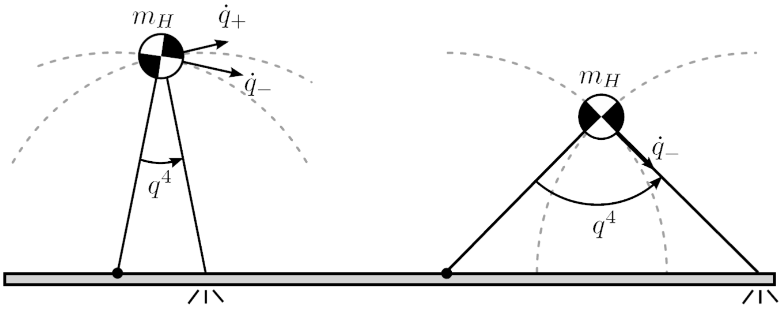

Figura 4.1: Comparison of the hip velocity before ($\dot{q}_-$) and after ($\dot{q}_+$) impact for two impact angles q_4.

With $\boldsymbol{U}$ an orthogonal matrix, and $\boldsymbol{U} = \boldsymbol{V}$ since $\boldsymbol{X}$ is symmetric. The numbers σ_i on the diagonal of the matrix $\boldsymbol{\Sigma}$ are called the singular values of $\boldsymbol{X}$. Note that the values σ_i may be zero. In fact, the rank of $\boldsymbol{X}$ is equal to the largest value r such that $\sigma_r \neq 0$. For $i > r$, $\sigma_i = 0$. The matrix $\boldsymbol{X}$ can act as a quadratic form on vectors $\boldsymbol{x}$, i.e. it can map a vector $\boldsymbol{x}$ to a number $\boldsymbol{x}^T\boldsymbol{X}\boldsymbol{x}$. When this quadratic form is applied to the unit sphere (all vectors satisfying $\boldsymbol{x}^T\boldsymbol{x} = 1$), the resulting set of vectors $\left(\boldsymbol{x}^T\boldsymbol{X}\boldsymbol{x}\right)\boldsymbol{x}$ forms an ellipsoid, and the radii of this ellipsoid are precisely equal to the singular values σ_i. Furthermore, the principle axes of the ellipsoid are given by the columns of the matrix $\boldsymbol{U}^T$ (the first column of $\boldsymbol{U}^T$ is the vector that is enlarged most by the quadratic form, and the last column of $\boldsymbol{U}^T$ is the vector that is enlarged least). We cannot use this singular value decomposition directly to study the singular value of $\boldsymbol{D}$, since the unit sphere $\dot{\boldsymbol{q}}^T\dot{\boldsymbol{q}} = 1$ has no physical meaning and would give coordinate-dependent results. Instead, we study the effect of $\boldsymbol{D}$ on vectors satisfying $\dot{\boldsymbol{q}}^T\boldsymbol{M}(\boldsymbol{q})\dot{\boldsymbol{q}} = 1$, i.e. directions with constant kinetic energy. To adapt the singular value decomposition to this situation, we use the Cholesky factorization $\boldsymbol{M}(\boldsymbol{q}) = \boldsymbol{G}^T(\boldsymbol{q})\boldsymbol{G}(\boldsymbol{q})$ (which exists since $\boldsymbol{M}$ is positive definite and symmetric), and determine the singular value decomposition of $\boldsymbol{X} = \boldsymbol{G}^{-T}\boldsymbol{D}\boldsymbol{G}^{-1}$. This decomposition again provides the principle directions of the quadratic form when applied to the unit sphere $\boldsymbol{x}^T\boldsymbol{x} = 1$. In addition, if we parameterize the vectors $\boldsymbol{x}$ as $\boldsymbol{x} = \boldsymbol{G}\dot{\boldsymbol{q}}$, we see that this decomposition gives the principle directions of the quadratic form:

$$\boldsymbol{x}^T\boldsymbol{X}\boldsymbol{x} = (\boldsymbol{G}\dot{\boldsymbol{q}})^T\left(\boldsymbol{G}^{-T}\boldsymbol{D}\boldsymbol{G}^{-1}\right)(\boldsymbol{G}\dot{\boldsymbol{q}}) = \dot{\boldsymbol{q}}^T\boldsymbol{D}\dot{\boldsymbol{q}} \tag{4.9}$$

When applied to the space

$$\boldsymbol{x}^T\boldsymbol{x} = (\boldsymbol{G}\dot{\boldsymbol{q}})^T(\boldsymbol{G}\dot{\boldsymbol{q}}) = \dot{\boldsymbol{q}}^T\boldsymbol{M}\dot{\boldsymbol{q}} \tag{4.10}$$

And hence, the singular value decomposition, constructed in this way, describes physically meaningful principle values σ_i and corresponding principle directions, given by the columns of $\boldsymbol{G}^{-1}\boldsymbol{U}^T$. Note that the singular values must be between zero and one, since no more that 100% and no less than 0% of the kinetic energy can be lost on impact.

Figures 4.2 and 4.3 shows a plot of the singular values for the compass bipedal walker with varying mass ratio $m_H : m$ and impact angle $q_4(T)$. Figure 4.4 shows the singular values and lists several principle directions for the impact velocity $\dot{\boldsymbol{q}}$, with

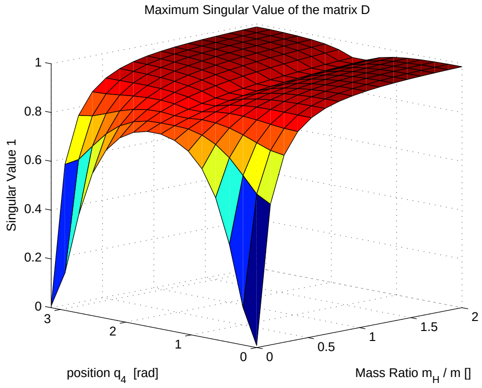

Figura 4.2: Maximum Singolar Value.

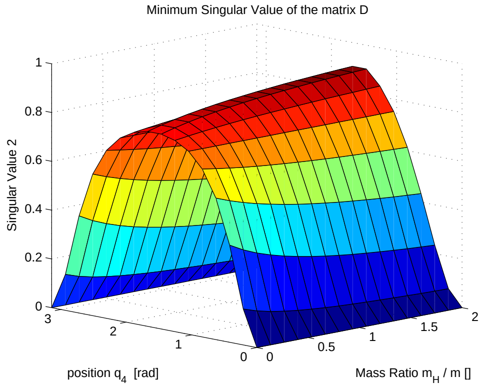

Figura 4.3: Minimum Singolar Value.

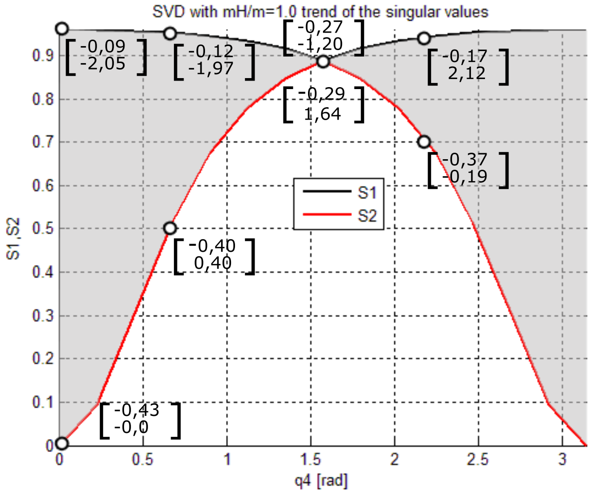

Figura 4.4: Trend of the singular values with mH/m=1.

the parameters fixed at $m = 1[kg]$ and $m_H = 5kg$. The figure shows the singular values describing the energy loss, i.e. the extreme cases of maximum possible loss and minimum possible loss. For general velocities not aligned with any of the principle directions, the energy loss will be somewhere between the singular values, i.e. in the darker area between the two curves in Figure 4.4.

For a given angle of impact, the velocity could then be chosen closer to the efficient direction to minimize energy loss. However, for some configurations (namely $q_4 = {}^{\pi}/_{2}$ or $m_H = 0$) the two singular values are the same, and hence the energy loss is constant for all velocity directions. The singular value analysis provides bounds on the energy loss during impact, and indicates efficient velocity directions for the end of a step. In this way, it can help suggest efficient walking strategies. For example, looking at Figure 4.4, it is efficient for small impact angles $q_4(T)$ to have an impact velocity that has large $\dot{q}_3$ and small $\dot{q}_4$ (i.e. moving the stance leg more than the swing leg), since then, the energy loss will be close to the lowest singular value. Note that the efficiency of the continuous dynamics is not taken into account yet, so the gaits that are the most efficient overall may still have less efficient impact angles and velocities. Besides for efficient studies, the energy loss computed into equation (4.6) can be used in the search for purely passive dynamic walking motion. For such motions, the gravitational energy converted to kinetic energy during a step must be equal to the kinetic energy lost on impact at the end of a step. For the compass model, this gives the following equation:

$$\begin{cases} \Delta P\,[n] = \Delta K\,[n] = \Delta E_{hs} \\ P^{-}\,[n] - P^{+}\,[n] = K^{+}\,[n+1] - K^{-}\,[n] \\ -2g\,(2m + m_H)\sin(\gamma)\sin\left(\frac{1}{2}q_4^{-}\right) = -\frac{1}{2}\dot{\boldsymbol{q}}_{-}^{T}\boldsymbol{D}\,(\boldsymbol{q})\,\dot{\boldsymbol{q}}_{-} \end{cases} \tag{4.11}$$

Which any passive (or otherwise energy-continuous) gait must satisfy. This equation also gives bounds on the minimally and maximally achievable speeds of the robot. If we choose for example $m = 1[kg]$, $m_H = 5[kg]$, $g = 9.81[m/s^2]$, $\gamma = 3°$ and $q_4^{-} = 0.5[rad]$, we obtain that $\Delta P\,[n] = -1.78[J]$ per step. Since the singular values of $\boldsymbol{D}$ are 1.0 and 0.22, it means that the kinetic energy on impact must be at least $1.78[J]$ and at most $1.78/0.22 = 8.08[J]$. No passive limit cycles can exist for velocities outside this range (at least for this choice of parameters).

4.3 Research of Passive Dynamic Walking (PDW)

The mechanisms that may show a passive attitude downhill there are not so many, and as noted in Previously, the existence of a passive gait of a mechanism generally depends on the mass distribution and angle of inclination of the terrain along which the system moves in addition to the layout of the system. The passive walking exists solely for robots that move downhill in order to exploit the gravitational force and therefore be able to compensate the loss of energy upon impact with the ground with the supplement of energy due to the potential energy that is converted into kinetic energy. One mechanism that has this type of walking, is the easier one we can imagine how bipedal walker mechanism and it is the compass like bipedal robot here called in this thesis Compass. This model was studied for a long time both for its simplicity (in fact, its equations of motion are relatively simple that they can also be easily calculated manually), and also because it is studying the simple mechanisms that we can easily understand some particular behavior of walker mechanisms that, for the complex ones is not of easy observation (e.g. passive stable limit cycles, or the phenomenon of bifurcation - See from literature [6]). An important aspect of this mechanism is the fact that there is just one type of SM that is possible. In fact, the model provides just one strike at the end of the gait (the one of the feet to the ground), and then the cycle re-start again from the same initial conditions. This aspect of this particular walking system make the optimization be easy and not computationally onerous, because there is just one SM to test (remember that SM have to be an input of the optimization routine) and so, there are not additional discrete parameters to add to the optimization routine.

4.4 PDW - Optimization Part 1

The optimization algorithm for this particular mechanism, is developed as was described in the section 3.1 about the general treatment. Therefore the optimization parameters are those in the table 4.1. It was chosen the configuration for which it is reached a passive gait ([36]) and was not investigated over the results that the variability of certain parameters may change.

Parameters	*Description*
links	2 (right and left leg).
n	6 (Degree of polynomials)
P_T	1 (there is only the strike on the ground).
P_M	3 (masses and length of links).
γ	$3°[deg]$
x_p	Parameter vector of length equal to 18 $(n \cdot links \cdot P_T + P_T + P_M)$

Tabella 4.1: Parameters of the optimization routine 1 - Compass Model

The parameters *param_body*, are in number P_M , as specified in chapter 2, and were bound within the sub-routine *Constraints* in order to fix them. The three parameters are:

m_H	$5[kg]$
m	$1[kg]$
l	$1[m]$

Tabella 4.2: Physical Parameters of Compass Model

The physical data of the system are corresponding to parameters of real systems whose lab tests showed the passive behavior. How was said previously, the optimization needs to be droven to the right direction by adding new constraints to the minimization process and then, after some iterations, remove them in order to find the correct result. The other constraints we considered are for example:

- The imposing a value for the final step time (T).
- The imposing of determined initial positions of the variables.
- The definition of a certain range in which the coordinates may vary.

The optimization converge to a result that is outlined as follow:

J (Cost Function)	$0.0009572[]$
T (Step Period)	$0,6079[s]$

Tabella 4.3: Optimization results 1

As we know, the optimization routine has like output also the coefficients of the polynomials which relate to the coordinates of the walker. The coordinates are reconstructed through the relation:

$$\boldsymbol{q}^i(t) = \sum_{j=0}^{n} b_{ij}\boldsymbol{t}^j = b_{i0} + b_{i1}\boldsymbol{t} + b_{i2}\boldsymbol{t}^2 + ... + b_{ik}\boldsymbol{t}^n \tag{4.12}$$

Where i is the index that's related to the $i-th$ coordinate, j is the index that scan the values from 1 to n that is the degree of the polynomial, $\boldsymbol{t}$ is the time vector, and b_{ij} are the coefficients of the polynomial, the ones have been just optimized.

4.4.1 Results Part 1

They are shown the results that are summarized by the feature of the coordinates position and velocity, and by the stick-diagram (respectively Fig.4.5 and Fig. 4.6).

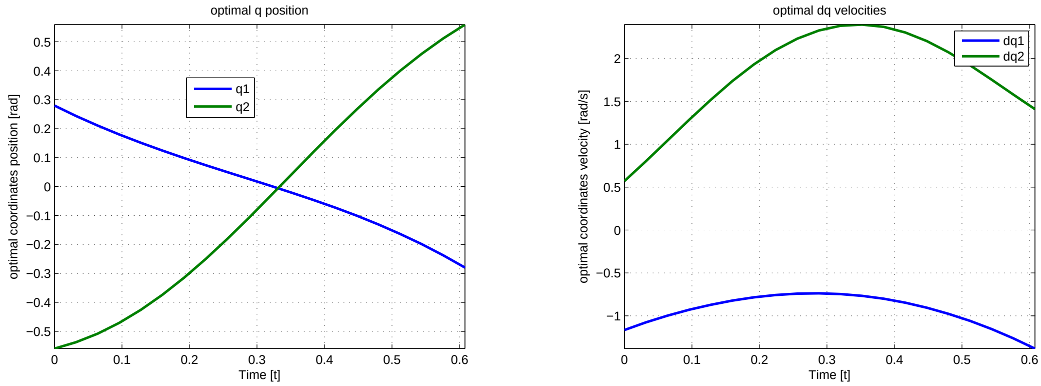

Figura 4.5: Optimal position of the coordinates of the Compass model. Opt. 1.

Figura 4.6: Optimal velocities of the coordinates of the Compass model. Opt. 1.

I want to represent the diagram below that is named Stick-diagram that represents the gait of the walking system as a set of overlapping photographs of many snapshots of the movement from the beginning of the step to the end.

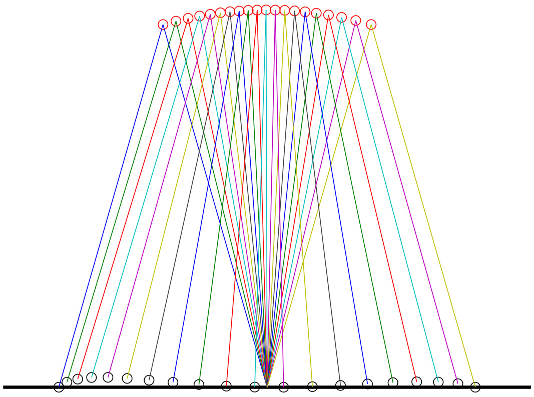

Figura 4.7: Stick diagram of the optimal gait. Opt. 1.

How we can see from the figure 4.7, we obtain a step that's characterized by the fact that the foot of the swing leg is constantly (apart the first moments of the step) grazing the ground and then the impact happen with a moderate downward velocity that makes the impact be energy lost efficient. The downward velocity of the foot in that case is approximately $0.37[rad/s]$. The optimization result doesn't give us any knowledge about the walking stability. For having an idea, we have to simulate the system with the obtained initial conditions and no actuation on the joints. We obtained the initial conditions like follows,

$$\boldsymbol{q}_+ = \begin{bmatrix} 0.279 \\ -0.559 \end{bmatrix} \quad \dot{\boldsymbol{q}}_+ = \begin{bmatrix} -1.165 \\ 0.571 \end{bmatrix} \tag{4.13}$$

That's the initial status of the optimization of the walking system's gait and the units are respectively [rad] and [rad/s].

4.4.2 Simulation and comparing - Part 1

So, we simulate and we obtain the following results:

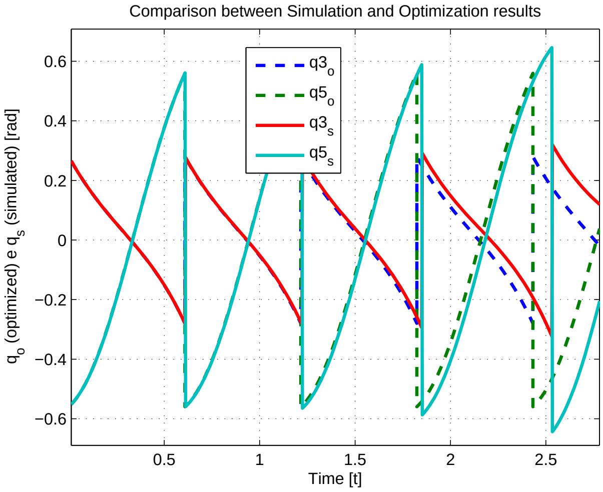

Figura 4.8: Comparison between the simulation results and optimization results of the compass like bipedal model (q_o, are the optimized coordinates and q_s are the simulated ones).

4.5 PDW - Optimization Part 2

The comparison of the two developments of the graphs is showing the coordinates evaluated respectively with the optimization solver (dashed line) and with the simulator (solid line), we can notice how the simulated curves starts with the initial condition imposed, taken from the ones of the optimization results, but it diverges soon (after few seconds) from the optimization curve because of the problem that the swing leg is not swung high enough, and the robot falls.

Apparently, although the computed gait is natural (indeed, the uncontrolled robot initially follows the computed trajectory perfectly), it is not stable.

The results suggest that stable walking may be obtained by raising the swing leg higher above the ground, in order to ensure that the foot makes contact and the next step can start. We can add an additional constraint to the optimization problem to enforce this, for example, a constraint that forces for the final downward velocity of the swing foot (just before impact) to be larger than some positive number v. The downward velocity (towards the ground) is given by the time-derivative of the relation 4.14 that describes the position of the foot of the swing leg (p_2). The constraint refers to the component along the y axes.

$$\begin{bmatrix} p_{2x} \\ p_{2y} \end{bmatrix} = \begin{bmatrix} q_1 - \sin(q_3) + \sin(q_3 + q_5) \\ q_2 + \cos(q_3) - \cos(q_3 + q_5) \end{bmatrix} \tag{4.14}$$

The additional constraint is:

$$\dot{p}_{2y} = -\sin(q_3)\,\dot{q}_3 + \sin(q_3 + q_5)\,(\dot{q}_3 + \dot{q}_5) \leq -v \tag{4.15}$$

For some large enough $v > 0$ (was chosen $v = 0.7$ [m/s]). Running the optimization routine gives result with $J = 0.0017$, so, higher than before (as expected since have been added a constraint), and the trajectories (positions and velocities) are shown in figures 4.9.

4.5.1 Results Part 2

The results are shown in the table 4.4 below:

J (Cost Function)	$0.00179991[]$
T (Step Period)	$0,7783[s]$

Tabella 4.4: Optimization results 2

The optimized curves, position and velocities.

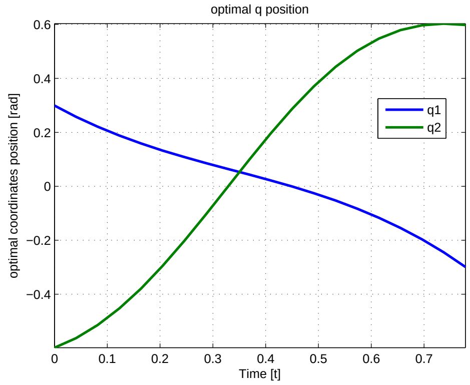

Figura 4.9: Optimal position of the coordinates of the Compass model. Opt. 2.

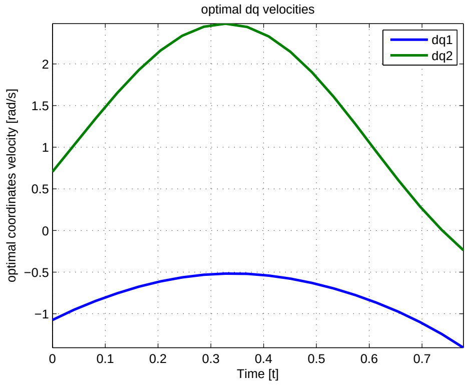

Figura 4.10: Optimal velocities of the coordinates of the Compass model. Opt. 2.

The optimization produce some results that are different from the ones reported in the section 4.4. Looking at the figures 4.9 and 4.10 reported above, we con notice how the coordinate q_5 is much more flat at the end of the gait respect the other that can be seen in the figure 4.5. As supporting that, we can notice how the velocity of the coordinate q_5 , now, has negative value in correspondence of the end of the gait. In addiction we can say that the optimization produce a result that have to be considered symmetrical for an entire walking cycle. That means the values of the optimal curves at the end of

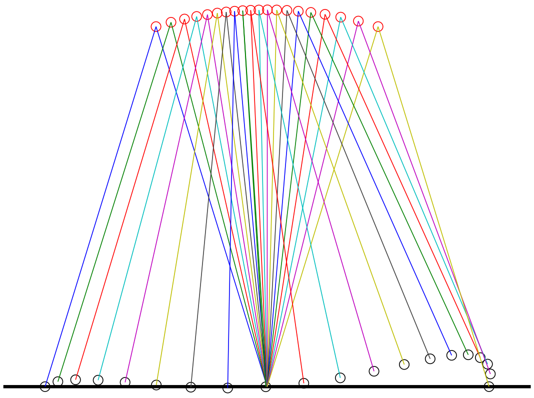

Figura 4.11: Stick diagram of the optimal gait. Opt. 2.

the gait, after using the re-labeling operator, have to be the same at the values of the curves at the beginning of the same gait. Thi is obtained constraining the optimization with some constraints that allow us to reach that symmetry. Note the relation for the re-labeling of the coordinates and the result in the Figure **??**.

$$\boldsymbol{q}_+ = \boldsymbol{G}\boldsymbol{q}_- = \begin{bmatrix} 1 & 1 \\ 0 & -1 \end{bmatrix} \boldsymbol{q}_- \Rightarrow \begin{cases} q_{3+} = q_{3-} + q_{5-} \\ q_{5+} = -q_{5-} \end{cases} \tag{4.16}$$

More explicitly, we can notice the stick-diagram in the Figure 4.11, that highlights the posture of the mechanism during a single gait. In contradiction with the previous stick-diagram, the swig leg, now, swung higher than before, in order to ensure and satisfy the constraint we add to the optimization. The value of the downward velocity of the swing leg's foot is, now, $0.899[rad/s]$. Like said before, the optimization result doesn't give us any knowledge about the walking stability. For having an idea, we have to simulate the system with the discovered initial conditions and no actuation on the joints. We have obtained values for the initial conditions of the optimized results like follows,

$$\boldsymbol{q}_+ = \begin{bmatrix} 0,299 \\ -0,598 \end{bmatrix} \quad \dot{\boldsymbol{q}}_+ = \begin{bmatrix} -1,075 \\ 0,705 \end{bmatrix} \tag{4.17}$$

That's the initial status of the optimization of the walking system's gait and the units are respectively [rad] and [rad/s].

4.5.2 Simulation and comparing Part 2

Showing the results of the simulation we can compare the previous results with the actual ones.

The result in this section show that, at least for this simple example, passive walking gaits can be found. The fact that there is still a nonzero cost function is due to the approximation of the trajectories by polynomials. The consequence of the approximation is also visible in the non perfect trace of the simulated curves (solid lines - red and

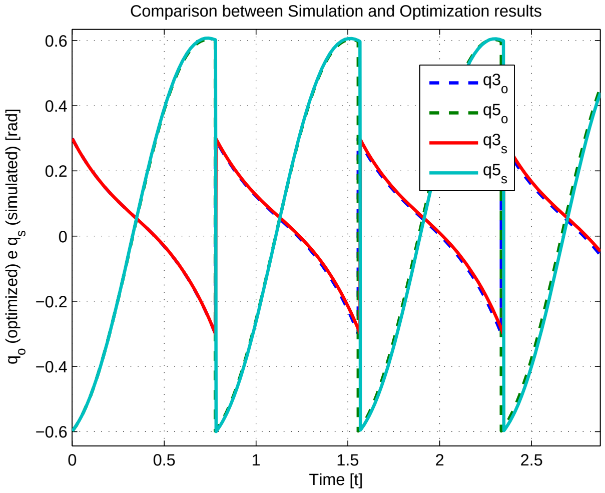

Figura 4.12: Comparison between the simulation results and optimization results of the *Compass* (q_o, are the optimized coordinates and q_s are the simulated ones).

azure) on the optimized curves (dashed lines - green and blue). This approximation doesn't impede the search for stable passive limit cycles, since if the limit cycle is stable with some practical region of attraction, it should attract the solution obtained by this polynomial approximation. For control purpose, the question whether an efficient limit cycle is stable or not is not so important; The controller can stabilize the cycle in case of disturbances anyway (provided that the system has enough control inputs). The important aspect of the optimized cycles is that *nominally*, little or no energy is required to follow them, and hence, that nominal walking is efficient.

CAPITOLO 5

Kneed Models: Optimization

Introduction In this chapter it is investigated the walking of the kneed models. In particular Knee and Dribbel models.
The mechanical models are the ones described in the chapter 2. The purpose is to investigate which is the much more effective mechanism for walking downhill and if the passive dynamic walking exists for these particular two systems (*Dribbel* and *Knee*).
In this Section it is firstly analyzed the optimal degree of polynomials n that better suits the coordinate trends trading off with computational burden. Then, it is developed the optimization routine for the model Dribbel first, and then for Knee model. These optimizations take into account not all the possible SMs for the mechanisms, but with some considerations about the cost function J, it will be possible to find reasonable results in according to the searched optimal gait.

5.1 Optimal Grade of Polynomials

In this section is treated a sensitivity analysis on the parameter n, the degree of the polynomial functions will represent the coordinates of the system.
For doing that, we made a series of tests with different step models, varying the parameter n, and observing how the cost function J , is consequently varying. There were considered SMs referred to both Dribbel and Knee in order to validate the analysis in general for both the kneed models treated in the following sections. In order to make these tests, we have to determine the SMs with which having some samples of optimizations results in order to further validate the research. For that purpose, I considered three SMs referring to Knee, and one referred to Dribbel. They are presented in the table 5.1.
I want to investigate the minimum value of n beyond which we don't have a significant reduction of the cost function J . That would mean that a higher value of n doesn't produce a better optimization in the sense of cost of actuation. The investigation starts performing the various optimizations. The sensitivity analysis for discovering the best n parameter consists in a trade-off between the computational burden due to the high degree of the polynomials and the minimum cost function value. This analysis was done with the four SMs described before. The parameter n was made vary between the values 4 and 9 and for every optimization, was evaluated the objective function value J. The results are shown in the figure below.

Taking a look to the figure 5.1, we notice how increasing over 6 the value n, of the degree of polynomials, the optimization doesn't produce a significant improvement (the cost

Step Model (SM)	*Description*
Model 1 $3n4str1\_1\_2\_gr$	Knee mechanism providind 4 strikes during the gat. The order of the strikes is defined by the sequence $1\_1\_2\_gr$ (1 is referred to the stance leg and 2 to the swing leg).
Model 2 $3n4str1\_2\_1\_gr$	Knee mechanism providind 4 strikes during the gat. The order of the strikes is defined by the sequence $1\_2\_1\_gr$ (1 is referred to the stance leg and 2 to the swing leg).
Model 3 $3n3str1\_2\_gr$	Knee mechanism providind 3 strikes during the gat. The order of the strikes is defined by the sequence 1_2_gr (1 is referred to the stance leg and 2 to the swing leg).
Model 4 $3n2str2\_gr*$	Dribbel mechanism (the $*$ define a Dribbel's SM) providind 2 strikes during the gat. The order of the strikes is defined by the sequence 2_gr (1 is referred to the stance leg and 2 to the swing leg).

Tabella 5.1: Step Models for the definition of the optimal degree of polynomials

function is stable around the lower value and it doesn't decrease). Another thing have to be noticed, is that the three models that refers to *Knee* (models 1,2 and 3) have almost the same values of the objective function J. At this point of this treatment, is difficult to say way the three models have almost the same cost function value for $n \geq 6$. Otherwise, it could be reasonable to think that whereas the first two models (1 and 2) differs only for the order of the strikes (indeed the number of the strikes is the same, 4, and the order is different: model 1 has a series like 1_1_2_gr, and model 2 has a series like 1_2_1_gr), the two models are redundant in the number of strikes (probably due to the two strikes that happen on the leg 1), and so the order of them has a poor influence on the objective function value. Analog consideration have to be made fot the model 3, that has one strike less than the models 1 and 2 but, for the same reason, it reachs the same objective function value of the previous models (This could be a proof of the presence of a redundant strike in the models 1 and 2). The model 4, that's referred to Dribbel, reachs a lower value of J but it stabilzes its value, also, for $n \geq 6$. It is shown, for example, the differences between the coordinates evaluated considering the optimization with model 2 and value $n = 6$ and $n = 9$. The figures 5.2 and 5.3 are showing that the differences between the two optimizations are negligible.

In the figure 5.2, there are represented all the coordinates of the optimization with $n = 6$ in blue, and of the optimization with $n = 9$ in red. Figure 5.3, indeed, is reported the maximum value of the error between the two optimization. The error is calculated like punctual difference between the coordinates for each time instant. This is not exactly

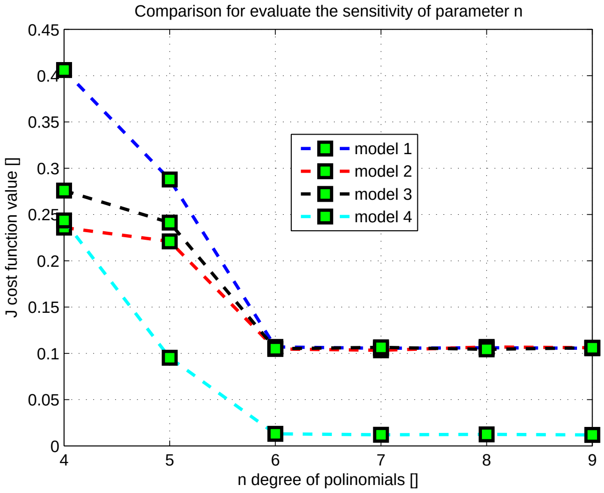

Figura 5.1: Diagram that shows the minimum number of parameter n that is useful for a proper optimization.

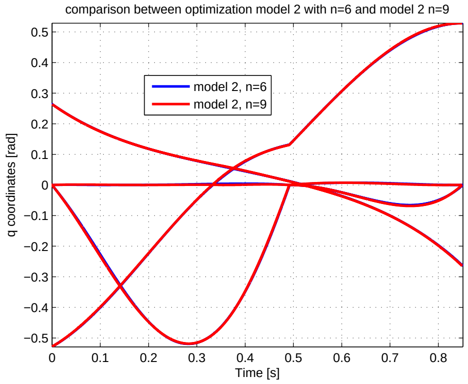

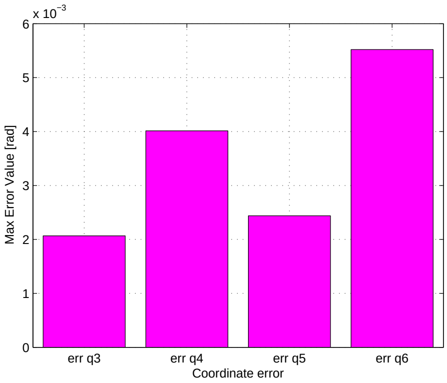

Figura 5.2: Comparison between the two optimizations with model 2 described before.

Figura 5.3: Histogram of the error between the two optimization with model 2 described before.

strict to do, because of the time vectors of the two results. In fact the final time instants are different and this brings that the instant in which the coordinates are evaluated are different from the two optimizations and so, the punctual difference from coordinates value at the same instant is not strictly correct in meanings. Otherwise, the two models have a final time instant that is not exactly the same but that is really close to each other. This brings as result that the punctual difference could be done without heavy practical errors. Indeed, the maximum value of the error is approximately 0.005 [rad] obtained with the coordinate q_4 and it is almost the 1% of the maximum coordinate excursion. In conclusion we have found the minimum value of the parameter n that is useful for obtaining a good optimization result. We take the minimum value in order to lighten the computational burden derived from the evaluation of the polynomials of high degree, for all the various optimization we will perform. Instead, all the following optimizations will be implemented with fixed n and equal to 6.

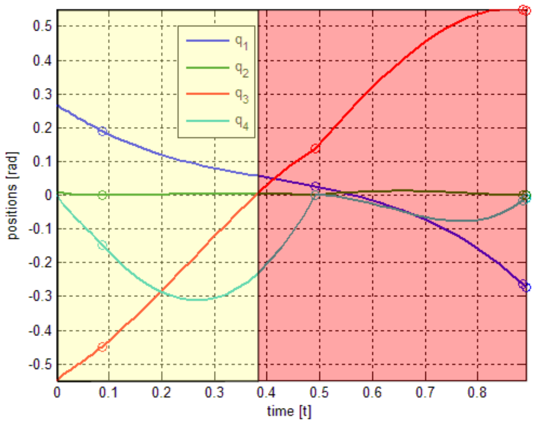

Figura 5.4: Graph with the areas of the first part and second part of the gait highlighted.

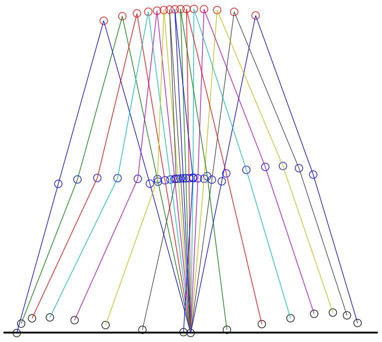

Figura 5.5: Stick Diagram representing the shape of the gait.

5.2 Optimization Results - General

Before performing the optimizations, it's useful define some useful concepts in order to better understand the results. In the following will be presented first, the parameter K for better clarifying the energy consumption of the actuators, and then, the concept of the degenerate strikes that will be useful to drive the research of the optimal movement of the mechanisms.

5.2.1 K parameter

In order to quantify the energy consumption associated to each degrees of freedom during a step, a K parameter for each d.o.f. is introduced. The K parameter is defined as:

$$K_i = \int |\tau_i| \, dt \tag{5.1}$$

where i is the index of the $i - th$ torque τ_i (i-th element of the vector $\boldsymbol{\tau}$).
Note that J is the weighted sum of the squared $\boldsymbol{\tau}$ vector, whereas K, is the integral over the step period of the absolute value of each τ_i.
One interesting instant that allows to separate the gait into two phases is the instant in which the swing leg passes the stance leg forward along the walking direction. This instant is characterized by the coordinate q_3 equal to zero.
Figure **??** shows the time histories of the d.o.f. during a single gait split into the two phases defined by $q_3 = 0$ From now on, it will called the phase evidenced in figure **??** with a light yellow color with the term *first part of the gait* and the other phase with the term *second part of the gait.* The K parameter has been evaluated for each of the parts outlined before.

5.2.2 Degenerate strikes

First to say, is that the degenerate strikes are always those which happen on the knees (coordinates q_4 and q_6). Remember that, for making the optimization be possible to converge, the number of strikes and their order, is defined a priori in the optimization

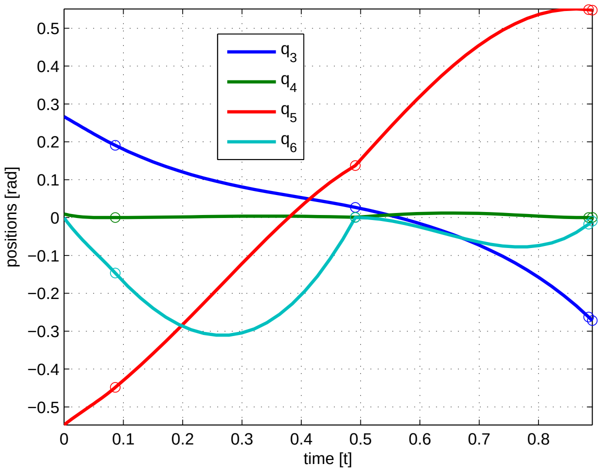

Figura 5.6: Example of result of an optimization routine. The SM is providing 5 strikes.

routine. This involves that, if the dynamical behavior of the mechanical model require a lower number of strikes than the ones provided by the SM, the strikes in surplus, will be positioned in order to minimize the OF and reduce the loss of efficiency. Thus, these strikes are often placed really close to the instant at which the relative coordinates of the two knees (q_4 and q_6) are reaching the zero line with a low velocity. This usually occurs at the beginning or at the end of the gait due to the symmetry of the walking gait due to the fact that the walking with knees will assume at the end (with the parameters used in this thesis), an approximated compass posture that is proper of compass bipedal mechanism. The strikes which position is collocated like explained before, are called degenerate, and the considered SM is probably not the optimal one. For these considerations, we can notice that in figure 5.6 (taken as example for illustrating the problem) there are at least two degenerate strikes. They are the two strikes that practically overlap the one to the ground at the end. Also the other strike on the *knee1*, the one that happen approximately at $t = 0, 1$, could be considered degenerate. That is, because it happen in an area in which the relative coordinate q_4 was grazing the ground with a really low derivate. The only non degenerate strike in this example is the one that happen on *knee2*. This strike happen at the instant around which the coordinate doesn't graze the zero line with moderate velocity. Contrary it strikes strongly (it reach the zero line with a high derivate) and after that, it diverges from that point with a really different slope. The degenerate strike, usually, doesn't provide a changing into the trend coordinates behavior, because of the less strength with which it happen due to the low derivate of the related coordinate at the impact instant. The presence of degenerate strikes is a sign of redundant strikes in the SMs, or a sign of the need of a different mechanical model for the walking particular purpose.

5.2.3 Optimizations Parameters

Before performing the optimizations we need to define the optimization parameters. The optimizations parameters are the following:

γ	3°
n	6
$StepModel$	varying

The parameters are the same for all the following optimizations in order to make the results be comparable.

5.2.4 Algorithm to determine the number of possible SMs.

It was decided to proceed with the optimizations, collecting them per groups in order to better understand the results step by step. It was performed first, the optimizations that refer to *Dribbel* and then the others, referred to *Knee*. The ones referred to *Dribbel* are collected in the group one, and the others, are collected in the groups from two to five, depending on the number of strikes of each group. Each group, in general, contains a certain number of possible SMs can be admissible with the considered number of strikes.

The number of possible SMs combinations, in general, could be evaluated with the following algorithm:

- Individuate the number of the strikes.
- The number of the *strike variables* is the number of the strikes minus one because the strike to the ground has a fixed position and it's always situated at the end of the gait.
- If the number of strikes is 2, there are just 2 possible combinations.
- If the number of strikes is grather than 2, assign the amount of strikes variables to the *knee1* or *knee2* in order to assign all the *strikes variables* to the knees in order to satisfy all the possible combinations (for example if strike var. is 2, we have to assign first 1 strike to each of the knees. Then 2 strikes to one knee and zero to the other and later do the opposite).
- Evaluating the number of combination for each assignment by the following equation:

  $$C_j = \frac{n!}{m_1!m_2!\cdots m_l!}$$

  Where n is the number of the strike variables and $m_1, m_2, \cdots m_l$ are the l multiplicities of the elements of the strike variables (taken in some order). C_j is the j-th multinomial coefficient where j is the index that runs all the combination of the assignments of strike variables that is possible.
- Sum all the coefficients C_j and obtain the number N_p of possible permutations that is possible to have changing the order of the strikes for a determine number of strikes per gait.

At the end, we obtain the number N_p of possible SMs into the group of optimizations. We have to try the different step models in order to find the proper one for the walking down-hill under test.

5.3 Group 1 - *Dribbel* Optimizations

In this section, it is investigated the step models of Dribbel and its effects on the gait efficiency. For doing that, have been done a series of optimizations varying the step models and observing how the objective function (J) changes.
The step model is defined like explained in the section 2.5 by some discrete parameters that have to be defined before starting the optimization algorithm. The mechanical model is the one treated in the section 2.3 and it provides the presence of only strikes on *knee2* and, of course, the one to the ground. For how the SM is defined, an infinite number of step models can be developed for this group of optimizations, simply adding an increasing number of strikes on the knees. Otherwise, the best in terms of cost of actuation is the one that provides just one strike on *knee2* and, at the end of the gait, the last one on the ground.
The best model, so, has only two strikes and is named with the nomenclature $SM1*$. Moreover, it will be investigated another SM that provides two *knee2* strikes in order to show the worsening of the walking efficiency taking into consideration more than one strike on *knee2*.
The model is named $SM2*$. The table below is summarizing the two SMs used in this group of optimizations.

$SM1*$	$362str2\_gr*$
$SM2*$	$362str2\_2\_gr*$

The sign $*$ is used to highlight the fact that the SM is referring to an optimization with Dribbel mechanism (because have been used the same notation for the codes of both the *Knee* and *Dribbel* models).

5.3.1 *Dribbel* - 2 strikes $SM1*$

Let's investigate, first, the $SM1*$. Running the optimization routine we obtain the results showed in the figures 5.7 and 5.8.

How can be noticed from the figures, the variable q_4 is kept locked to the value zero for all the duration of the gait. This could be observed in particular in the stick diagram in the figure 5.8. It shows the posture of the system during the gait and we can notice how the stance leg remains straight for all the duration. Notice that the mechanical lock happens after *knee2* strike (represented by the coordinate q_6 that reaches the value zero) and after that, the coordinate q_6 remains locked till the end of the gait. The OF value of this optimization is $J = 0,012$. For a better understanding on the energy torque consumption, can be shown the histogram (figure 5.9) of the K parameters of the torques taken individually.

The numbers of x axis are referring to the torques of the system respectively to τ_3, τ_5 and τ_6. How can be understand from the histogram, the torque that is much required is τ_6, but, how better understandable later, the amount of torque required is very low compared with the following results.

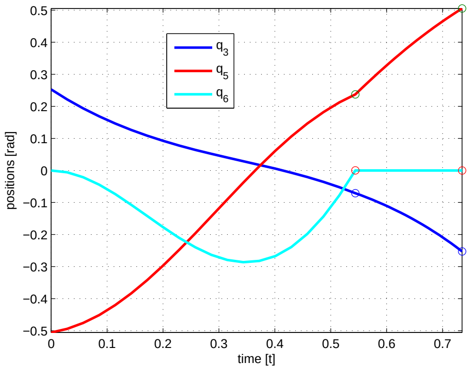

Figura 5.7: Trend of the curves representing the position of the links of the mechanical system (Dribbel) with $SM1*$. In the figure are represented the instants in correspondence of which the strikes happen.

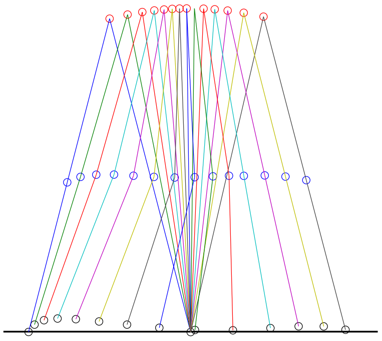

Figura 5.8: Stick Diagram representing the shape of the gait. 2 strikes $SM1*$

5.3.2 *Dribbel* - 3 strikes $SM2*$

This model is providing 3 strikes per gait.
This model was tested because it wants to demonstrate how other different models over the $SM1*$ will provide worst results in terms of walking efficiency.
With this model two knee strikes are expected, and for ensures the mechanical lock of the swing leg happen only in correspondence of the second *knee2* strike.The results are shown in the figures 5.10 and 5.11.

The coordinates trend in the figure 5.10 is showing the presence of the two *knee2* strikes. Despite of this, one of them, the second in time order, have to be consider degenerate. Only by zooming the area between the two strikes on knee2, can be noticed how the coordinate q_6 swings very a little bit far from the zero line till the second strike happen, and then the mechanical lock is activated. This model have a problem of redundancy of strikes and so, this SM is not proper for describe an efficient walking behavior.
The objective function value in this case is $J = 0,234$ that is much higher that before. Some considerations could be done also with the histogram of energy torques consumption in the figure 5.12.

How can be easily noticed, the much required torque is, like before, τ_6, but the global amount of torques energy is the very much more respect to the previous model ($SM1*$). In the histogram the scale of the y axis is kept equal to the scales used for the previous histogram obtained in the previous section. This was done, in order to be able to compare the histograms.
The other optimizations adding more strikes to the SM have been gave up because the OF values of each were much higher as many strikes have been added. In conclusion the best SM for the 3 d.o.f. mechanism walking down-hill, is the $SM1*$. It will be compared with the best results of others groups of optimizations. In the following are investigated the results obtained with optimizations using *Knee* model.

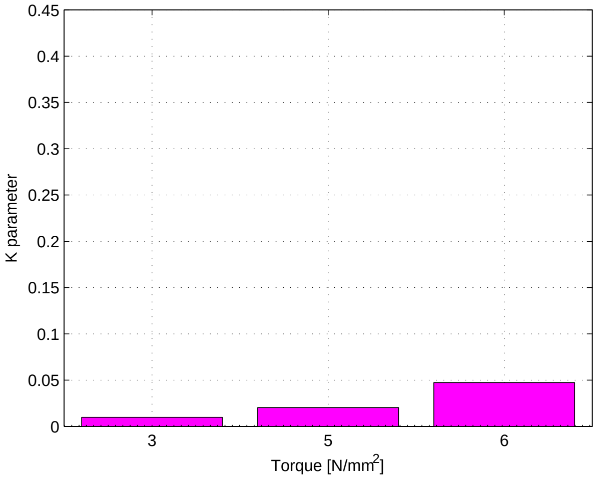

Figura 5.9: Histogram representing the cost of actuation with the parameter K for each of the joint actuators. It's referring to the optimization with $SM1*$

5.4 *Knee* Optimization - Overview

In this section, I have investigated the step models of the 4 d.o.f. mechanism (*Knee*) and its effects on the gait efficiency.

To show the results, it was decided to divide the various optimizations into groups for better understand.

The groups are divided depending on the number of the strikes that happen during the gait period. For example, the investigation will start from the optimizations with various SMs that provide two strikes in the gait period. Inside that group, we analyze all possible combinations of SMs that could be allowed by the mechanism constraints and then, we change the group considering one with a higher number of strikes (proceeding in ascending order we will take the group with 3 strikes) and we do the same of before. That method allow us to discover strengths and weaknesses of each group in order to discover a guideline for optimizations which are subsequently, allowing us to be able to drive the analysis choosing or discarding the subsequent SMs, if they are suitable or not to the walking behavior.

5.4.1 Group 2 - 2 strikes SMs

The research starts with the assumption that the step model provides at least one strike to the knee (for example the one of the swing leg) because we are investigating the effect of the knee strikes on the walking gait, against the compass model that has the only strike to the ground. With these assumptions, the easiest step model we can find, for that particular mechanical system, is the SM providing two strikes: for example, one on the knee of the swing leg, and the last one to the ground. The number of possible combinations for this group of step models is evaluable from the algorithm of the paragraph 5.2.4 that is concretized like:

In that case the evaluation of the number of combination that are permitted is simple and the value is 2. The two different step models are:

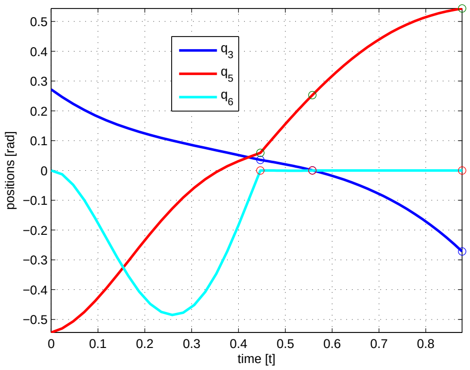

Figura 5.10: Trend of the curves representing the position of the links of Dribbel with $SM1*$. In the figure are represented the instants in correspondence of which the strikes happen.

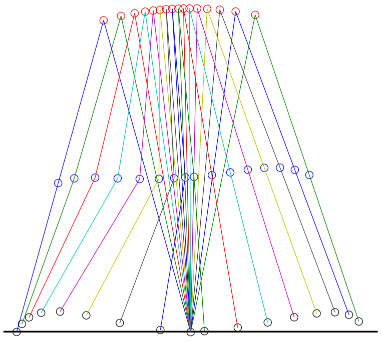

Figura 5.11: Stick Diagram representing the shape of the gait. 3 strikes $SM2*$

2 Strikes	**Possible combinations**	**Multinomial Coeff.**
⇓	$\begin{cases} 1 & k1 \\ 0 & k2 \end{cases}$	$C_1 = \frac{n!}{m_1!m_2!} = \frac{1}{1} = 1$
1 Strike Variables	$\begin{cases} 0 & k1 \\ 1 & k2 \end{cases}$	$C_2 = 1$
Total	⇒	$N_p = 2$

Tabella 5.2: Scheme for the evaluation of number of possible SMs for the imposed number of strikes

$SM1$	$362str1\_gr$
$SM2$	$362str2\_gr$

The parameters of the optimization are all the same and are the one detailed before in the section 5.2.3.

2 Strikes - $SM1$

The SM provides two strikes: one on the knee of the stance leg and the other on the ground. The optimization routine shows the following results:
For a better understanding of the energy consumption associated to the actuation torques we are reporting the K parameter histogram:
We can see from the histogram that the joint that requires the greatest torque is q_6 for which the parameter K is approximately equal to 0.35. In addition, can be noticed how the greatest amount of torque required happen in the second part of the gait.
The curves of the Fig. 5.13, in particular the ones that define the coordinates q_4 and q_6, have an unexpected development during the gait. In particular, the coordinate q_6 graze

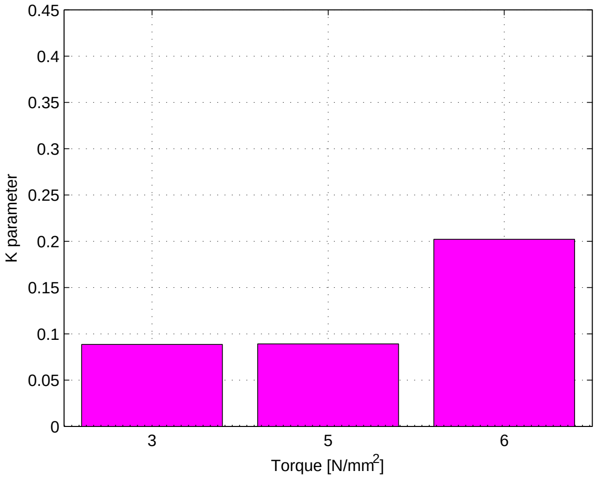

Figura 5.12: Histogram representing the cost of actuation with the parameter K for each of the joint actuators. It's referring to the optimization with $SM2*$

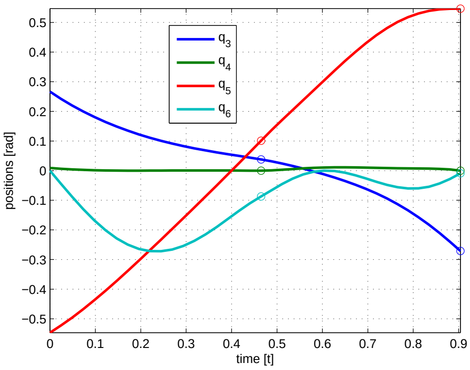

Figura 5.13: Trend of the positions of the links with 2 strikes $SM1$. In the figure are represented the instants (circles) in correspondence of which the strikes happen.

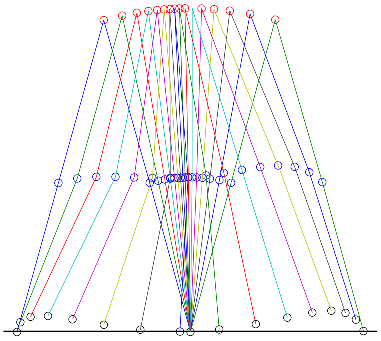

Figura 5.14: Stick Diagram representing the shape of the gait. 2 strikes $SM1$

the zero value at $t \simeq 0,6$ without impacting with it and this is an unexpected behavior of the optimized curves that may mean that an additional strike for that coordinate needs to be added in the SM.
The coordinate q_4, in addition, is grazing the zero line for all the duration of the gait. Because of this, the strike on *knee1* is degenerate. This is an unexpected behavior and could be an indicator of the fact that a different number of strike or a different dynamical model could be more suitable to this walking purpose.

Thus, from these consideration, can be plausible to think that an additional strike on the *knee2* seems to be necessary for the walking efficiency.

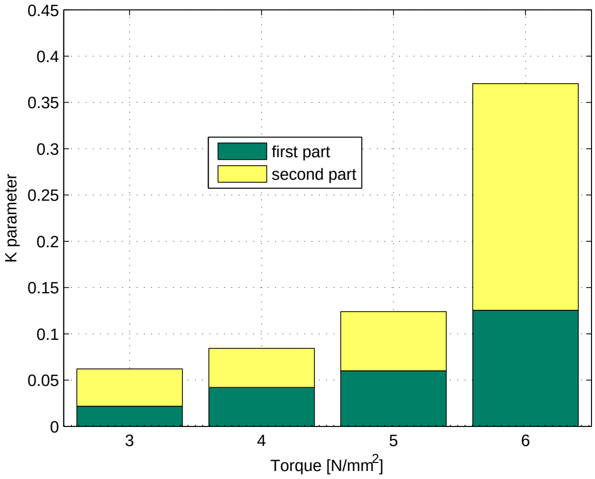

Figura 5.15: Histogram representing the parameter K. The numbers from 3 to 6 are the torques relative to the i-th joint. 2 strikes $SM1$

2 Strikes - $SM2$

The other possible step model, involving the presence of two strikes, is the case in which we have the presence of the knee strike on the swing leg and not on the stance leg ($SM2$ $362str2\_gr$). The parameters of the that optimization are the same of the one before, and so, the results are shown below:

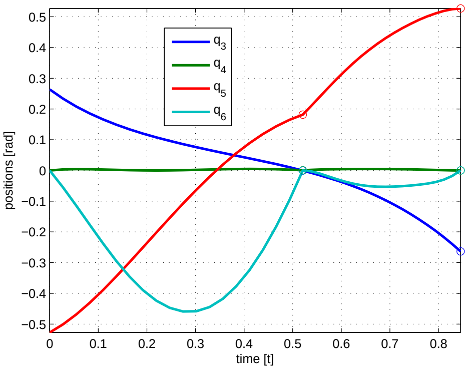

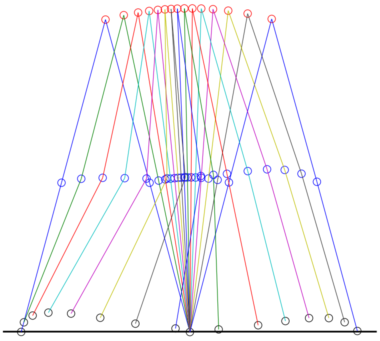

Figura 5.16: Trend of the positions of the links with the $SM2$. In the figure are represented the instants (circles) in correspondence of which the strikes happen.

Figura 5.17: Stick Diagram representing the shape of the gait. 2 strikes $SM2$

Like before, I represent the same histogram for a better understanding of the costs of the actuation.

Like was done before, the histogram in the figure 5.18 is representing the amount of torque required during the whole gait, considering torques individually. Like before, the torque that is required the most is the one related to the coordinate q_6 that reaches the value approximately of 0.23. So, the amount of torque required with $SM2$ is smaller than the one obtained with $SM1$. In addition, the amount of the torque τ_6 is less

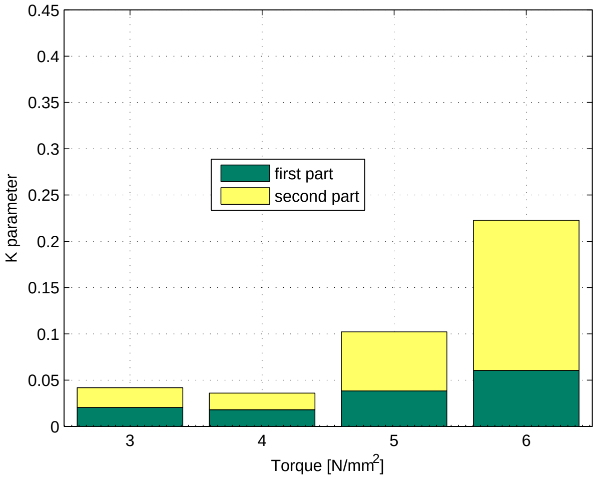

Figura 5.18: Histogram representing the parameter K. The numbers from 1 to 4 are the torques relative to the i-th joint. 2 strikes $SM2$

required because of the presence of the *knee2* strike in the second half of the gait. The other torques are not required like τ_6 is, and they are comparable with the values obtained with the optimization with the $SM1$ (figure 5.15).

We report the objective function values of the two optimization showed below:

2 Str - $SM1$	$J = 0,326$
2 Str - $SM2$	$J = 0,209$

How we can see from the table above, the model that presents a lower cost in terms of actuation is $SM2$. These optimizations show how the presence of the strike on *knee2* (if it happen in the second half of the gait period) is effective for the gait efficiency. Dealing with the coordinate q_4 , can be noticed that it always grazes the zero value during the whole duration of the gait. Like before, it's unexpected, and could be an indicator of the fact that the mechanical model used is wrong (remember the results obtained with *Dribbel* model). This is well understandable also in the stick diagram (Fig.5.17) above, where we can notice how the upper part of the stance leg remains aligned with the lower part for all the gait long.

5.4.2 Group 3 - 3 strikes SMs

The second group it is investigated is the one that provides 3 strikes for the SMs every gait. The number of the SM of that group is defined through the algorithm defined in the previous paragraph. The algorithm provides the scheme that defines the number of possible combinations of SMs that can be seen in the table 5.3.

At the end we obtain a number of $N_p = 4$ different SMs for that group and we obtain the following table that summarize the different four SMs

We had considered all the models for trying to understand if there are some configurations that produce an efficient optimization in terms of costs of actuation. For that analysis we run the optimization of all of the SMs and we'll make some considerations

3 Strikes	**Possible combinations**	**Multinomial Coeff.**
⇓	$\begin{cases} 1 & k1 \\ 1 & k2 \end{cases}$	$C_1 = \frac{n!}{m_1!m_2!} = \frac{2}{1} = 2$
2 Strike Variables	$\begin{cases} 2 & k1 \\ 0 & k2 \end{cases}$	$C_2 = 1$
	$\begin{cases} 0 & k1 \\ 2 & k2 \end{cases}$	$C_3 = 1$
Total	⇒	$N_p = 4$

Tabella 5.3: Scheme for the evaluation of number of possible SMs for the imposed number of strikes

3 Str - $SM1$	$363str1\_2\_gr$
3 Str - $SM2$	$363str2\_1\_gr$
3 Str - $SM3$	$363str1\_1\_gr$
3 Str - $SM4$	$363str2\_2\_gr$

about the objective function value J and on the shape of the coordinates graph. The analysis starts running the optimization with the $SM1$. The parameters are the same of the previous group in order to let the results be comparable.

3 Strikes - $SM1$

The model provides three strikes in order for which happen first, the strike to the *knee1* (i.e. the stance leg's knee), second, the strike to the *knee2* (i.e. the swing leg's knee) and, at the end of the gait, the strike to the ground. The Fig. 5.19 represents the trend of the curves of the position evaluated by the optimization routine and the stick diagram Fig. 5.20.
How we can see from the figure 5.19, the trend of the coordinates is almost regular and the instant of the strikes are neat separated and well defined into the gait. Despite of this, the coordinate graph, like the optimizations of the group 1, show an unexpected trend. In fact, the coordinate q_4 has a trend for which it swings very close around the value zero and it remains the same for all the duration of the gait. This fact brings as result that the strike on *knee1*, the one that happen at $t \cong 0,2$, could be considered degenerate cause of the proximity of the coordinate q_4 to the zero line in that area. The objective function, in this case, has value $J = 0,1051$.

3 stikes - $SM2$

Let's analyze the optimization that uses the $SM2$. That model provides three strikes in order for which happen first, the strike to the *knee2*, second, the strike to the *knee1* and, at the end of the gait, the strike to the ground. The optimization parameters are

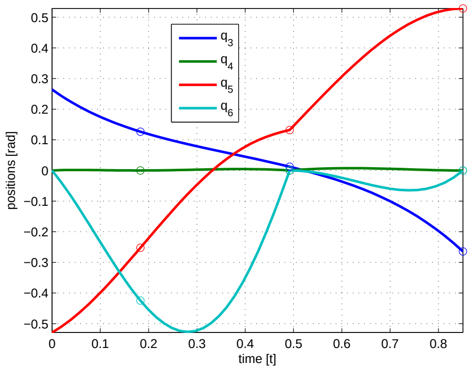

Figura 5.19: Trend of the positions of the links with the $SM1$. In the figure are represented the instants (circles) in correspondence of which the strikes happen.

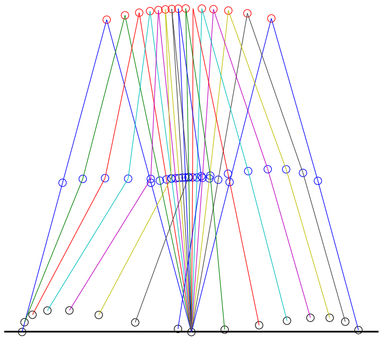

Figura 5.20: Stick Diagram representing the shape of the gait. 3 strikes $SM1$

the same of before, and so, we can plot the results in terms of trend of coordinates and stick diagram.

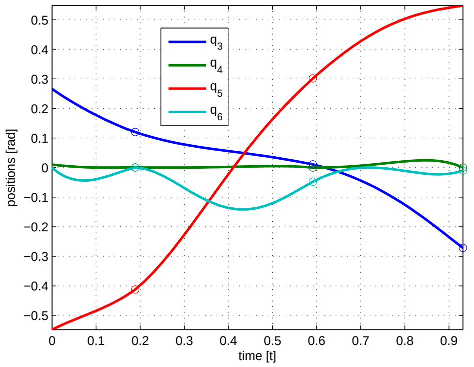

Figura 5.21: Trend of the positions of the links with 3 strikes $SM2$. In the figure are represented the instants (circles) in correspondence of which the strikes happen.

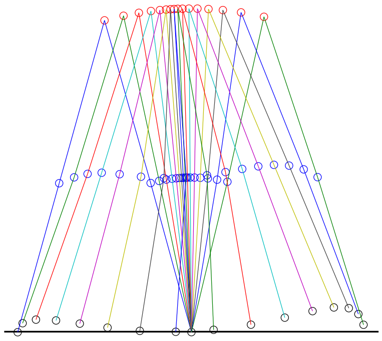

Figura 5.22: Stick Diagram representing the shape of the gait. 3 strikes $SM2$

From the figure above we can notice how the shape of the gait is very different from the one analyzed before. In that case, we can notice how the swing leg swings higher than the case of before, and the coordinate q_6 swings much less than the one obtained with $SM1$. This fact is probably due to the presence of the knee2 strike before the knee1 strike and that make the system be less efficient than the one before. The efficiency is testified by the value of the objective function that is much higher and it's $J = 0,511$. Like before, we can notice the degeneration of the strike on knee1 despite of the strikes are spaced enough into the gait. In addition, we notice how the line in green, that is referred to the coordinate q_4 , is grazing the zero line for all the duration of the gait. That is, how said before, a sign of the inadequacy of the mechanical model or of the SM used. The other optimization results that missing in that group are showed below and they refers to the optimizations routines that use the SMs 3 and 4 (read from the Table **??**). The optimization parameters are always the same in order to make the optimizations be comparable.

3 stikes - $SM3$ and $SM4$

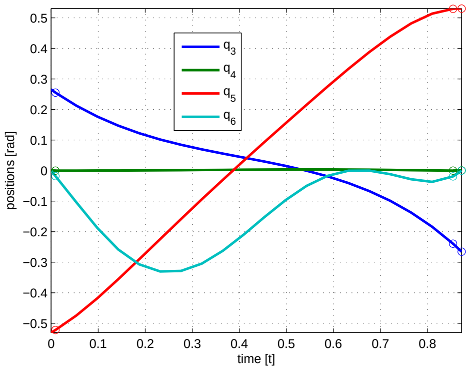

Figura 5.23: Trend of the positions of the links with 3 strikes $SM3$. In the figure are represented the instants (circles) in correspondence of which the strikes happen.

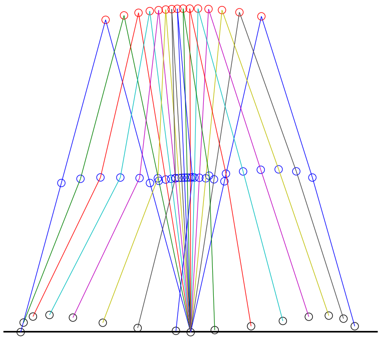

Figura 5.24: Stick Diagram representing the shape of the gait. 3 strikes $SM3$

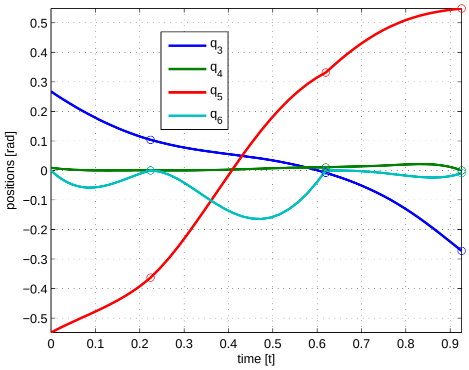

Figura 5.25: Trend of the positions of the links with 3 strikes $SM4$. In the figure are represented the instants (circles) in correspondence of which the strikes happen.

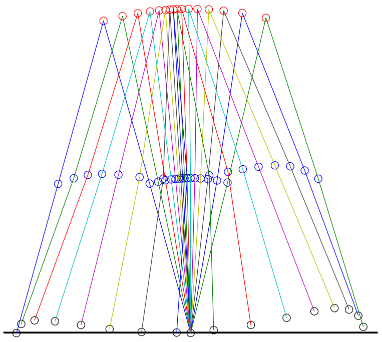

Figura 5.26: Stick Diagram representing the shape of the gait. 3 strikes $SM4$

The previous results are better understandable if we also report the OF values of the various optimization routines. For the optimization with the $SM3$, the OF value is $J = 0,599$, and for the optimization with $SM4$, the OF value is $J = 0,397$. Considering the entire group of optimizations, the better result in terms of cost of actuation is the result obtained with the $SM1$ ($J = 0,1051$), the other results have a much higher OF value and so, they are less suitable to characterize this particular type of walking down-hill.

It's interesting to investigate the reason why and the characteristics of the SMs are not suitable. It was discarded the model that provides the *knee2* strike before the *knee1* strike, and the model that has no strikes on the *knee2*. These models had the worse optimization results ($J = 0,599$ and $J = 0,511$ respectively). The $SM4$, that provides 2 strikes for *knee2* has a better result (comparing for example with the $SM2$) because of the presence of another strike on the knee2 in the second half of the gait period (take a look to the figure 5.25). This shows how the *knee2* strike is effective for the walking efficiency, but the presence of two *knee2* strikes worst the results than the case with just one *knee2* strike. It is well highlighted in the histograms 5.27 and 5.28.

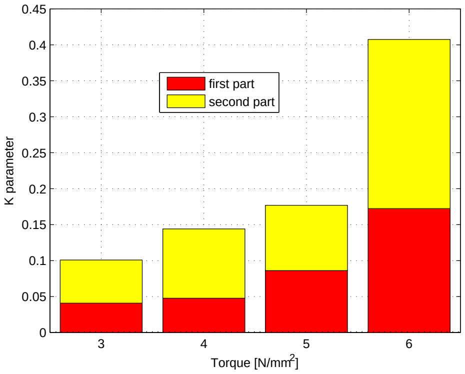

Figura 5.27: : Histogram representing the cost of actuation of the torques singularly, in which is highlighted the share between the two parts of the gait. It's referring to the optimization with $SM2$.

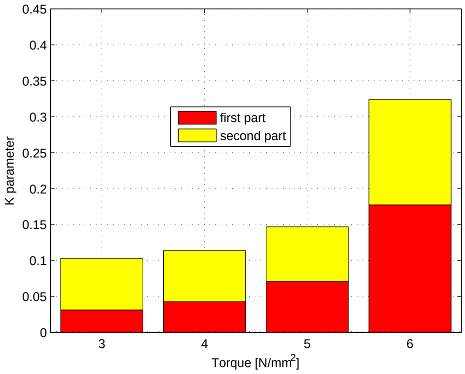

Figura 5.28: Histogram representing the cost of actuation of the torques singularly, in which is highlighted the share between the two parts of the gait. It's referring to the optimization with $SM4$.

The first histogram is referring to the optimization with $SM2$, and the second, to the one with $SM4$. The pieces in red are the share of torques are referred to the first part of the gait, and the pieces in yellow, are referring to the second part. The two models differs substantially of the presence of one additional strike on q_6 for the optimization with $SM4$. It could say that, because the presence of the strike referred to the coordinate q_4 (degenerate), for $SM2$, doesn't produce a consistent effect on the dynamic behavior of the walking system. That can be reasonably observed in the figure 5.21 in which can be noticed that in correspondence of the instant in which the strike of q_4 happens, there are no evident perturbation of the behavior of the other curves (thing that happens, for instance, in correspondence of the instant of the strike referred to q_6 , and the curves behave much different as stronger is the strike we are considering). The fact could be verified also numerically showing the values of the velocities of the coordinates before and after impact.

The table 5.4 above, is showing the velocities pre and post knee1 impact of the optimization routine with the $SM2$. Note that the velocity of the coordinate q_4 is zero after impact how is expected. The velocities post impact are showing a global deviation from the velocities pre impact that is in percentage around 1%. The global deviation from the velocities is evaluated with the following equation (5.2):

$$dev\% = \frac{norm\left(\dot{q}_{-}\right) - norm\left(\dot{q}_{+}\right)}{norm\left(\dot{q}_{-}\right)} \tag{5.2}$$

The amount of global deviation of the values of the table 5.4 is very poor comparing with the deviation between the velocities are referred to the strike to the *knee2* that is

Velocities pre	**Value [rad/s]**	**Velocities post**	**Values [rad/s]**
$\dot{q}_{1-}$	-1.0348	$\dot{q}_{1+}$	-1.1124
$\dot{q}_{2-}$	-0.1590	$\dot{q}_{2+}$	0
$\dot{q}_{3-}$	0.7322	$\dot{q}_{3+}$	0.6598
$\dot{q}_{4-}$	-1.3361	$\dot{q}_{4+}$	-1.3457

Tabella 5.4: Tables representing the values of velocities just before the knee1 impact, and just after that. The values refers to the optimization results with the SM2.

around of 20%. The values of the velocities pre and after *knee2* impact are reported in the table 5.6.

Velocities pre	**Value [rad/s]**	**Velocities post**	**Values [rad/s]**
$\dot{q}_{1-}$	-0.9370	$\dot{q}_{1+}$	-0.9358
$\dot{q}_{2-}$	-0.1316	$\dot{q}_{2+}$	-0.1603
$\dot{q}_{3-}$	0.6475	$\dot{q}_{3+}$	0.4459
$\dot{q}_{4-}$	-0.6935	$\dot{q}_{4+}$	0

Tabella 5.5: Tables are reporting the velocity values just before and just after the knee2 impact. The values are referred to the optimization with SM2.

How can be noticed from the tables above, the velocity value of the coordinate $\dot{q}_4$ after impact is zero as expected. Looking at the figures 5.27 and 5.28 they are showing that τ_4 has a consistent decrease (from the opt. with $SM2$ to the one with $SM4$) because of the happening of the second *knee2* strike in the second half of the gait. Despite of this, the happening of the strike on *knee2* is not always effective for the walking efficiency. In fact, the comparison between the two figures 5.29 and 5.27 is showing how the presence of *knee2* strike has opposite effect on walking efficiency.

In the figure 5.29 is shown the histogram of K parameter of the optimization with $SM1$, compared with the figure 5.27 that's referring to the one with $SM2$. Both the models are providing one strike on *knee1* and one on *knee2*, but the order is changed. The one referring to $SM1$, is much more effective that the one referring to the $SM2$. In particular, can be noticed that both the part of the gait are stressed the less than the others of the figure 5.27. For instance, if the strike on *knee2* happen in the second part of the gait, the strike would be effective for the walking efficiency, but if it happen on the first part, it will be not effective, and it will reduce the performances. In conclusion, the model that suits better the efficient walking behavior, is the one ($SM1$) that provides the *knee2* strike in the second part of the gait period. The trend coordinates is the one

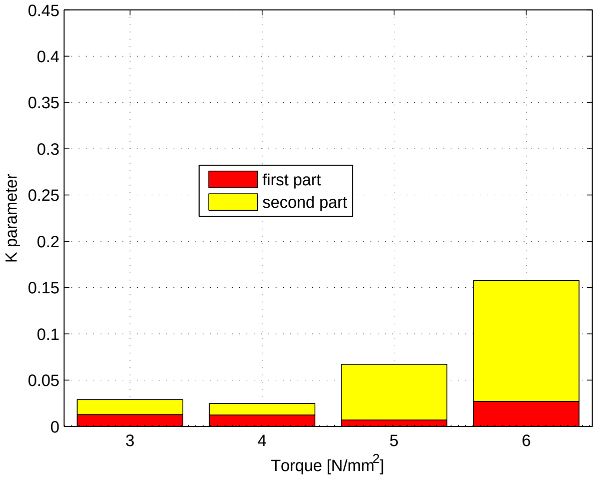

Figura 5.29: Histogram representing the cost of actuation of the torques singularly, in which is highlighted the share between the two parts of the gait. It's referring to the optimization with $SM1$

shown in the figure 5.19 and the OF value is $J = 0,1051$. In further optimizations we would like to individuate, in advance, the models we are sure will provide worst results in according with the considerations made in this paragraph and in the previous.

5.4.3 Group 4 - 4 strikes SMs

We are now investigating the group of SMs that are characterized for having four strikes. The number of possible SMs is evaluated with the algorithm presented before and in particular we obtain the following diagram.

4 Strikes	**Possible combinations**	**Multinomial Coeff.**
⇓	$\begin{cases} 2 & k1 \\ 1 & k2 \end{cases}$	$C_1 = \frac{n!}{m_1!m_2!} = \frac{6}{2} = 3$
	$\begin{cases} 1 & k1 \\ 2 & k2 \end{cases}$	$C_2 = 3$
3 Strike Variables	$\begin{cases} 0 & k1 \\ 3 & k2 \end{cases}$	$C_3 = 1$
	$\begin{cases} 3 & k1 \\ 0 & k2 \end{cases}$	$C_4 = 1$
Total	⇒	$N_p = 8$

Tabella 5.6: Scheme for the evaluation of number of possible SMs for the imposed number of strikes

Step Model	**Summary Code**
$SM1$	$364str1\_1\_2\_gr$
$SM2$	$364str1\_2\_1\_gr$
$SM3$	$364str1\_2\_2\_gr$
$SM4$	$364str2\_1\_1\_gr$
$SM5$	$364str2\_1\_2\_gr$
$SM6$	$364str2\_2\_1\_gr$
$SM7$	$364str1\_1\_1\_gr$
$SM8$	$364str2\_2\_2\_gr$

How can be seen from the scheme in the table 5.6, this group provides a maximum number of $N_p = 8$ different SMs but with the previous considerations made for the groups 2 and 3, we can individuate some of them that are not proper for our purpose, in order to not reporting the results for not complicate over the treatment.
Table **??** that follows, is summarizing the possible SMs we can have in this group.
The table above is representing all the eight possibilities of SMs.
Remembering the previous results and considerations, we can indicate in advance the models will provide worst results. They are the models are providing only strikes on one of the two knees (for example the $SM8$ and $SM7$) , and the models that provide the happening of the strikes of the *knee2* in the beginning of the gait (for example models $SM6$, $SM5$, $SM4$). We are sure that the OF values we can find running those optimizations will be higher or much higher than the results we can obtain with the other SMs.
For Instance, we can show the only results of the models $SM1$, $SM2$ and $SM3$. The parameters of the various optimizations are the same of the optimizations before. Let's show the results of the optimization with the $SM1$.

4 Strikes - $SM1$

The above results are showing how the trend of the curves is similar to the best ones of the previous group. (I'm referring to the $SM2$ of the group 2 and $SM1$ of the group 3). This optimization show an OF value that is $J = 0,1069$ and that's comparable with the other OF values of the best optimizations of the other groups analyzed till now. From the figure 5.30 we can notice how both the strikes on the *knee1* have to be considered degenerate. The first, because of the proximity to the beginning of the gait period, and the second, because the trend of the coordinate q_4 (the one in green) is almost linear and grazing the line of zero how the optimizations analyzed before. (That could be a confirm of the fact that the dynamical model used for describing the behavior of that mechanism walking down-hill could be un-optimal).

4 Strikes - $SM2$

How can be noticed, the model provides the strikes in that order: first, happen the strike on *knee1*, then the strike on *knee2* and then again, on *knee1*. The results in the graphs above, have almost the same shape of the curves found in the previous optimization. From the figures 5.32 and 5.30 we can notice how the change of model

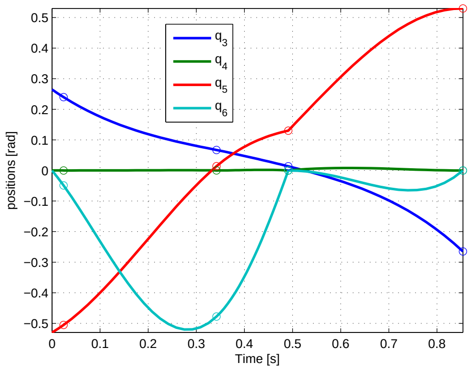

Figura 5.30: Trend of the curves representing the position of the links of the mechanical system with the $SM1$. In the figure are represented the instants in correspondence of which the strikes happen.

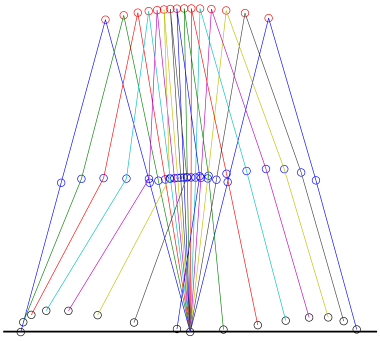

Figura 5.31: Stick Diagram representing the shape of the gait. 4 strikes $SM1$

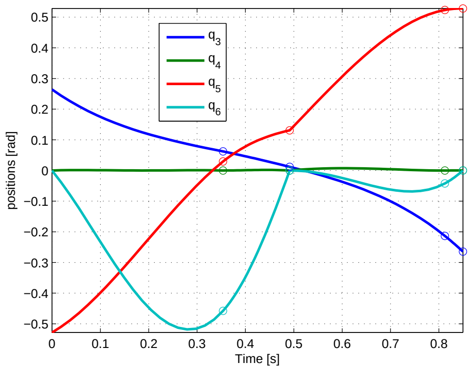

Figura 5.32: Trend of the curves representing the position of the links of the mechanical system with the $SM2$. In the figure are represented the instants in correspondence of which the strikes happen.

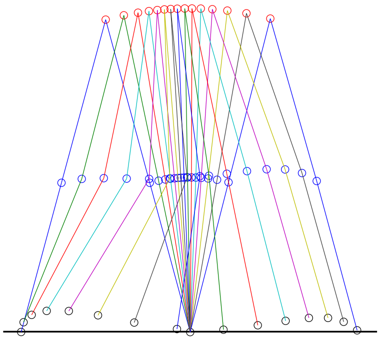

Figura 5.33: Stick Diagram representing the shape of the gait. 4 strikes $SM2$

between these two optimizations (the one with $SM1$ and $SM2$), doesn't produce a considering difference in terms of OF value. In fact, in that case, $J = 0,1047$, that is really close to the one obtained before. Like previously, the coordinate q_4 (the one in green) is grazing the zero line and both the strikes on knee1 have to be considered degenerate. This can be observed in the coordinate graph because the happening of the degenerate strikes doesn't produce a significant variation into the coordinates behavior because of the pour strength with which the strike happen. The fact that the OF value is close to the one obtained with the optimizations made for the groups 1 and 2, allow us to understand that additional strikes (those degenerate) are redundant and some of them need to be removed because they don't produce any advantage for the walking efficiency.

4 Strikes - $SM3$

The model is the $SM3$ and it is providing first, the strike on *knee1* and then, two strikes in a row on *knee2*. That model shows the results we can see in the figures 5.34 and 5.35:

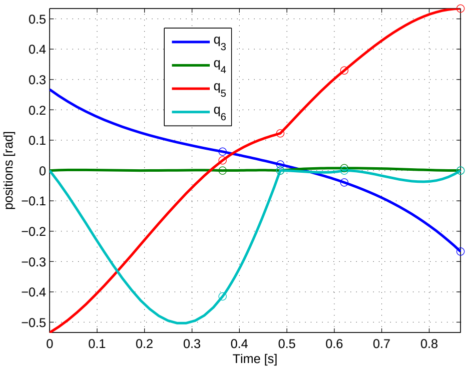

Figura 5.34: Trend of the curves representing the position of the links of the mechanical system with the $SM3$. In the figure are represented the instants in correspondence of which the strikes happen.

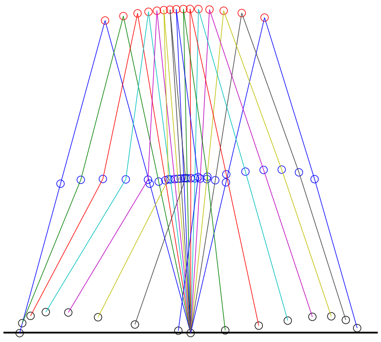

Figura 5.35: Stick Diagram representing the shape of the gait. 4 strikes $SM3$

The OF value of this optimization is $J = 0,1124$. The value is a little bit different, and worst, from the ones obtained before, and that's because the presence of two strikes on knee2 doesn't procure any improvement in the walking efficiency but moreover, it hampers the natural behavior that the model would have with the presence of only one *knee2* strike. In this SM can be noticed two degenerate strikes: the first one is the one on *knee1* and the second is the *knee2* strike that happen at $t \cong 0,6$. The figure 5.36 is showing the histograms reporting the value of the parameter K of both the SMs 2 and 3 in comparison.

From the figure 5.36, can be notice that the two SMs have more or less the same trend of parameter K. The presence of the additional strike on knee2 with the $SM3$ ensures that the results in terms of parameter K, are a little bit worst respect to the one with $SM2$, and the worsening is distributed quite uniformly over the four torques. For this group we can take like the proper model, the $SM2$, the one with the *knee2* strike between the other two *knee1* strikes. The choice was made considering the model with the lower value of the parameter J. Despite of this, the *knee1* strikes are degenrate and so, this model is not proper for this walking purpose.

5.4.4 Group 5 - 5 strikes SMs

The number of possible combinations of SMs is obtained with the same algorithm we used for the other groups. The algorithm is sintesized by the scheme in the table 5.7: The number of the possible SMs for that group of strikes is $N_p = 16$ different SM. They are summarized in the tables below.

The table **??** is reporting all the codes of the possible SMs we can have performing five strikes per gait. How was done for the group 4, we will not test every possible model because the timing of every single optimization is computationally onerous, and test

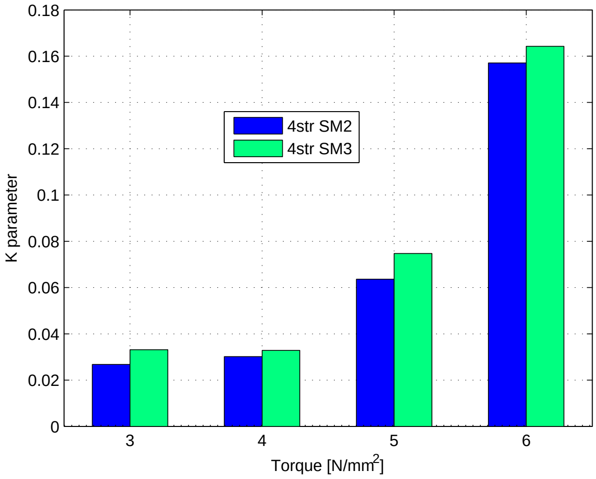

Figura 5.36: Histogram representing the comparison between the K parameters of the optimizations with $SM2$ and $SM3$.

5 Strikes	**Possible combinations**	**Multinomial Coeff.**
⇓	$\left\{\begin{array}{ll} 4 & k1 \\ 0 & k2 \end{array}\right.$	$C_1 = \frac{n!}{m_1!m_2!} = \frac{24}{24} = 1$
	$\left\{\begin{array}{ll} 3 & k1 \\ 1 & k2 \end{array}\right.$	$C_2 = 4$
4 Strike Variables	$\left\{\begin{array}{ll} 2 & k1 \\ 2 & k2 \end{array}\right.$	$C_3 = 6$
	$\left\{\begin{array}{ll} 1 & k1 \\ 3 & k2 \end{array}\right.$	$C_4 = 4$
	$\left\{\begin{array}{ll} 0 & k1 \\ 4 & k2 \end{array}\right.$	$C_5 = 1$
Total	⇒	$N_p = 16$

Tabella 5.7: Scheme for the evaluation of number of possible SMs for the imposed number of strikes

every single model could take too much time.
For this reason, it will test the only models that it's already known that could be proper for the down-hill walking. Our considerations are driven by the results obtained from the previous optimizations.
In fact, we obtained that the proper model for that walking must provide one strike on *knee2*, and the others four (we are considering 5 strikes for that group) on *knee1*. These results allow to discard all the models from SM6 to SM16, because they all provide more than one strike on *knee2*, and the $SM1$, because it doesn't provide any strike on *knee2*. From some other considerations made in the previous paragraphs, the

Step Model	**Summary Code**	**Step Model**	**Summary Code**
$SM1$	$365str1\_1\_1\_1\_gr$	$SM9$	$365str2\_1\_1\_2\_gr$
$SM2$	$365str1\_1\_1\_2\_gr$	$SM10$	$365str2\_1\_2\_1\_gr$
$SM3$	$365str1\_1\_2\_1\_gr$	$SM11$	$365str1\_2\_1\_2\_gr$
$SM4$	$365str1\_2\_1\_1\_gr$	$SM12$	$365str1\_2\_2\_2\_gr$
$SM5$	$365str2\_1\_1\_1\_gr$	$SM13$	$365str2\_1\_2\_2\_gr$
$SM6$	$365str1\_1\_2\_2\_gr$	$SM14$	$365str2\_2\_1\_2\_gr$
$SM7$	$365str1\_2\_2\_1\_gr$	$SM15$	$365str2\_2\_2\_1\_gr$
$SM8$	$365str2\_2\_1\_1\_gr$	$SM16$	$365str2\_2\_2\_2\_gr$

happening instant of the knee2 strike during the gait is really important. Was obtained that if the strike happen in the first half of the gait (and in particular if it happen long before the swing leg has passed the stance leg), the strike is not effective on the walking efficiency and the cost of actuation rise up consistently. For that reason we decided to show the only optimizations that could produce good results in term of value of the OF.

5 Strikes - SM3 and SM4

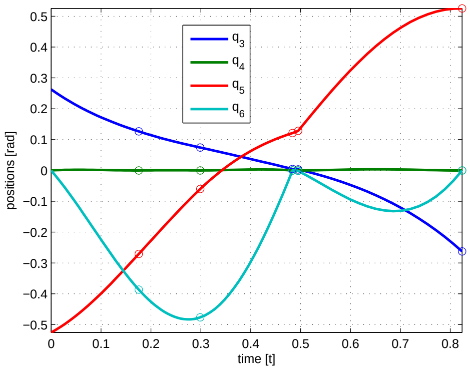

Figura 5.37: Trend of the curves representing the position of the links of the mechanical system with the $SM3$. In the figure are represented the instants in correspondence of which the strikes happen.

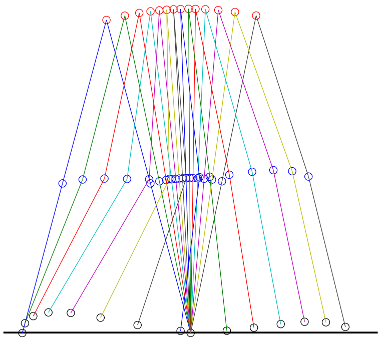

Figura 5.38: Stick Diagram representing the shape of the gait. 5 strikes $SM3$

The results of the figures above, are completely understandable if we report the value of the OF for both the optimizations. The optimization with the $SM3$ has $J = 0,1081$ and the one with $SM4$ has $J = 0,267$. These results are showing how the best model for that group is the $SM3$. Can be said, in addition, that both the models $SM3$ and $SM4$ present three degenerate strikes each. The additional strikes on the *knee1* are not effective for the walking efficiency but, moreover, they are redundant and unnecessary. In fact, the $SM4$ provides the happening of the two latest strike on the *knee1* almost at the end of the gait and they are practically overlapped to the final strike on the ground. In general, all the *knee1* strikes have to be considered degenerates, because of the

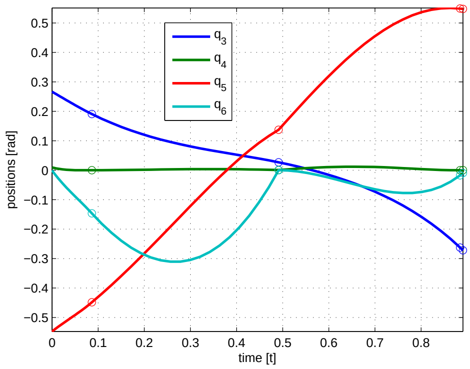

Figura 5.39: Trend of the curves representing the position of the links of the mechanical system with the $SM4$. In the figure are represented the instants in correspondence of which the strikes happen.

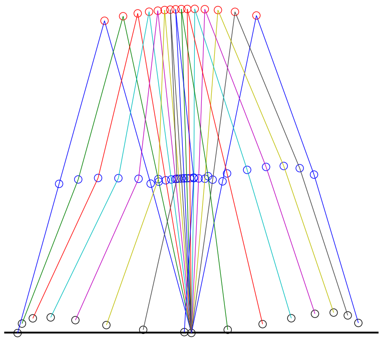

Figura 5.40: Stick Diagram representing the shape of the gait. 5 strikes $SM4$

coordinate that grazes the ground for all the duration of the gait. This is an unexpected behavior of the optimization results probably due to the improper mechanical model used. It seems to be much proper the 3 d.o.f. model (Dribbel) used in the optimizations of the group 1.

5.5 Summarizing the obtained results

Remembering the other optimizations made with other groups of strikes we can summarize a little, the obtained results. In the group 1 were investigated the optimizations involving the 3 d.o.f. mechanism. Those results had shown how that mechanical model is proper for walking down-hill because of the fix stance leg and the compass posture at the moment of the strike to the ground. In this group of optimizations, the best is the one that provide only one *knee2* strike and it doesn't presents degeneration. The other model, the $SM2*$ that provides two *knee2* strikes, showed the presence of one degenerate strike. With the group 2, were studied the SMs related to the 4 d.o.f. mechanical model. Was obtained that the presence of the strike on knee2 was very relevant in the efficiency of the walking gait. On the other hand, we found an unexpected thing in the walking behavior. The coordinate q_4 in fact, always graze the line of zero without moving far from it. This fact was a little bit unexpected and other models adding more strikes were investigated in order to check it out. The comparison between the two figures 5.14 and 5.16 is showing the deep differences between the two only models provided into this group, and the value of the OF strongly bends towards the SM is providing the *knee2* strike ($SM2$) The OF value in that case was $J = 0,23$.
Considering the group 3, was confirmed the hypothesis done with the models of the group 2. The model that better suits the walking downhill is the model that provides the *knee2* strike into the gait. From the figure 5.19, we can see how the shape of the curves and their trends are really similar to the ones found for the model with two strikes (figure 5.16). The OF value, also, is close, despite of this, it leads us to choose the model with three strikes because it's better (OF value $J = 0,1051$). The *knee1* strikes are all degenerate strikes because of the trend of the coordinate q_4. At this

Group	**Relative Step Model**
Group 1 - 2 Strikes, *Dribbel*	$SM1*$
Group 2 - 2 Strikes, *Knee*	$SM2$
Group 3 - 3 Strikes, *Knee*	$SM1$
Group 4 - 4 Strikes, *Knee*	$SM2$
Group 5 - 5 Strikes, *Knee*	$SM3$

point the choice seems to be driven by the previous results. Increasing the complexity of the models adding new strikes to the SMs, some models that behave similar to the one with 3 strikes obtained before are expected to find. In addition, that model is expected to be the best for that group of SMs. The model would be something that provides just one strike on the *knee2*, and missing strikes on the *knee1*. That's because of the previous optimizations results and considerations. With the group 4, how said before, the best SM was the one showed in the figure 5.32. That model is really close to the one outlined before with the three strikes models. They differs obviously on the presence of an additional strike on the *knee1* for the model of the fourth group. This additional strike is positioned after the *knee2* strike, and that seems to be degenerate as well as the others *knee1* strikes, because happens really close to the end of the gait in which happen the strike on the ground. This could be due to the redundancy of the strikes for this SM or due to the mechanical model used (remember that with the 3 d.o.f model, the *knee1* strikes were not allowed and so, no possible degenerate strike on that knee could happen). For the optimizations of the fifth group was obtained the best SM to be the $SM3$ whose coordinates trend is shown in the figure 5.37.
The model provides three degenerate strikes symptom that there are unuseful strikes provided by this SM. After this group of optimizations, was decided to not go further with adding strikes to the SMs because it was found that the results obtained with the optimizations of the group 3, 4 and 5 (Indeed with 3, 4 and 5 strikes each) were almost the same (considering the optimal solution of each group) and the models were providing degenerate strikes as much as additional strikes were considered. Proceeding further with the addition of the strikes, the results in terms of J doesn't change but rather, they increase a little bit as much as the strikes are added.
The table **??** is collecting the best optimization SM for every group.

The figure 5.41 is showing the results of the best optimizations of each group without the ones of the group 1 (the one related to Dribbel).

How it is easily to notice, the best SMs for the groups 3, 4 and 5, have almost the same J value, a little bit increasing between the best SMs of the group 4 and 5. This is an interesting result because, how said before, increasing the number of strikes over a certain value (in that case the minimum is four strikes really close to the value obtained with three strikes), it doesn't procure a benefit on the walking efficiency.

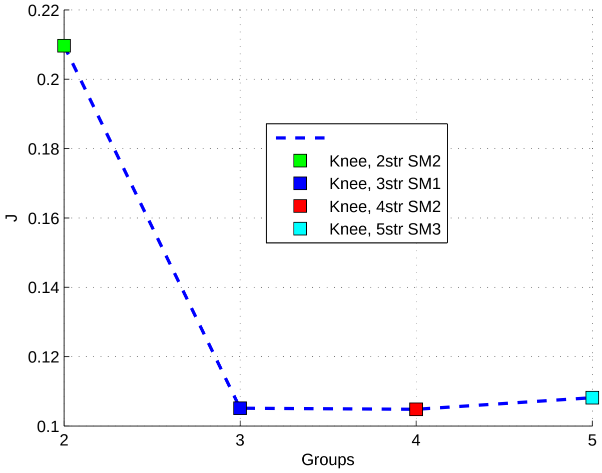

Figura 5.41: Values of the OFs of the best optimization of each group.

5.6 Comparison between best models

The group 1 reveal the best model to be $SM1*$ that present an OF value $J = 0,012$. This model shows a result that is much less than the best value we obtained with the *Knee* optimizations. Comparing, for example the model $SM1*$ of the group 1 with the $SM2$ of the group 3 (that's the best for the Knee optimizations), can be obtained the figures 5.43 and 5.44.

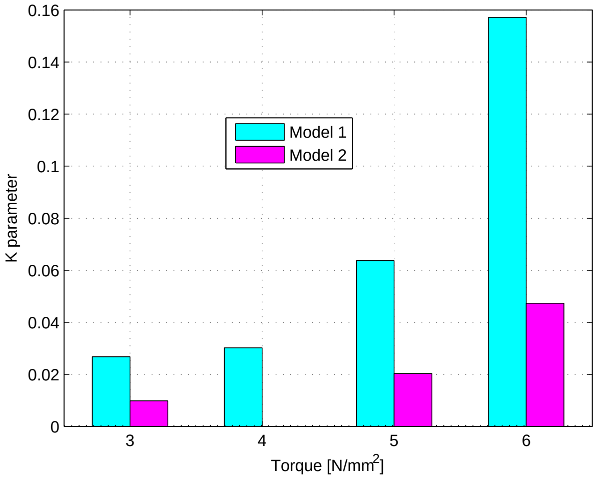

Figura 5.42: Comparison between the best SMs of Dribbel and Knee optimizations.

The above histograms are showing how the differences are neat especially on the torque related to the coordinate q_6. In addition, the great amount of energy cost of actuation for the *Knee* model is happening in the second half of the gait period. In the first half, the energy cost is really small. Contrary, the amount of energy cost with *Dribbel* model is concentrated in the first half of the gait and the cost of actuation in the second half,

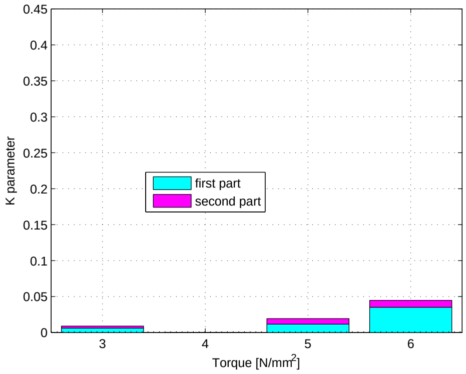

Figura 5.43: Histogram reporting the K parameters of the $SM1*$ with Dribbel mechanism.

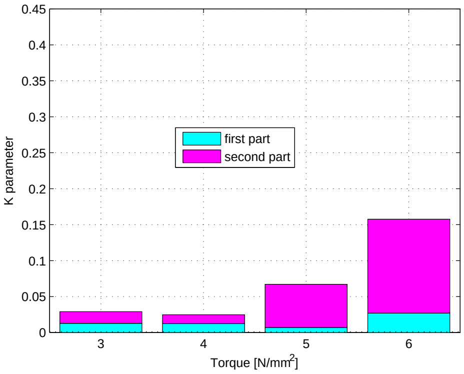

Figura 5.44: Histogram reporting the K parameters of the $SM1$ with Knee mechanism with 3 strikes.

is much less than in the first part, and the combination of the two parts of actuation ensure that is obtained a better results in terms of J respect to the *Knee* model. After all the previous optimizations was obtained that the model that best fits the bipedal down-hill walking (with our imposed parameters) is Dribbel with $SM1*$. The SM is defined such as happen one strike on the *knee2* and, at the end of the gait, the one on the ground. The best coordinates are, therefore, the one reported in the figure 6:

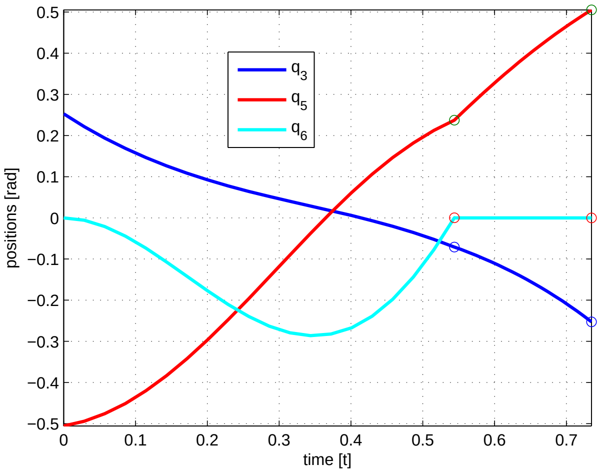

Figura 5.45: Trend of the curves representing the position of the links of the mechanical system (Dribbel) with the $SM1*$. In the figure are represented the instants in correspondence of which the strikes happen.

CAPITOLO 6

Trajectory Tracking Control

Introduction In this chapter it will simulate the optimal trajectories found in the previous chapter (5) with the optimization method. It was found that the optimal kneed mechanism for walking down-.hill with the parameters outlined in the section 5.2.3, is *Dribbel*. The optimization routines gives as result the coordinates trend visible in the figure . This coordinate trend is related to the $SM1*$ described in the section 5.3.1 which presents only two strikes during the gait. The first strike happen on the knee2 approximately at the middle of the gait, and the second one is the final strike on the ground. The objective function value in that case is equal to $J = 0,012$ that is much higher than the one obtained with the optimization of *Compass*. This could mean that *Dribbel* couldn't exhibit a passive dynamic walking over a terrain with the value of slope we imposed that is $\gamma = 3°$. Anyway, the purpose is to test it in simulation for verify these statements and eventually applying a certain control law in order to make it to walk. The mechanical model was described in the section 2.3 How was said for the simulation of the model Compass, the optimization routine doesn't say anything about the stability of the walking cycle, and, this need to be proved with the simulation of the model. The simulation model, needs to provide the implementation of knee locking mechanism because of the walking behavior of this particular walker.

6.1 *Dribbel* and knee-locking mechanism

The walking of this model is the one shown in the figure 6.1.

The walking motion was divided into four phases. The knee is unlocked at toe-off, and the thigh and shank of the nonsupport leg swing freely (a) until the angle of the shank once again matches the angle of the thigh. At this point the knee is fully extended, and the biped experiences an instantaneous impact as the knee strikes its limit and locks (b). The thigh and shank of the nonsupport leg now swing as one unit, effectively reducing the model to the simplicity of the compass gait biped (c) until the tip of the nonsupport leg collides with the ground in another impact (d). Again we assume an instantaneous transition from nonsupport leg to support leg, and the biped immediately begins taking another step. The phase (c) in which the mechanism behaves like a compass bipedal walker is characterized by having the swing leg locked in straight position due to the electromagnets in the knee-cups. This particular behavior of the mechanism is modeled considering an additional control action (activated only on the swing leg's knee) into the mechanical equation that has the purpose to keep the leg straight after the knee strike. The equation changes like in the following:

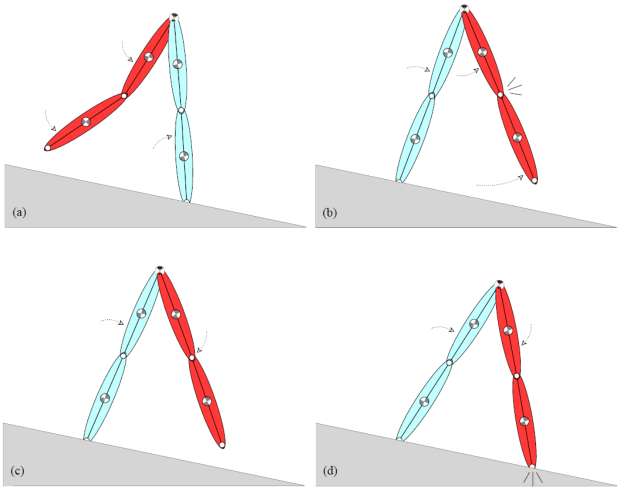

Figura 6.1: The four phases of the down-hill walking with Dribbel

$$\boldsymbol{M}(\boldsymbol{q})\ddot{\boldsymbol{q}} + \boldsymbol{C}(\boldsymbol{q},\dot{\boldsymbol{q}})\dot{\boldsymbol{q}} + \boldsymbol{V}(\boldsymbol{q}) = \boldsymbol{\tau} - \boldsymbol{J}_r^T\boldsymbol{\lambda}_r \tag{6.1}$$

Where $\bar{\boldsymbol{M}}_i(\bar{\boldsymbol{q}}_i) \in \mathbb{R}^{m\times m}$ is the mass matrix of system and collects the inertial terms, $C(q,\dot{q}) \in \mathbb{R}^{m\times m}$ collects together elements of centrifugal force and Coriolis forces, the term $V(q) \in \mathbb{R}^{m\times 1}$ collects the elements of gravity, while $\tau \in \mathbb{R}^{m\times 1}$ is the vector of torque applied to the system and $\boldsymbol{J}_r^T\lambda_r$ is the locking torque that ensures to keep straight the swing leg. m is the number of degrees of freedom that in this case is equal to 3. While the knee is unlocked, $\lambda_r = 0$ When the nonsupport knee is fully extended, we want to enforce the locking constraint $q_6 = 0$ to keep the nonsupport leg straight. Differentiating this constraint is obtained $\dot{q}_6 = 0$ or

$$\begin{bmatrix} 0 & 0 & 1 \end{bmatrix}\dot{\boldsymbol{q}} = 0 \tag{6.2}$$

Defining $\boldsymbol{J}_r = \begin{bmatrix} 0 & 0 & 1 \end{bmatrix}$, differentiating again could be obtained:

$$\boldsymbol{J}_r\ddot{\boldsymbol{q}} = 0 \tag{6.3}$$

And it's possible to solve the equation (6.1), for $\ddot{\boldsymbol{q}}$ and finding:

$$\ddot{\boldsymbol{q}} = -\boldsymbol{M}(\boldsymbol{q})^{-1}\left[\boldsymbol{C}(\boldsymbol{q},\dot{\boldsymbol{q}})\dot{\boldsymbol{q}} + \boldsymbol{V}(\boldsymbol{q}) - \boldsymbol{\tau} + \boldsymbol{J}_r^T\boldsymbol{\lambda}_r\right] \tag{6.4}$$

And reducing the notation defining $\boldsymbol{h}(\boldsymbol{q},\dot{\boldsymbol{q}}) = \boldsymbol{C}(\boldsymbol{q},\dot{\boldsymbol{q}})\dot{\boldsymbol{q}} + \boldsymbol{V}(\boldsymbol{q}) - \boldsymbol{\tau}$, it is possible to substitute equation (6.4) into (6.3) obtaining:

$$\boldsymbol{J}_r\ddot{\boldsymbol{q}} = -\boldsymbol{J}_r\boldsymbol{M}(\boldsymbol{q})^{-1}\left[\boldsymbol{h}(\boldsymbol{q},\dot{\boldsymbol{q}}) + \boldsymbol{J}_r^T\boldsymbol{\lambda}_r\right] \tag{6.5}$$

And solving for λ_r is obtained:

$$\lambda_r = \begin{cases} 0 & \text{if} \quad \text{knee} \quad \text{unlocked} \\ -\left[\boldsymbol{J}_r\boldsymbol{M}(\boldsymbol{q})^{-1}\boldsymbol{J}_r^T\right]^{-1}\boldsymbol{J}_r\boldsymbol{M}(\boldsymbol{q})^{-1}\boldsymbol{h}(\boldsymbol{q},\dot{\boldsymbol{q}}) & \text{if} \quad \text{knee} \quad \text{locked} \end{cases} \tag{6.6}$$

The two different values of λ_r have to be implemented into the dynamic equation in order to switch correctly from the 3 d.o.f. configuration to the one with 3 d.o.f. as well, but behaving like 2 d.o.f. model.

6.2 Uncontrolled Simulation

In this section it will investigated if the passive dynamic walking for *Dribbel* exists. For doing that, let's simulate the model with no control action $\boldsymbol{\tau} = \mathbf{0}$, except the one required for the knee locking mechanism ($\boldsymbol{J}_r^T \lambda_r$). The simulation starts with the same initial conditions obtained with the optimization algorithm:

$$\boldsymbol{q}\left(t_0\right) = \begin{bmatrix} 0,252 \\ -0,505 \\ 0 \end{bmatrix} \quad \dot{\boldsymbol{q}}\left(t_0\right) = \begin{bmatrix} -1,44 \\ 0,270 \\ 0 \end{bmatrix} \tag{6.7}$$

Where $\boldsymbol{q}\left(t_0\right)$ and $\dot{\boldsymbol{q}}\left(t_0\right)$ are the initial state variables of the model under simulation. Their units are respectively $[rad]$ and $[rad/s]$. The simulation routine produce the results shown in the figure 6.2.

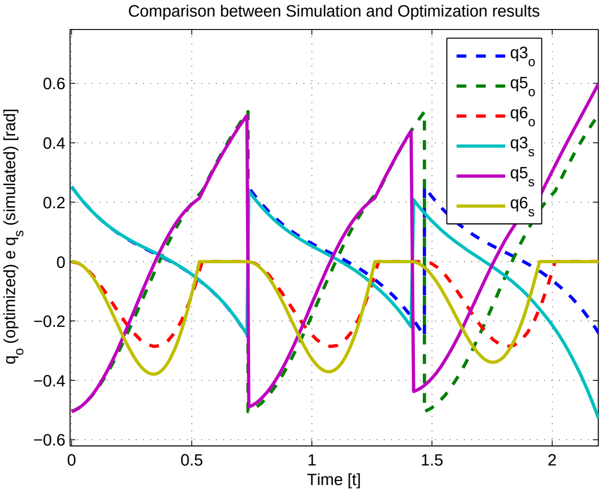

Figura 6.2: Comparison between the simulation of the uncontrolled *Dribbel*, and the optimized curves. Dash line are the optimized curves, and solid line is the simulation.

In the figure is showed the trends of the optimized positions with dashed line, and the trends of the simulated positions with solid line. Notice how the coordinate q_6 reaches the zero value in correspondence of the knee strike, and then, it remains the same till the end of the singe gait. Moreover, the figure 6.2 is showing how the simulation of the robot with optimal initial conditions and zero control effort (except knee locking) highlights that the computed gait is not fully passive. While the ankle (q_3) and hip (q_5) joints passively follow the computed gait quite closely, at least in the initial phase, the knee joint (q_6) deviates severely. Still, despite this difference, the computed gait is a fair approximation of a passive (or at least efficient) motion of the walker and indeed the uncontrolled robot takes a few step before falling over.

6.3 Controlled motion

Like obtained in the previous section, the passive dynamic walking for Dribbel, with the characteristics used in this thesis, doesn't exist. In order to make the robot walk with the optimal trajectories found in the previous chapter, we need to introduce a controller with a control law in order to make the system follow the reference trajectories defined before. It is chosen to use a type of PD control law, because of the co-located nature of the control actions, that will provide stability on trajectories tracking purpose.
The control law is defined like:

$$\boldsymbol{u} = k_p\left(\boldsymbol{q}_r - \boldsymbol{q}\right) + k_d\left(\dot{\boldsymbol{q}}_r - \dot{\boldsymbol{q}}\right) \tag{6.8}$$

Where the parameter k_p is the gain of the proportional control referred to the difference between the reference position and the simulated position; the parameter k_d is the derivative gain referred to the difference between the velocities (reference and simulated).
There are used the same gains for all the three control actions $u \in \mathbb{R}^{3\times 1}$ referred to the three degrees of freedom. The main problem with this control law is modeling the tracking of the trajectories during the simulation routine. This problem is characterized by the fact that the reference trajectories are discontinuous in correspondence on the final instant of a step. The problem is that the system is controlled with a PD control law, and so, it will follow the reference as better as the controller is well performed depending by the gains k_p and k_d. Despite of this, there will always be a difference between the simulated and the reference curves. This difference could be a problem in correspondence of a strike (ground) if the reference curves reaches the strike configuration in advance respect the simulated ones. This is, because immediately after that, the reference changes and the simulated curves, that have not reached its strike instant jet, are forced to follow the reference that is different despite of the reference just before the strike (this is due to the re-labeling operator of the coordinates).
This could be easily understand considering the figure 6.3. In this figure is shown the final instant of a step that links to the next step. The represented function has no other meaning but the one to show this problem's mechanism.

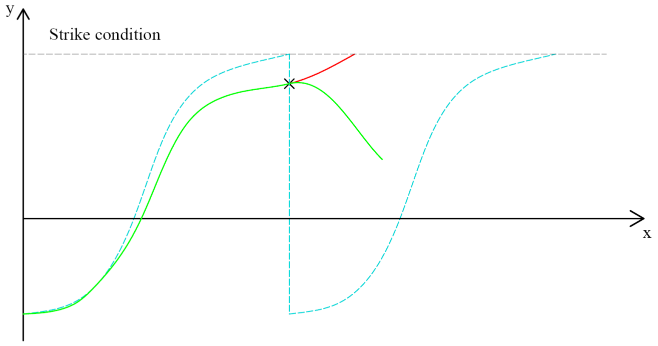

Figura 6.3: Problem of trajectory tracking for hibrid mechanical systems.

The dashed line is the reference, and the solid line is the simulated coordinate. How we can see, if the reference line reaches its strike instant before the simulated one does it, the reference changes an instant after, and the simulated curve is forced to follow the new reference function before having its strike. This condition is conceptually wrong to do it but in practice, it never happen because the little difference, that is kept between the reference and the simulation due to some proper gains of the control law (this is true for the non perturbed walking behavior). Anyway, in the following is introduced a dynamic reference in order to avoid the problem outlined before.

6.3.1 Dynamic Reference

The problem about the discontinuity of the reference, practically speaking, is not a severe problem if the magnitude of the difference between the reference and simulated curves is little. This is obviously dependent, in general, by the magnitude of the control action. The dynamic reference consist into extend the reference along the polynomial function defined for the considered part of the gait. In particular, remembering what was said in the section 3.1, the reference of every part of the gait, bounded by the various strikes that happen, is defined by the use of polynomial functions (N_p in numbers) whose coefficients are the parameters optimized into the optimization routine. The extension of the reference is made along the polynomial function defined by its coefficients. In practice, when the reference trajectories reach the strike instant, if the simulated curves have not reached the strike criterion jet (for example, the knee2 strike criterion is $q_3 = 0$), the reference is extended along its polynomial function till the strike criterion is reached even by the simulated curves. The figure 6.4 is showing this mechanism and the area of extension is highlighted.

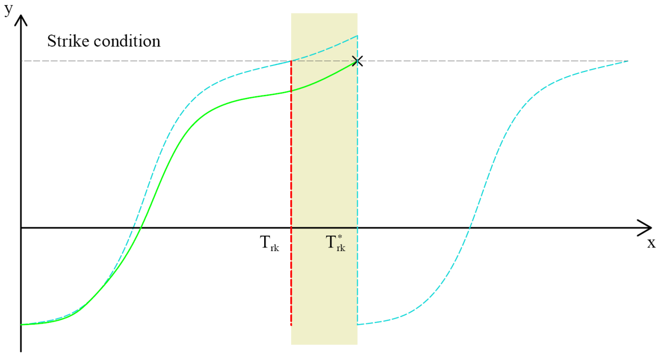

Figura 6.4: Dynamic reference mechanis.

For some appropriate gains values, the extended reference will be absorbed in the next steps by the control law; it is appropriate to chose the gains in order to consider this type of re-absorption. The definition of the polynomial is the one made in the section 3.1, and it is defined into the time range $t \in [0, T_{rk}]$ where T_{rk} is the time instant of the $k-th$ strike happen during the walking cycle. The subscript r stands for reference and indicates the time instant is the one of the reference curves. If, during the walking, the position reference reaches the strike configuration before the simulated curves does, the reference is extended over to the range $t \in [0, T^*_{rk}]$.
T^*_{rk} is the extended time instant of the $k-th$ strike that coincides with the simulated walking model time strike. The choice of extending the reference along the polynomial functions is dictated by the fact that the regularity of the functions between the strikes, and their smoothness due to the optimization, are properties that allow us to extend

preserving the direction that the reference had at the strike instant. This is true only if the extension persist in a small time range. This happen for all the practical simulations we had tested in the following (Otherwise some problems happen when the perturbation of the state variables is introduced).
This mechanism is used also for the intermediate strikes of the gait. The knee strikes are characterized by a consistent change into the reference slope of the coordinates trend (like shown in the figure 6.10), and using this reference mechanism, the reference strike instant's characteristics are preserved till the effective strike instant of the simulated model happen. The figure 6.10 is showing the configuration for which the knee strike happen.
The configuration provides the relation $q_3 = 0$ at the time instant *Tknee*.

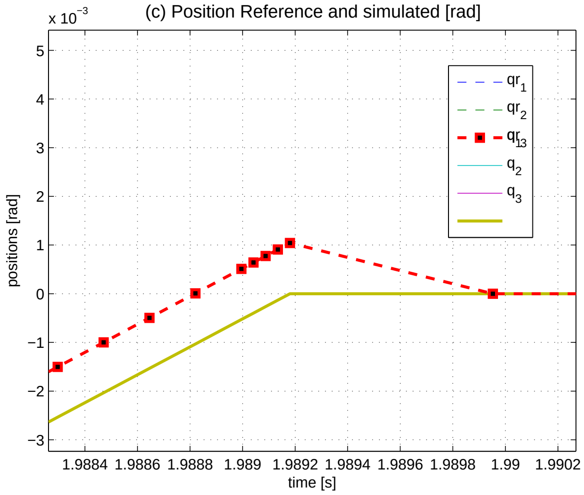

Figura 6.5: Particular of the knee strike of a simulation result.

The figure is zooming the particular of the knee strike. Notice how the reference line (q_{r3} - dashed) should change slope in correspondence of the intersection with the zero line because of the strike that occur. Despite of this, the reference is extended along the polynomial function in order to make the simulation follow a proper reference (reference that has the same direction of the function defined at the strike instant's reference) till the strike happen in correspondence of $q_3 = 0$. When the simulated model reaches the strike configuration (t=Tknee), the reference is reset and it starts again from t=Tknee, with the polynomial function of the next part of the walking cycle.

6.3.2 Optimal control parameters

In this section are evaluated the parameters k_p and k_d that are the gains of the proportional and derivative part of the control law respectively. These gains, have been set making some consideration on the work (W) required by the walking system. The Work for every step is defined like:

$$W_k = \int_0^{T_k} \boldsymbol{\tau}_k \cdot \boldsymbol{q}_k dt \, [J] \tag{6.9}$$

Where $\boldsymbol{\tau}_k$ is the vector of the torques value of the $k-th$ step of the walking and $\boldsymbol{q}_k$ is position vector of the values of the $k-th$ step. This analysis is computed considering the non perturbed motion of the system beginning with the optimal initial conditions obtained in the section 5.3.1. The value of the work done by the system is evaluated for the only first step of the entire walking simulation because it is investigated the optimal values of parameters k_p and k_d that makes the system to remains close to the desired trajectories without diverge from it. In fact, how can be seen from the figure 6.2, that illustrates the trend of the coordinates with zero control effort and optimal initial conditions, the system falls down in the third step of its walking, and so, considering the only first step, preserve to consider values of work of divergent steps like, for example, the third in the figure 6.2. This happen for same couple of gains that are too little for keep the system stable, and make it diverges after few steps. The figure **??** is showing the surface of the work values evaluated making the parameters k_p and k_d vary into the ranges: $k_p \in [0, 350]$ and $k_d \in [0, 150]$. All the simulations performed, end at $t_f = 3.5\,[s]$ that consist, if the gait is stable, to performing an amount of 6 entire steps.

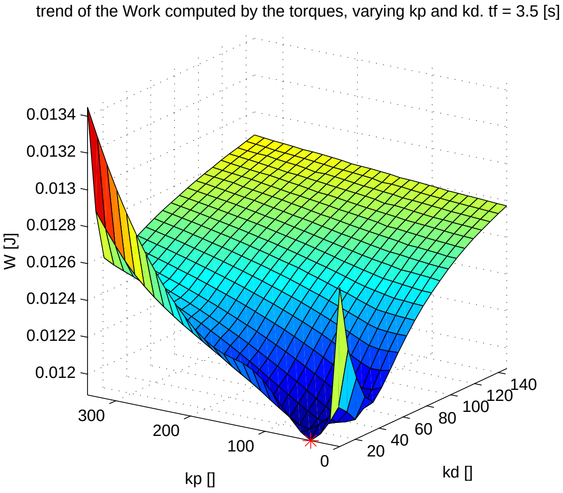

Figura 6.6: Surface representing the work of the actuators varying the control input parameters.

The figure is highlighting the point that individuates the minimum of the surface in the domain defined before. How can be easily noticed, the surface has a neat minimum (the minimum is represented by the red mark) in correspondence of really low values of both the parameters k_p and k_d. The 3D figure was cutted in correspondence of zero values of the parameter k_d for let the figure to be represented properly, because for those values, the work (W) provided very high valors. So, another important thing is that for lower values (close to the zero) of the parameters, especially for lower values of the parameter k_d , the control system quickly diverges from the optimum. The quickly diverge is due to the fact that the control actions doesn't reach so good to keep the coordinate system to follow the reference, and so, the error (position and velocities errors) rises, and the control actions, and consequently the work do the same.

The loss of optimality of the control actions can worst till the case in which the system becomes unstable. It is, for example, when both the parameters are zero. For higher values from the minimum of k_p and k_d, the W arise, but less sharply that previously

and for really high values (k_p more than 300, and k_d more than 140), the surface tends to stabilize its trend around a certain value. Says that, it could be effective focus the research around the minimum value found in the figure 6.6, thickening the mesh of the surface and focusing on a much more little range of parameters. From the previous considerations can be investigated the first part of the previous parameters range in order to find a local minimum point of the surface that suits our purpose of finding the lowest possible values of the parameters that ensures stability of the walking (at least for the first 6 steps).
The figure 6.7 is plotting the desired surface defined into restricted ranges of parameters. This time, $k_p \in [0, 30]$, and $k_d \in [0, 15]$.

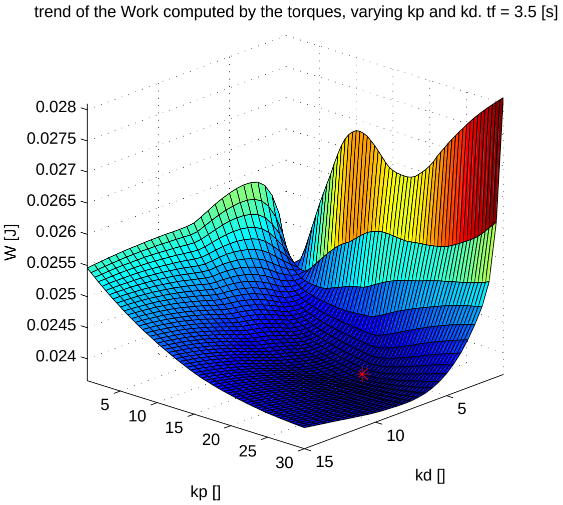

Figura 6.7: Surface representing the work of the actuators varying the control input parameters. It's a detail of the figure 6.6.

Zooming the area, it is easy to notice how the figure shows a local minimum point of the surface, and it happen for reasonable low values of the parameters. The minimum is in correspondence of $k_p = 19,5$ and $k_d = 5,5$. It is important to notice how the surface, for lower value of the parameters, rise up consistently till the maximum that is obtained, like expected, in correspondence of the edges in which $k_p = 0$ and $k_d = 0$. The surface, in addition, rise a little bit for higher values of the parameters (higher than $k_p = 19,5$ and $k_d = 5,5$), and then it tends, for high values of the parameters, to the values of the figure 6.6 showed before. That means that a local minimum value of the surface exists and we can use that minimum for identifying the optimal parameters. The optimal parameters are:

$$k_p = 19,5 \quad k_d = 5,5 \tag{6.10}$$

The obtained results are better defined considering also the RMS function of the position error. Those results, in fact, are the best in terms of work computed from the actuators but nothing is known about the position error we make with these parameters. Indeed, it is useful to define the quantity:

$$RMS_{err,k} = \overline{err_k}^2 + \sigma^2_{err,k} \left[rad^2\right] \tag{6.11}$$

$$\boldsymbol{err}_k = \boldsymbol{q}_{r,k} - \boldsymbol{q}_k \, [rad] \tag{6.12}$$

Where $\overline{err_k}$ is the mean of the position errors ($\boldsymbol{err}_k$) of the $k-th$ step, $\sigma_{err,k}$ is the standard deviation of the errors in the $k-th$ step length, and $\boldsymbol{q}_{r,k}$ is the position vector of the reference defined in the $k-th$ step. The RMS of the position error is a value defined with the same characteristics with which was defined the work of the system. The value is defined for the only first step, and the system is let started with the optimal initial conditions and with no perturbation.
The obtained surface with the same range of parameters $k_p \in [0, 30]$, and $k_d \in [0, 15]$ is the following figure 6.8;

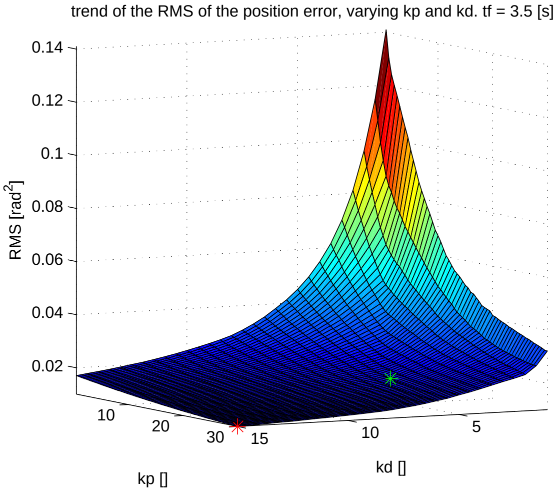

Figura 6.8: Surface representing the RMS of the error between simulated and reference curves varying the control input parameters.

The figure 6.8 is showing the trend of the RMS surface varying the control action's parameters. The red mark on the edge of the domain is the local minimum of the surface, defined in this domain, and the green mark, is the one related to the minimum of the work defined in the figure 6.7; the minimum of RMS is, like expected, in correspondence of the maximum value of the parameters (in this domain $k_p = 30$, and $k_d = 15$), and this is because the control law is always stable due to the control actions nature and this brings the fact that the error always decrease while increasing the control parameters.
Physically happen that the control action is much more performant than the optimal one defined before, and make the system follow the reference much better and quickly than before, and the position error globally reduce. In this way reduce also the extended period of each single step due to the dynamic reference described in the previous section. The extended period of the reference trajectories is function of the control actions, and in particular, as much the control action is performing, as the extended period is short, and, to the limit, it becomes zero (that means perfect trajectories tracking).

6.4 Simulation with optimal control parameters

At moment, *Dribbel* needs to be tested with the optimal control parameter in order to verify the statements about its stability and good tracking. The parameters of the simulations are:

- No perturbation of the initial state.
- 3° slope of the terrain
- $t_f = 3,5$ $[s]$ final time of the simulation
- $k_p = 19,5$
- $k_d = 5,5$
- $x_0 = x_{0,opt}$ initial state conditions are the optimized one
- SM of the walking is $SM1*$ with its reference trajectories $\boldsymbol{q}_r$, $\dot{\boldsymbol{q}}_r$ and $\ddot{\boldsymbol{q}}_r$

All these parameters provide the following coordinate trends result shown in the figure 6.9.

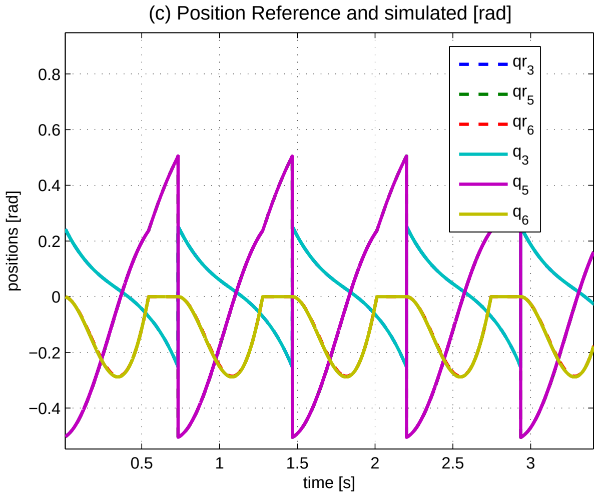

Figura 6.9: Trend of the simulated and reference coordinates with optimal control law.

Looking at the figure 6.9, can be noticed how the system is stable (the control law is able to drive the system's coordinates despite of the tendency of being unstable), and evolves in time, emulating the reference with a good precision and accuracy. The amount of error is shown in the figure 6.10 below, and can be noticed how the most of the position error is related to the coordinate q_6 , and the amount is around $3.5 * e - 3$ $[rad]$. At the beginning of the figure the transitional during which the error is going to stabilize, is probably due to the problem of how many significant digits have been considered in the definition of the initial conditions of the simulation routines.
From the figure 6.11 can be noticed how the most of the work done by the actuators is done by the torque τ_6 referred to the coordinate q_6 . The amount of work done by the actuators for every step is around the value of $W = 0,012$ [J].

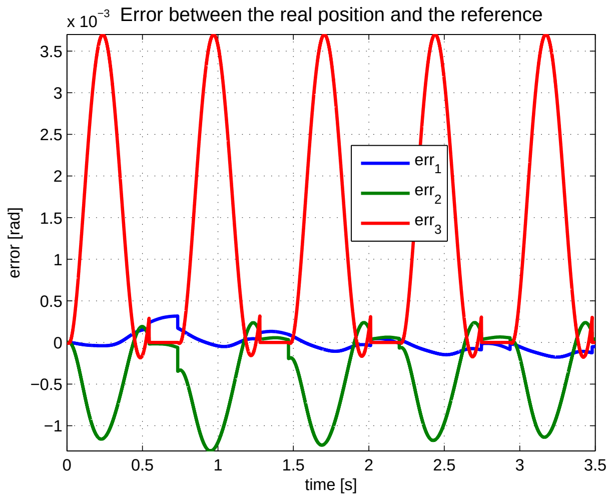

Figura 6.10: Error between the real positions and the reference of the three coordinates.

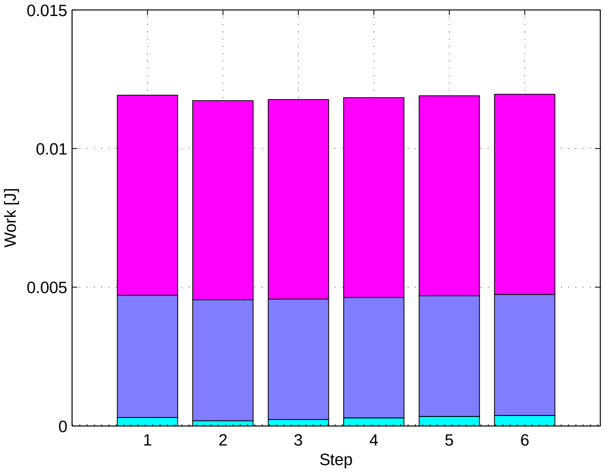

Figura 6.11: Work per step; the three columns azure, purple and pink are represented the work of the toque 3, 5 and 6 respectively.

6.5 Compare with other movement trajectories

The obtained controlled movement of the previous pharagraph is the one with which the minimum control input is required, and for which the walking is stable. For prove it, it is useful to test other movement trajectories as reference, and control the system with the control law defined before. These movemets are obtained trhough the optimization algorithm imposing some other constraints to the optimization routine. The constraints were for example:

- Imposing a knee strike's time instant.
- Impose a final time instant of the gait.

With these additional constraints, the obtained movements of the system are tested in simulation with the same control law defined before. The results are the following in the figures 6.12, 6.13 and 6.14 Imposing knee strike's time instant referred to the final time $t_f - T_{knee1} = 0,15$ is obtained:

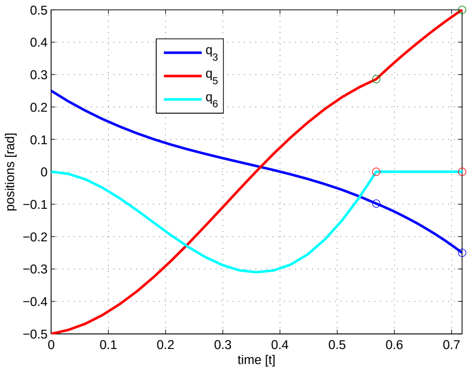

Figura 6.12: Trend of the curves representing the optimizaed coordinates.

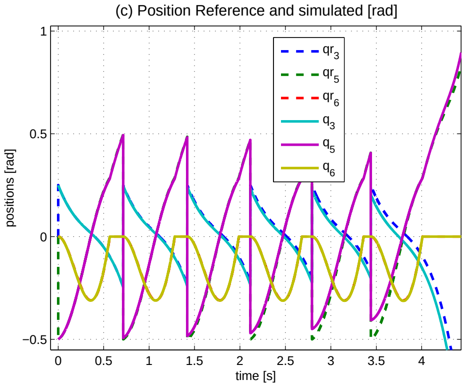

Figura 6.13: Trend of the simulated and reference coordinates with optimal control law befined in the previous pharagraph.

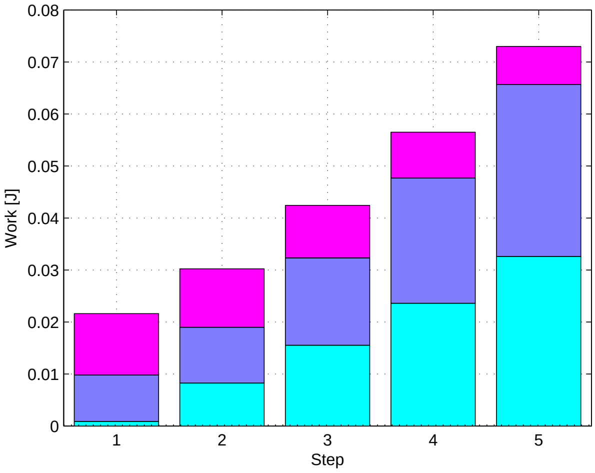

Figura 6.14: Work per step; the three columns azure, purple and pink are represented the work of the toque 3, 5 and 6 respectively.

And for and imposed final time instant $t_f = 0,65$ the results are in the figures 6.15 and 6.16

In this case the amount of work for the only first step is around $W = 0,057$ [J], amost 5 times the value obtained with the optimal movement obtained in the figure 6.11. How was expected, the control law designed in the previous paragraph is not able to drive the coordinates movements as well as was done for the optimal trajectories of the figure 6.9. Can be noticed how the control law defined before is not sufficient for a perfect trajectory tracking and it causes instability of walking considering both the simulations shown in the figures 6.15 and 6.12. How was said in the section 4.5.2, for

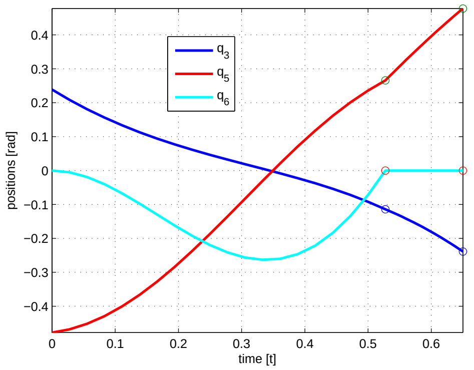

Figura 6.15: Trend of the curves representing the optimizaed coordinates.

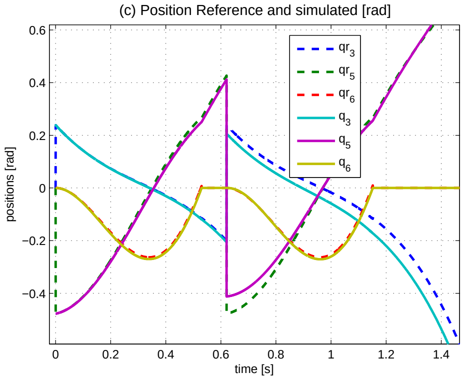

Figura 6.16: Trend of the simulated and reference coordinates with optimal control law befined in the previous pharagraph.

control purpose, the question whether an efficient limit cycle is stable or not is not so important, because it is always possible to keep the walking stable chosing some high enough coltrol parameters. Otherwise in this case we are talking about an efficient controlled walking limit cycle that is unstable with zero control effort. This bring as consequence that a minimum of control input energy is required for make the walking be stable over time.

With these considerations, the analysis of stability of this controlled system should be interesting considering the stability with its nominal control action that is the one obtained in the section 6.3.2.

CAPITOLO 7

Global stability of Dribbel

7.1 Introduction

In this chapter, it is investigated the walking stability of *Dribbel*'s motion found in the previous chapters. The walking stability, as outlined before, has not a real sense with a control purpose. In this case, otherwise, the walking limit cycle obtained with the control law defined in the section 6.3.2, is such that the control input is optimal in the sense of trajectories tracking and control action effort (in particular it was found the optimal control parameters that minimize the work done by the actuators). In this sense, the purpose of the stability analysis is to investigate the stability of *Dribbel* walking down-hill with the optimal control input parameters defined before. The stability anasysis was developed introducing some perturbations on the system's state variables at the beginning of the first step, in order to observe the walking behavior, and if the system falls down after a certain number of steps (unstable) or if the perturbation is re-absorbed from the control law and the system continue along its walking limit cycle (stable).
The concept of walking limit cycle is defined in the section 3.1. To study the of stability of the walking cycle have to be considered the step-to-step function (Stride function) of which was discused, again, in the section 3.1.

7.2 Limit Cycle verification

The first step of the analysis of the stability of Dribbel walking is to determine the walking limit cycle that in this case should be represented by the obtained result of the optimization routine. For verifying the walking limit cycle we can use another optimization function of MatLab (*lsqnonlin*) that solves the last-squares non linear problem of finding the state variable vector $\boldsymbol{x}^*$ for which

$$\boldsymbol{x}^* = \boldsymbol{F}\left(\boldsymbol{x}^*\right) \tag{7.1}$$

where $\boldsymbol{F}\left(*\right)$ is the step-to-step function, that maps the initial conditions of a step into themselves of the next step, through the integration of continuous dynamic and through the projection operators and, the re-labeling operator in addition to the knee locking mechanism. $\boldsymbol{x}$ is the state variables vector defined like $\left[\begin{array}{cccccc} q_3 & q_5 & q_6 & \dot{q}_3 & \dot{q}_5 & \dot{q}_6 \end{array}\right]^T$. $\boldsymbol{x}^*$ is the fixed point, meaning that the output of the function is the same as the input. The limit cycle is obtained numerically imposing the minimization of the difference between the input and output state varibles $min_x \left| \boldsymbol{F}(\boldsymbol{x}) - \boldsymbol{x} \right|$. The implementation of the previous minimization gives as result the $\boldsymbol{x}^*$ state variable vector of the limit cycle walking of the system. The minimization function provides a initial state varibles vector from which make the minimization proceeding and it was chosen the obtained optimal state initial vector. The obtained $\boldsymbol{x}^*$ is really close to the optimal initial state variables $\boldsymbol{x}_{0,opt}$ defined with the optimization routine of the section 5.3.1.

$$\boldsymbol{x}^* = \begin{bmatrix} 0,2527 \\ 0,5053 \\ 0 \\ -1,1437 \\ 0,2693 \\ 0 \end{bmatrix} \quad \boldsymbol{x}_{0,opt} = \begin{bmatrix} 0,2525 \\ 0,5051 \\ 0 \\ -1,1439 \\ 0,2690 \\ 0 \end{bmatrix} \tag{7.2}$$

The differences between the two state vectors are really pour probably due to numerical errors of the optimization routine. From the obtained new state variables $\boldsymbol{x}^*$, we can run the simulation of the walking down-hill of *Dribbel* and verify the limit cycle that's expected to obtain with these initial conditions. The limit cycle could be easily shown through the limit cycle diagram shown in the figure 7.1.

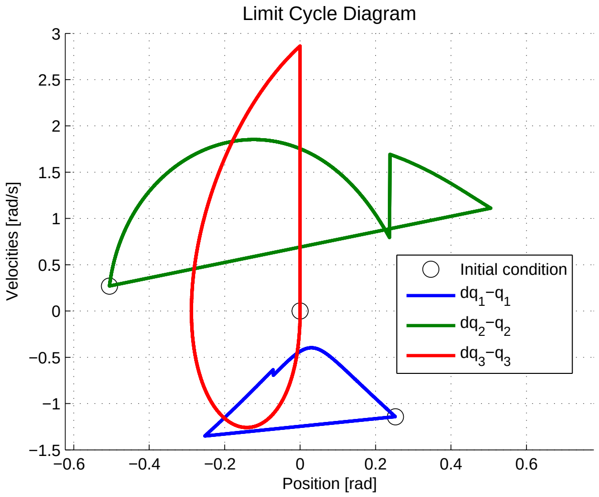

Figura 7.1: Limit Cycle Diagram. The dark marks indicate the state value of the steps initial conditions.

The obtained curves are showing how, for every coordinate of the system, the initial position state variables are mapped the same at the beginning of every step through the step-to-step function $\boldsymbol{F}(*)$ (it is not understandable from the diagram but the simulation was performed for a series of 6 steps in a row). The state variables obtained is the vector $\boldsymbol{x}^*$ that is a fixed point of the Poincaré surface into the Poincaré map showed in the figure 3.2 in the section 3.1.

7.3 Global Stability

The stability analysis was developed considering the Global stability analysis of the walking mechanism through the use of Basin of Attraction Diagrams. The analysis of

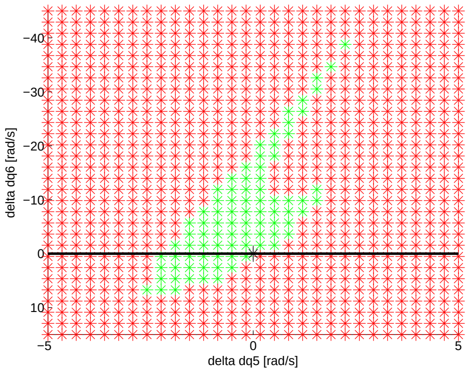

Figura 7.2: Basin of attraction $\Delta\dot{q}_6$ - $\Delta\dot{q}_5$

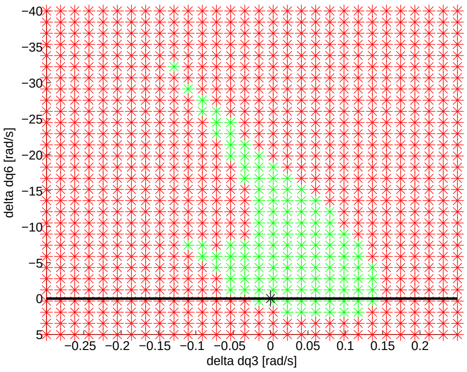

Figura 7.3: Basin of attraction $\Delta\dot{q}_6$ - $\Delta\dot{q}_3$

simulation starts from this initial optimal condition perturbating the nominal initial state (the velocities in particular) and observing the evolution of the coordinates over time during the walking. There are simulated the dynamics for different velocities using the fixed point positions of the coordinates of the system ($q_3 = 0,2527$, $q_5 = 0,5053$ and $q_6 = 0$). This method is taken from the one proposed by [42]. A state is considered stable if its last two consequtive steps of the walking have an initial condition state vector difference that is within a threshold of 0,001 [rad] for the positions and 0.01 [rad/s] for the velocities . It is also assumed that if a large amount of steps are taken (50), the model will walk forever. The resulting figures of the basin of attraction are shown in Figures 7.2, 7.3 and 7.4 with the fixed point marked with a black plus marker. The basin of attraction are characterized by markers over the considered range of perturbations, of different colors depending on if the walking is stable or not (red mark if the walking is unstable, and green if it is).

The basin of attraction have on their axis the perturbation of the state variables. Considering the perturbation $\Delta\dot{q}_6$, is important to say how the respective basin of attractions in the figures 7.2 and 7.3, present a black line in correspondence of the value zero of the perturbation $\Delta\dot{q}_6$, dividing the diagrams in two areas. The area of negative values of the perturbation is admissible because there is congruency between the perturbation and the physical constraints of the model. The area with positive values, otherwise, is not admissible, because at the beginning of the gait *Dribbel* has a compass posture and is not allowed to the lower part of the legs to over-extend. For those reasons, these diagrams have to be considered for the only area with negative values of the $\Delta\dot{q}_6$ perturbation. The velocities of the initial state vector are defined like defined in the eqaution (7.3).

$$\dot{\boldsymbol{q}} = \dot{\boldsymbol{q}}^* + \Delta\dot{\boldsymbol{q}} \tag{7.3}$$

Where $\dot{\boldsymbol{q}}^*$ is the fixed point velocity vector, and $\Delta\dot{\boldsymbol{q}}$ is the vector of the perturbations. For an easy representation, there were shown the basin of attraction considering two perturbed velocities at a time. The basin of attraction diagrams are shown in the following.

How can be easily notice from the figures 7.2, 7.3 and 7.4 is that the range in which the velocity $\dot{q}_3$ may vary (obtaining a stable walking) is very narrow comparing with the ranges of the velocities $\dot{q}_6$ and $\dot{q}_5$ that produce a stable walking also with really

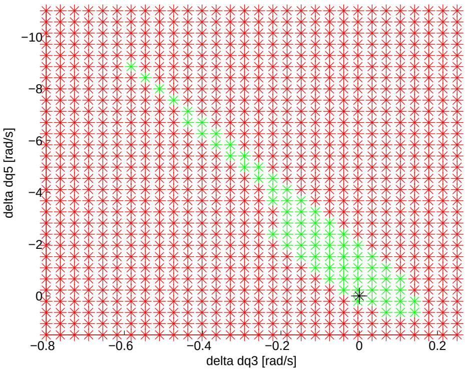

Figura 7.4: Basin of attraction $\Delta\dot{q}_5$ - $\Delta\dot{q}_3$

high disturbances. For example, taking a look to the figure 7.2, can be noticed how the velocity $\dot{q}_6$ may vary in a very large range of values of disturbaces. From the figures emerges that the possible values of the disturbances for which the walking remain stable is very different from the various considered coordinates. In particular, can be noticed how the maximum amount of disturb (for which the walking is stable) on $\dot{q}_6$ is (more or less) one order of magnitude bigger than the disturb on $\dot{q}_5$ and another order of magnitude bigger than $\dot{q}_3$ disturb. That means that on stability purpose, a disturb on the velocity of the coordinate q_3 compared with a disturb of the same value, but acting on the coordinate q_6, for example,is much more effective to bring the system to be unstable because of the little basin of attraction that the system has along the axes of the $\dot{q}_3$ disturb.
For the stability analysis it was considered the ground clearance of the swinging foot like a determinant parameter for the stability. In particular, if the swinging foot hits the groung (ground clearance $gc = 0$) before the time instant in which the *knee2* strike should happen, the simulation is stopped and the walking is considered unstable because the constraints of the walking model were violate (the compass posture at the end of the gait was not reached).
Another aspect that is important to outline, is that the dynamic reference that is used to drive the trajectories tracking control, was not providing saturation on a certain limit value. This brings that when the area of extension of the reference is big (caused, for example by great perturbances), the reference continue evolving along its polynomial function without saturate. if the entity of the extension is big, the reference changes in unexpected way due to the polynomial and the controlled system try to track the reference introducing the necessery torques to the actuated joints. The dynamic reference, was developed for using with no applyed perturbations or at least, with just a little perturbation on the state variables. If the amount of the perturbation is consistent, the approach with dynamic reference is not proper and should be modified for example adding a saturation on the references coordinates or thinking another way to construct the reference.

CONCLUSIONS

In this thesis were analyzed the three mechanical bipedal walkers called *Compass*, *Dribbel* and *Knee*. It was found that the best model for walking down-hill is *Compass*, because (with the physical parameters chosen in this thesis) is the only one that can exhibit a passive dynamic walking.

With the example of *Compass*, it was tried to find an efficient walking movement for the kneed models in order to walk along a terrain of 3° slope. The obtained results from the optimization algorithm shows how *Dribbel* is the best kneed model for the studied walk. The obtained results outlined how the best SM for this particular mechanism is the one that provides only two strikes during a single gait. The first one happen in correspondence of the *knee2* and the second one, at the end of the gait, to the ground. The optimization algorithm was constructed considering the objective function (OF) related the torques of the ideal back-driveble actuators, whose are functions of the coordinates and velocities and accelerations of the system. This algorithm was developed in order to optimize the parameters of the polynomial functions that describe the coordinates over the entire gait period. The optimization results have been considered of general validity cause of the great amount of optimization routines performed for considering the most of the possible combinations of step models describing the walking behavior of the mechanical models.

The optimization results, and the simulation also, showed how no passive dynamic walking was found for *Dribbel* and that the obtained passive walking was unstable.

After that was developed a control action in order to make Dribbel to walk performing a stable walking. The control action was developed with a simple PD control law, but the parameters of the controller (k_p and k_d) were obtained such as they minimuze the work done by the actuators over a single gait period. The parameters obtained in such way, are optimal parameters for a stable and energy efficient walking behavior. The obtained parameters were used in order to evaluate the stability of the walking perturbing the velocity vector $\dot{\boldsymbol{q}}$ around its nominal values that are the ones obtained from the optimization algorithm. The result was that the control law is really robust for perturbations acting on the velocity $\dot{q}_6$ and $\dot{q}_5$ allowing perturbations bigger that one order of magnitude respect of the maximum value of the velocity for the $\dot{q}_6$ and of the same order of magnitude for $\dot{q}_5$. The velocity $\dot{q}_3$ is, on the other hand, really sensitive to the perturbations; in fact there are allowed perturbations of approximately one order of magnitude less than the maximum value reached during the nominal walking gait.

The obtained walking motion for Dribbel was the most efficient one and the applyed control law was defined to be optimal for a stable walking. Those conclusions are valid for the considered bipedal models (with their physical parameters) and for the control law used in this thesis. changing the physical parameters or the control law, the results

may change consistently.
The parameters used are the most common ones used in the litterature that referred to real walking systems developed in the recent years.

BIBLIOGRAFY

[1] M. Vukobratović and D. Juriĉiĉ. Contribution to the synthesis of biped gait. *IEEE Transactions on Bio-Medical Engineering*, BME-16(1):1-6, January 1969.

[2] M. Vukobratović and J. Stepanenko. *Mathematical models of gerneral anthropomorphic systems.* Mathematical Biosciences, 17:191-242, 1973.

[3] M. Vukobratović and J. Stepanenko. *On the stability of anthropomorphic systems.* Mathematical Biosciences, 15:1-37, 1972.

[4] M. Vukobratović, B. Borovac, and D. Surdilovic. *Zero-moment point - proper interpretation and new applications.* In Proceedings of the IEEE/RAS International Conference on Humanoid Robots, pages 237-244, Tokyo, Japan, 2001.

[5] A. Goswami. Foot rotation indicator (FRI) point: *A new gait planning tool to evaluate postural stability of biped robots.* In Proceedings of the IEEE International Conference on Robotics and Automation, pages 47-52, Detroit, Michigan, May 1999.

[6] A. Goswami. *Postural stability of biped robots and the foot rotation indicator (FRI) point.* International Journal of Robotics Research, 18(6):523-533, 1999.

[7] Y. Fujimoto and A. Kawamura. *Simulation of an autonomous biped walking robot including environmental force interaction.* IEEE Robotics and Automation Magazine, 5(2):33-42, June 1998.

[8] C.-L. Shih. *Ascending and descending stairs for a biped robot.* IEEE Transactions on Systems, Man, and Cybernetics - Part A: Systems and Humans, 29(3):255-268,May 1999.

[9] H. Miura and I. Shimoyama. *Dynamic walk of a biped.* The International Journal of Robotics Research, 3(2):60-74, 1984.

[10] S. Kajita, F. Kanehiro, K. Kaneko, K. Yokoi, and H. Hirukawa. *The 3D linear inverted pendulum mode: A simple modeling for a biped walking pattern generation.* In Proceedings of the IEEE/RSJ International Conference on Intelligent Robots and Systems IROS, pages 239-246, Lausanne, Switzerland, 2001.

[11] Napoleon, S. Nakaura, and M. Sampei. *Balance control analysis of humanoid robot based on ZMP feedback control.* In Proceedings of the IEEE/RSJ International Conference on Intelligent Robots and Systems IROS, pages 2437-2442, Lausanne, Switzerland, 2002.

[12] T. Sugihara and Y. Nakamura. *Contact phase invariant control for humanoid robot based on variable impedant inverted pendulum model.* In Proceedings of the IEEE International Conference on Robotics and Automation, pages 51-55, Taipei, Taiwan, 2003.

[13] S. Collins, A. Ruina, R. Tedrake, and M. Wisse. *Effcient bipedal robots based on passive-dynamic walkers.* Science, 307:1082-1085, February 2005.

[14] T. McGeer. Powered flight, child's play, silly wheels and walking machines. *In Proceedings of the IEEE International Conference on Robotics and Automation*, pages 1592-1597, 1989.

[15] T. McGeer. Dynamics and control of bipedal locomotion. *Journal of Theoretical Biology*, 163:277-314, 1993.

[16] S. H. Collins, M. Wisse, and A. Ruina. A three-dimensional passive-dynamic walking robot with two legs and knees. *The International Journal of Robotics Research*, 20(7):607-615, July 2001.

[17] M. Spong and F. Bullo. Controlled symmetries and passive walking. *In Proceedings of the IFAC Triennial World Congress*, Barcelona, Spain, 2002.

[18] S. Collins, A. Ruina, R. Tedrake, and M. Wisse. Effcient bipedal robots based on passive-dynamic walkers. *Science*, 307:1082-1085, February 2005.

[19] J. Yamaguchi, S. Inoue, D. Nishino, and A. Takanishi. Develpment of a bipedal humanoid robot having antagonistic driven joints and three DoF trunk. *In Proceedings of the IEEE/RSJ International Conference on Intelligent Robots and Systems IROS*, pages 96-101, Victoria, Canada, 1998.

[20] H. Miura and I. Shimoyama. Dynamic walk of a biped. *The International Journal of Robotics Research*, 3(2):60-74, 1984.

[21] T. Sugihara. Mobility Enhancement control of Humanoid Robot Based on Reaction Force Manipulation via Whole Body Motion. *PhD thesis, Department of Mechano-Informatics*, The University of Tokyo, Tokyo, Japan, 2004.

[22] T. Sugihara and Y. Nakamura. Contact phase invariant control for humanoid robot based on variable impedant inverted pendulum model. *In Proceedings of the IEEE International Conference on Robotics and Automation*, pages 51-55, Taipei, Taiwan, 2003.

[23] K. Doya. Walking pattern learning robot. *Journal of the Robotics Society in Japan*, 8(3):117, 1990.

[24] K. Matsuoka. Mechanisms of frequency and pattern control in the neural rhythm generators. *Biological Cybernetics*, 56:345-353, 1987.

[25] T. Arakawa and T. Fukuda. Natural motion generation of biped locomotion robot using hierarchical trajectory generation method consisting of GA, EP layers. *In Proceedings of the IEEE International Conference on Robotics and Automation*, pages 211-216, Albuquerque, New Mexico, USA, 1997.

[26] V. Duindam, S. Stramigioli, Modeling and Control for efficient Bipedal Walking Robots, vol. 53, 2009

[27] J. Adolfsson, H. Dankowicz, and A. Nordmark, 3d passive walkers: Finding periodic gaits in the presence of discontinuities, Nonlinear Dynamics, vol. 24, pp. 205-229, 2001.

[28] F. Anderson and M. Pandy, A dynamic optimization solution for vertical jumping in three dimensions, *Computer Methods in Biomechanics and Biomedical Engineering, vol. 2,* pp. 201-231, 1999.

[29] Acary, V. & Brogliato, B. (2003), Towards a Multiple Impact Law: the 3-Ball Example, *in Actes du Sixième Colloque National de Calculs des Structures*, Vol. 2, pp. 337-344.

[30] Glocker, C. (2001), On Frictionless Impact Models in Rigid-Body Systems, *Philosophical Transactions of the Royal Society London* 359(1789), pp. 2385-2404.

[31] Glocker, C. (2004), Concepts for Modeling Impacts without Friction, *Acta Mechanica 168*, pp. 1-19.

[32] Beekman, N. (2004), Analysis and Development of a 2D walking machine, *Master's thesis, University of Twente.*

[33] Dertien, E. C. (2005), Realisation of an Energy-Efficient Walking Robot, *Master's thesis, University of Twente.*

[34] van Oort, G. (2005), Strategies for Stabilizing a 3D Dynamically Walking Robot, *Master's thesis, University of Twente.*

[35] Dirk Wollherr, (2005) Design and Control Aspects of Humanoid Walking Robots *Lehrstuhl für Steuerungs und Regelungstechnik Technische Universität München*

[36] Goswami, A., Thuilot, B. & Espiau, B. (1998), 'A Study of the Passive Gait of a Compass-like Biped Robot: Symmetry and Chaos', *International Journal of Robotics Research* 17(12), pp. 1282-1301.

[37] Asano F. Efficiency Analysis of 2-period Dynamic Bipdal Gaits *The 2009 IEEE/RSJ International Conference on Intelligent Robots and Systems* October 11-15, 2009 St. Louis, USA

[38] Asano F. Zhi-Wei L. (2008), Underactuated Virtual Passive Dynamic Walking with an Upper Body, *2008 IEEE International Conference on Robotics and Automation* Pasadena, CA, USA, May 19-23.

[39] F. Asano and L. Zhi-Wei, Asymptotically stable biped gait generation based on stability principle of rimless wheel *Robotica (2009) volume 27, pp. 949-958. Cambridge University Press*

[40] Gomes, M. & Ruina, A. (2005), A Walking Model with No Energy Cost. *In revision, J. of Theor. Biology.*

[41] Trefethen, L. & Bau, D. (1997), Numerical Linear Algebra, *Soc. for Industrial and Applied Math.*

[42] Vanessa F. Hsu Chen, with Passive Dynamic Walking with Knees: A Point Foot Model 2005